Promoting the Reactivity of Nano-scale Zero-valent Iron for Water Treatment: Mechanisms and Application

アハマド, モハマド, エルサイエド, アハマド, アリ, カリル

https://doi.org/10.15017/1866339

Thesis on

Promoting the Reactivity of Nano-scale Zero-valent Iron for Water Treatment: Mechanisms and Application

By

Ahmed Mohamed Elsayed Ahmed Aly Khalil

Supervised by

Assoc. Prof. Osama Eljamal

Department of Earth System Science and Technology

Interdisciplinary Graduate School of Engineering Sciences

Kyushu University

Japan

September 2017

Promoting the Reactivity of Nano-scale Zero-valent Iron for Water Treatment: Mechanisms and Application

A THESIS SUBMITTED IN PARTIAL FULLFILMENT OF THE

REQUIRMENTS FOR THE DEGREE OF

Doctor of Philosophy (Ph.D.)

By

Ahmed Mohamed Elsayed Ahmed Aly Khalil

Supervised by

Assoc. Prof. Osama Eljamal

Department of Earth System Science and Technology

Interdisciplinary Graduate School of Engineering Sciences

Kyushu University

Japan

September 2017

Abstract

Nano-scale zero-valent iron (nZVI) has been the research spotlight for numerous researches in water treatment and environmental applications over the last decade. It has proved its high pollutant removal efficiency and reactivity to treat several contaminants via diverse mechanisms. Owing to its unique properties such as excellent magnetic properties, surface modifiability, extremely small size and high surface area to volume ratio, nZVI is the emerging technology for water purification. However, the search for methods to improve the removal efficiencies of contaminants and their kinetic reduction rates by nZVI is unstoppable, especially in order to decrease the dosage amount required for decontamination. In addition, nZVI has some concerns about its reliability in environmental applications due to its limited mobility and fast agglomeration. Modifying nZVI surface and supporting nZVI particles on a carrier were the proposed solutions to boost the reactivity and solve the aforementioned issues. The nZVI-based reagents were synthesized and then characterized using a variety of analytical equipment, such as transmission electron microscopy, surface characterization analyzer, X-ray diffraction and laser diffraction particle size analyzer, then applied in different water treatment experiments to examine their performances. Nitrate and phosphate were chosen to be the under-investigated contaminants of this study to represent the enhanced mechanisms of removal on applying modifications, which are common mechanisms among numerous contaminants treated by nZVI. Their removal performance was carefully investigated via several batch experiments at various copper ions addition/loading ratios, different conditions of pH, presence/absence of oxygen, distinctive pollutant concentrations and so forth. Optimum addition ratio of $CuCl_2/Fe^0$ was collected from experimental results, which was used to conduct the rest of batch experiments.

The presence of copper ions during nitrate reduction imposes two electrochemical reactions; one stimulates iron corrosion and another reaction causes hydrogen-catalytic reduction of nitrate. Both reactions boosted removal efficiency and kinetics around 3.5 times more than that by ordinary pristine nano-Fe^0 alone, i.e. nitrate removal time was greatly reduced. In case of phosphate, the presence of copper chloride effectively enhanced the

adsorption capacity of phosphorus as it produced copper ferrite spinel on nZVI particles' surface, which can adsorb phosphorus and increase its rate of adsorption, and also it stimulated nZVI corrosion. The adsorption capacity of phosphorus in case of nZVI in the presence of copper chloride was greater by ca. 80% than that of nZVI without copper chloride. This modification greatly boosted reaction kinetics and removal efficiency, and decreased the dependency of remediation on pH of medium and dissolved oxygen presence.

Among 25 composites of synthesized nZVI on activated carbon (AC) support under different preparation and treatment conditions, thermally-treated granular AC-supported nZVI was selected at optimum nZVI/AC mass ratio and treatment conditions. This study introduced thermal treatment of AC before supporting nZVI, which modified its textural and surface chemistry properties to attract contaminant anions with a higher affinity towards nZVI. The novel composite succeeded in increasing the removal efficiency of nitrate by 50% and of phosphate by 100% from their aqueous solutions and of nitrate by 170% along with a complete removal of phosphate from their solution. Regarding the contaminants, their removal mechanisms were carefully inspected, and their Interference studies with the treatment efficiency were conducted including the investigation of interference of domestic wastewater, humic acid, anions of sulfate and phosphate, cations of cuprous and cupric, and calcium carbonate (hardness). Results showed the significant negative impact of interference of most substances (except copper ions) on the nitrate reduction and the superiority of optimized nFe(0)/AC by ca. 27% to ca. 183% increase in treatment efficiency over nZVI. All removal profiles of most batch experiments were described by kinetic formulation models that fitted experimental data with high accuracy and precision.

Concerning material conservation, a regeneration of nZVI materials and recovery of phosphate contaminant were successfully achieved. The regenerated nZVI, recovered from spent synthesized nanoparticles, regained full and complete removal performance.

Finally, the nZVI-based reagents were implemented in a developed application of a laboratory-scale continuous flow system (LSCFS) in order to test their performances and discover the challenges that can face actual operations. The results showed another improvement in removal efficiency and convenience in operation. To sum it up, the novel composite of combined modified copper ions addition and heat modified AC-supported nZVI can be a suitable reagent and a versatile material for applications in water treatment systems.

Acknowledgements

The whole praise, prostrations and supplications are to Allah who aided me in every moment of this project and helped me in finishing this work.

The studies presented in this dissertation were completed and submitted in partial fulfillment of the requirements for the degree of Doctor of Philosophy (Ph.D.) from Kyushu University, Interdisciplinary Graduate School of Engineering Sciences, Department of Earth System Science and Technology.

Special precious thanks to my dear supervisor Assoc. Prof. Osama Eljamal who was always offering continuous help, support and advice. I would like to express my sense of indebtedness and sincere gratitude to him as I even felt that he worked very hard for my success in accomplishing this work. I have learned from him commitment, follow-up, good usage and management of time and a lot others.

I want also to thank Prof. Nobuhiro Matsunaga, and I show him my appreciations for all efforts he made. He was always beside us in difficult moments. I am grateful to him for helping us in these situations. It has been an honor working in the laboratory of Prof. Nobuhiro Matsunaga, Prof. Yuji Sugihara and Assoc. Prof. Osama Eljamal.

I am indebted to Prof. Yuji Sugihara, Assoc. Prof. Takahiko Miyazaki, Prof. Naoki Hirose, and Assoc. Prof. Osama Eljamal for assessing this thesis and for their valuable review comments and questions.

I should be thankful to prof. Satoshi Hata, Asst. Prof. Hikaru Saito, Asst. Prof. Skander Jribi, and Assoc. Prof. Takahiko Miyazaki for giving me help and support in carrying out some analytical investigations of this research.

Table of Contents

List of Figures

List of Tables

CHAPTER 1

INTRODUCTION

Chapter 1 Introduction

Nowadays the scientific communities in the environmental field spend considerable efforts to research nanoparticles and their high reactivities and removal capacities of different severe contaminants. One of the materials that several researchers showed it high level of interest is nano-scale zero-valent iron (nZVI). They conducted numerous researches to study its properties and test its reactivity against a variety of contaminants. This Introduction section discusses the problem of contaminated water, hazardous nature of contaminants investigated in this thesis, common methods used for removal of these pollutants, and background overview on nanotechnology as an evolutionary remediation technology, focusing on nanoparticles (in particular nZVI) and their important applications in general and in environmental remediation in specific. A great concern and focus are given to the nano-scale zero-valent iron throughout the whole section as this chapter will handle information about the general methods of its synthesis, modifications, its practical application in laboratory and on macro scale, and prospects and risks related to its usage in environment.

1.1. Problem statement

Recently, the world attests an increasing demand on water. Globally, the utilization of water supplies is doubled every 15 years. The struggle to afford clean water, and keep up with the rapid growing essential need of it, is a great challenge for human beings. As a result of population growth, human overpopulation, deterioration of water quality and global climate change, the World Health Organization (WHO) declared that over than 40% of the world population competitively utilize scarce water resources. Thus, more than two billion people have no enough pure water access [1]. Specifically, over 780 million people suffer in finding improved drinking water sources [2].

The pollution is spreading side by side with industry. For instance, there are complex and varied mixtures of heavy metal ions, abundant in wastewaters coming from a wide range of industries, such as smelting of metals, manufacturing of metal alloys, electroplating and electronic products [3]. Over one billion cubic meters of such wastewaters are discharged in

China alone each year [4]. Today, Above 140 million people in over 70 countries are under threat of poisoning from arsenic-contaminated water [5]. This is because it occurs naturally in deep levels of ground water, but becomes dangerous when wells are dug too deep and used as a main water supply without proper treatment. In fact, there have been over 20 major incidents reported in Asia, but arsenic-contaminated water has also been found across the United States. As it seems that ground water is no far from the danger of pollution. European Environment Agency has identified an estimated 20,000 polluted sites and another 350,000 potentially contaminated sites required remediation. In USA, the Environmental Protection Agency has recognized between 235,000 and 355,000 sites that need cleanup at an estimated cost of between $174 and 253 billion [6]. These sites were discovered to be contaminated with chlorinated organic compounds, nitro aromatics and others.

Both nitrate and phosphate form nutrient pollution with accompanied health issues and environmental problems. Concentrations of nitrate in rainwater reached 5 mg/L in industrial regions, while the concentration in surface water can exceed normal range (0–18 mg/L) due to agricultural runoff, human or animal wastes and other sources of waste. In Europe, Nitrate concentrations have gradually increased in the last few decades and have sometimes doubled over the past 20 years in many countries. For example, the nitrate concentration experienced average annual increase of 0.7 mg/l in some rivers in the United Kingdom. The natural occurring levels of nitrate and nitrite in groundwater do not exceed 4–9 mg/L and 0.3 mg/L, respectively. However, the nitrate concentration can tremendously increase reaching several hundred milligrams per liter because of agricultural activities, such as the case in groundwater of an agricultural area in India of concentrations up to 1500 mg/L [7]. In USA, nitrate concentration exceeded the guideline value (50 mg NO_3^-/L according to World Health Organization) in 40 surface water and 568 groundwater supplies at the start of the last two decades. The excessive release of nitrogen and phosphorus compounds causes detrimental effects of eutrophication to many lakes and surface waters around the globe. Concerning the environment, Problems, such as the oxygen depletion, biodiversity reduction, lower light transmission and generation of algal blooms, occur when the phosphorus concentration exceeds 0.02 mg/L in lakes at the threshold at which eutrophication starts [8]. Addressing human health, nitrate (NO_3^-) contamination transforms into nitrite (NO_2^-) that increases toxicity level, resulting in blue baby syndrome, liver damage, cancer and so forth

[9]. Hence, both contaminants depict high measures of pollution in water, which should be efficiently and effectively treated.

It becomes a real necessity, due to the enormous pressure and competition on water supply, to remediate unconventional water supplies (e.g., wastewater, contaminated fresh water, sea water, storm water, brackish water and so on). In spite of the critical situation of water management, nanotechnology can present eminent solutions to develop water treatment systems and improve their performance. The devastating need for a versatile material for water treatment directed our research efforts towards nanomaterials, especially nZVI. The implementation of nanomaterials in water purification centers and units is termed by its low reliability on large infrastructures and economic employment of unconventional water sources. This results in expanding the existing water supply and solving a vast of environmental problems that affect directly all living things.

1.2. Background overview

It is a must to overview the background of the contaminants targeted for treatment in this research and moreover the sector of technology attached with the treatment reagent (nZVI).

1.2.1. Major contaminants of eutrophication

Nitrate and phosphate are considered from the major eutrophication causing contaminants in water. Moreover, each one of them expresses more danger and threat to the human and environment.

1.2.1.1. Nitrate

Nitrate is one of the well-known severe contaminants, which is regarded as the main concern in the treatment of groundwater and surface water. Nitrate pollution is considered as a nonpoint source, which results from agriculture runoff, nitrogenous fertilizers, animal manure, industrial and domestic wastewaters, septic systems waste, etc. This pollution has a great influence on the wells in the rural area in which shallow ground water exists, and residents mainly depend on them for drinking water purpose. In most cases, when nitrate (NO_3^-) is reduced to nitrite (NO_2^-), toxicity increases significantly, and the latter causes methemoglobinemia, which is formed because of combining nitrite with blood hemoglobin.

This methemoglobinemia leads to blue-tinged blood for babies, especially under six-month-old [10]. Furthermore, the human being is subjected to several diseases, such as cancer, liver damage and so forth, as a result of excessive release of nitrogen compounds and its consequences of eutrophication and drinking water pollution [9]. Thus, For prevention purpose, several entities and agencies, such as WHO (World Health Organization) and US-EPA (Environmental Protection Agency), have assigned the maximum contaminant level (MCL) for nitrate at 50 mg/L (NO_3^-) [7] and 10 mg/L (NO_3^--N, measured as nitrogen) [11], respectively. The environmental quality standards for human health in Japan have set the limit of nitrate and nitrite contamination in water to 10 mg/L (N) [12].

Several technologies were suggested and employed to remove nitrate from water. Decontamination of nitrate can be carried out using biological or physicochemical processes such as adsorption, biological denitrification, reverse osmosis, ion exchange and chemical reduction [10, 13-21]. However, these methods suffer some drawbacks. For example, adsorption process has some problems as it has strong pH and temperature dependency, and the spent adsorbent is difficult to dispose. Ion exchange and reverse osmosis require frequent regeneration of the media, and they generate secondary brine waste streams, that is why ion exchange and reverse osmosis are accounted as relatively expensive processes. Although biological denitrification is the most widely used method for drinking water treatment and can convert nitrate to nitrogen, it is incomplete and insufficient in contaminant removal, and slow. In addition, biological denitrification generates excessive biomass and soluble microbial products in which further treatment should address them. Concerning chemical reduction methods, they show fast kinetic rates and high removal efficiency. Moreover, chemical reduction methods transform into non-toxic or less toxic species depending on reaction conditions. Therefore, nanomaterials, owing to their high reactivities, could offer the best performance for the chemical reduction technique.

1.2.1.2. Phosphate

Discharges of wastewater, agricultural areas runoff and landfill leachate into the water bodies are the most common pollution source of chemical compounds and constitutes the main risk for reduced water quality [22-24]. One of these pollutants is phosphorus (P), originates from different sources such as fertilizers and animal feed run-off (from agriculture wastewater

[25]), detergents (from industrial wastewater [26]), and sewage water [27]. It can be found in water with forms of orthophosphates, polyphosphates, and organic phosphates [28, 29]. High level of phosphorus concentration (at phosphate concentrations > 0.1 mg/L [30]) in water bodies is known to cause massive algae bloom and eutrophication [31]. Eutrophication results in the depletion of oxygen that leads to fish death and effects on aquatic environment. On the other hand, phosphorus is an essential nutrient for all forms of life and cannot be replaced by other species. Phosphorus is mostly obtained from mined rock phosphate, and existing rock phosphate reserves could be exhausted in next 50 – 100 years [32, 33].

In order to reduce the negative effects of overloading the ecosystems with phosphorus and recover it for reuse as fertilizers [29], it is necessary to investigate various techniques and materials for removing and recovering phosphorus from wastewater effluents. These techniques are the chemical precipitation and adsorption with metal salts (of iron, alum, magnesium or lime), EBPR (Enhanced Biological Phosphorus Removal), crystallization and constructed wetlands (by action of plants) [34, 35]. Because of mud problem of precipitation [36], inefficiency and high cost of reverse osmosis [37] and drop in performance (at low P concentrations) of biological methods, the adsorption with chemical precipitation technique stands as a prominent and promising method among all other methods, and it is considered as the main commercial process. As mentioned, the important matter is not only eliminating the phosphorus, but also recovering and recycling it. This will benefit industry and society as phosphorus is used in producing fertilizers. All tertiary wastewater facilities remove phosphorus by chemical or biological method as a non-recyclable material (as metal-phosphate precipitates or precipitates together with numerous other waste materials as sludge). If nanomaterials could solve this focal recovery issue along with high performance in elimination of phosphorus and with low treatment cost, that would lead to the application of this new emerging technology for water treatment replacing (or placing aside to) the common ones. In addition, if this nanomaterial is versatile enough to eliminate nitrate that usually presents side by side with phosphorus, it will be a great triumph for treatment.

1.2.2. Nanotechnology

"There's Plenty of Room at the Bottom"! This is how nanotechnology started to be recognized in the modern era when the physicist Richard Feynman, a Nobel laureate, gave a

talk with that title on December 29, 1959 at a meeting of an American Physical Society at the California Institute of Technology (CalTech) [38]. Richard Feynman (Fig. 1-1a [39]) showed a technique by which engineers and scientists would have the ability to control individual molecules and atoms. Via this way, he introduced the concept related to nanotechnology. Not long enough until Professor Norio Taniguchi (Fig. 1-1b [40]) introduced the new term "nanotechnology" at the University of Tokyo in 1974. After that, in 1986, professor K. Eric Drexler continued to use the "nanotechnology" term in his book entitled "Engines of Creation: The Coming Era of Nanotechnology" [41] in which he showed that the nanoparticle is an assembler that can be controlled to build a structure of itself and other copies.   However, the technology itself was used by the people of the pre-modern era. For example, during the medieval period, in the 17th century, the Middle-eastern Arab faced the crusaders with a very special and extraordinary strong type of swords known as "Damascus blades" (Fig. 1-1c [42]). The secret of their strength was uncovered to reveal the nanotechnology employed by the ancient blacksmiths to the steel of blades [43]. They implemented nanotech manufacturing of the steel blade using carbon nanotubes and iron, proving that people of the old ages were inadvertently (or might be intentionally) applying nanotechnology in their lives.

Nanotechnology is the process of manipulating material on the level of nano-scale, ranging from size of 1 to 100 nm (nanometers). Through this definition, the nanotechnology includes a wide and broad range of applications in number of fields such as molecular engineering, organic chemistry, microfabrication, environmental engineering, catalysis, molecular biology, surface science, etc.

(a)   (b)   (c)
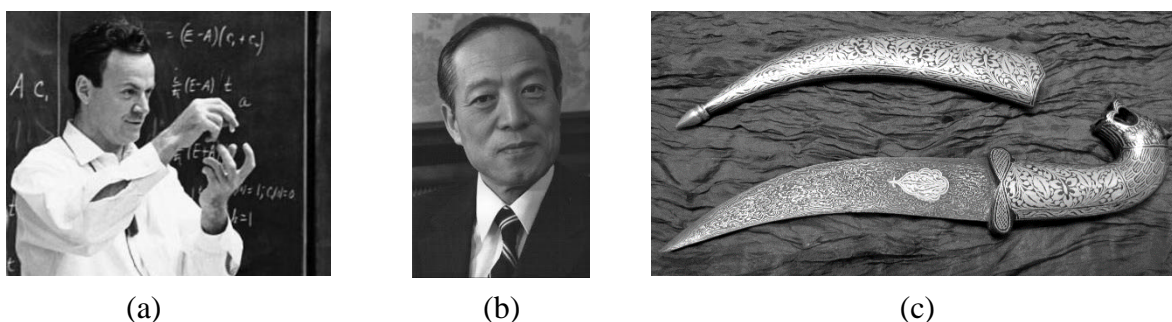
Fig. 1-1. a) Physicist Richard Feynman, (b) Professor Norio Taniguchi and (c) the Damascus blade used by Saladin's troops in the medieval era.

Promoting the Reactivity of nZVI for Water Treatment

The nano-scale is one of different scales that describes the matter in its tiny size form distinguishing it from the micro-scale, macro-scale and so on. The limitations of this nano-scale is between 1 to 100 nm. One nanometer is equal to the one billionth of a unit meter (i.e., 1 nm = 10^{-9} m). To add a good description and illustrate more, if the nanometer size is compared to the size of a meter, it resembles the size of a marble to that of the earth [44]. Another interesting facts that the average size of bacteria is 1000 nm, and the smallest of these, Genus Mycoplasma (a kind of bacterica), has a length of about 200 nm while the size of virus is around 100 nm (the upper size limit of nanomaterials). The DNA double-helix is around 10 nm in length and 2 nm in diameter. The glucose molecule occupies a space of 1 nm (the lower size limit of nanomaterials). However, the water molecule size is 10^{-1} nm (i.e., 1 A^{o}), so nanotechnology works very close to the molecular scale.

Nanomaterials are known for their unique magnetic, optical, electrical and thermal properties connected to their nanoscale size that can make these materials appropriate for different applications in which they compete with other materials [45]. For example, nanotubes are used to store the solar energy; electricity is generated from nano-structural oscillations using piezoelectric-crystals; nanomembranes are applied for water purification; self-cleaning (self-sanitizing) tissues work by exposure to sunlight; and nanowire bacteria remediate the sites polluted by radioactive uranium.

These nanomaterials are synthesized based on two types of approaches, the bottom-up approach and top-down approach. The bottom-up approach comprises the construction of organic and inorganic assemblies or structures through the arrangements of molecule-by-molecule or atom-by-atom, this is denoted as molecular nanotechnology. For instance, the bottom-up approach involves chemical reaction processes such as chemical emulsion reactions, chemical vapor deposition, electrochemical method, liquid quenching, etc. On contrary, the second approach denominates as top-down approach which is firmly connected to size reduction of bulk materials to nano-scale dimensions. These conventional blocks of materials are broken down at nanometric levels into nanoparticles by the means of etching techniques and mechanical attrition , such as solid-state silicon methods for microprocessors fabrication, high energy ball milling for nanoparticles production and so forth [46].

The applicability of nanotechnology is rapidly evolving in this current 21st century, and it is expected to dominate the era along with the information technology and

biotechnology, so as to be designated as the engines of technological development and innovation of this age. The applications of nanotechnology are so far abundant and diverse in varieties of fields. Nano materials, nano sensing, nano-molecule simulation and nano characterization are four basic aspects of future progression in nanotechnology field. The application of this technology cover wide range of sectors including medical treatment, biology, energy resource, electronics, aviation and military. Nanotechnology contriputed to improving petroleum exploration technology which advances it in the effective evalution of the oil reservoir space by nano fine characterization technology, monitor of characteristic parameters of petroleum reservoir by nano sensing, efficacious support for enhanced recovery and well drilling using suitable nanomaterials, and accurate determination of adsorption and desorption mechanisms of oil and gas and their migration laws in non-Darcy model by nano-molecule simulation [47]. For instance, reservoir nano-robots are injected into oil reservoirs providing real-time recording, storage of data (e.g., reservoir pressure and temperature, fluid type and viscosity, pore morphology, etc.) and then data transfer to the receivers. A promising technology like this obtains the spatial resolution of reservoir higher than that acquired by logging, seismic and 3D core scanning analysis. Similarly, other kinds of nano devices can be an effective cure for the medical treatment of cancer. Nanovectors are solid or hollow structures of size range 1–1,000 nm designed for the targeted delivery of detection agents and anticancer drugs to the defected cells [48]. Definitely, the applications of nanotechnology are many and increasing in numbers accompanied by several advancements and breakthroughs, and the current study focuses mainly on the applications of nanotechnology in water treatment and in particular nano-scale zero-valent.

1.2.3. Nanotechnology for water treatment

In general, nanotechnology can take different forms for application in water remediation such as sorption, membrane process, photocatalysis, disinfection and microbial control, and sensing and monitoring [49].

Nanomaterials exhibit sorption property as a useful tool to treat contaminated water through physical and chemical process by absorption, adsorption and ion exchange [50]. Adsorbents, in particular, act as polishers to eliminate inorganic and organic compounds from water and wastewater. Extreme high specific surface areas, tunable surface chemistry, short

intraparticle diffusion distance and controllable pore size are essential properties of nanomaterials that make them eligible to improve water treatment processes. The purpose of treatment focused mainly in removing heavy metals and organic and inorganic chemicals. The most common nanomaterial classifications are carbon-based nano-adsorbents, metal-based nano-adsorbents and polymeric nano-adsorbents. Carbon nanotubes (CNTs) and their oxidized forms have proven their higher efficiency than activated carbon in removing organic and heavy metals, respectively, then reused in 10 regeneration and reuse cycles with relative stability in the metal adsorption capacity [51]. Despite their hydrophobic graphitic surface that results in bundles formation and surface area reduction, they can adsorb polar organic compounds via various contaminant-CNT interactions such as π-π interactions, covalent bonding, hydrogen bonding, electrostatic interactions and hydrophobic effect. Therefore, CNTs are valid for adsorption of recalcitrant contaminants and contaminant preconcentration of organic compounds and heavy metals [51, 52].

Regarding metal-based nano-adsorbents, metal and metal oxides nanoparticles are efficient adsorbents for heavy metals and radionuclides [53]. Adsorption of these types are a strong function in specific surface area (SSA). Increasing specific surface area has a direct effect with increasing the adsorption capacity of metal ions and speeding up their kinetics. For instance, by reduction of particle size of magnetite (Fe_3O_4) from 300 to 11 nm, subsequently specific surface area normalized adsorption capacity increased, consequently its arsenic (As) adsorption capacity expanded more than 100 times [54]. This behavior is known as the "nano-scale effect" which appears in case of particle size below 20 nm and results in the formation of new vacancies and adsorption sites. Also this effect has a large impact on the magnetism of some iron oxides magnetic nanoparticles, e.g., nano-magnetite and nano-maghemite ($\gamma–Fe_2O_3$). The magnetic nanoparticles on size reduction become superparamagnetic which can easily be attracted to a low-gradient magnetic field. Overall, metal-based nano-adsorbents are cost-effective reagents characterized by high adsorption capacity, low production cost, easy separation by magnets and efficient regeneration.

Another type of sorbents that are capable of removing both heavy metals and organic compounds is the polymeric nano-adsorbents such as dendrimers. These tailored nanomaterials are composed of a hydrophobic interior shell for adsorption of organics and

hydrophilic polar branches of hydroxyl or amine groups (or etc.) responsible for heavy metals adsorption [55].

Advances in nanotechnology incubated membrane materials and processes. These physical barriers have major challenges related to membrane selectivity versus permeability and high-energy consumption connected to driving pressure and fouling. Functional nanomaterials possess unique properties that when incorporating into membranes, they improve permeability, mechanical and thermal stability, fouling resistance and new functions as contaminant degradation [49]. Nanotechnology served membrane materials/processes and produced modified membranes. For example, nanofiber membranes reject micron-sized particles and can be used as a pretreatment unit [56]. Nanocomposite membranes exploit the doping of hydrophilic metal oxide nanoparticles (e.g., Al_2O_3 [57], TiO_2 [58], and zeolite [59]) to reduce fouling by increasing the membrane hydrophilicity. Thin film nanocomposite (TFN) membranes enhance the membrane permeability by adding nanomaterial dopants such as nano-zeolites [60]. Magnetic nanomaterials, which are easy to separate and reuse, are used in forward osmosis, to recover the draw solute through flocculation [61].

Therefore, nanotechnology can participate greatly in water treatment. In particular, a specific nanomaterial possess the capability to treat a great variety of undesired constituents in water through efficient ways, different mechanisms and high-speed kinetics. It is one of the most extensively researched and applied nanomaterial in the remediation of water and soil. Nano-scale zero-valent iron is the basic material and main pillar of this whole research work.

1.3. Nano-scale zero-valent iron

Nano-scale zero-valent iron is a versatile material for water treatment. It is found in literature expressed with different symbols such as nZVI, NZVI, F, nFe(0) or n-Fe^0, and usually nZVI is used in this work. The following literature explores in brief the most of the aspects and features of nZVI technology for water treatment, focusing on the theory of work, mechanisms of operation, applications and environmental impact, but it is essential to have a quick grasp about zero-valent iron before reviewing nZVI that attracted the research spotlights.

1.3.1. Zero-valent iron

Iron (Fe) is ranked as the fourth abundant element in the earth`s crust (5.63% wt) comes after oxygen (O, 46.1%), silicon (Si, 28.2%) and aluminum (Al, 8.23%) [62]. It is available, cheap, non-toxic, easy to produce and a reactive metal with standard reduction-oxidation potential (E^0=-0.44 V). It appears that ZVI position in the electrochemical series based on the redox potential value permits it to reduce water and the oxidized ions of Cd, Co, Ni, Sn, Pb, H, Cu, Hg, Ag, Cr, Au, Mn and others. The publications on ZVI constitutes around 90% of all publications based on ISI (Institute for Scientific Information) Web of Knowledge data base (academic citation indexing and search service) [1]. ZVI has been applied successfully to remediate wastewater and ground water contaminated with heavy metals (in nano-form) [63-65], arsenic [66, 67], nitroaromatic compounds (NACs) [68, 69], phenol [70, 71], chlorinated organic compounds (COCs) [72], dyes [73] and so forth.

Zero-valent iron (ZVI) material comprises all scales of iron element in its zero-valent state, which includes granular form, micro-scale zero-valent iron (mZVI) and nano-scale type (nZVI). ZVI is general term for iron metals, which (if particles) are composed of iron core and shell cover of two layers (of iron oxide hydroxides), formed due to the strong oxidation tendency of ZVI especially nano-size [74]. Concerning nZVI, it is observed that its publications was around 16% of the whole publications on ZVI [1]. It appears that the size of the zero-valent iron particle is an important factor to determine its efficiency and efficacy in the contaminant removal. It was found that nanoscale zero valent iron (nZVI) is more superior to microscale zero valent iron (mZVI) as it provides larger specific surface area and higher reactivity in the removal of contaminants. With same nZVI and mZVI surface area concentrations used in batch reactors to remove phosphate, efficacy of the nano-ZVI was greater 13.9 times than that of micro-ZVI particles [75], referring to the nano-scale effect discussed previously.

1.3.2. Removal of hazardous contaminants by nZVI from water bodies

Nano-scale zero-valent iron transforms the contaminants from toxic species into non-toxic or less toxic ones. The removal mechanisms are various as they appear in Fig. 1-2. It is clear that any type of these mechanisms (reduction, oxidation, co-precipitation, precipitation and adsorption) can occur simultaneously with others for the same contaminant. Mainly,

adsorption is involved in all treatments and reduction is the most common mechanism (controlling step) for a serious of contaminants such as NACs, COCs, some heavy metals (HMs), nitrate and so forth. The removal mechanism bares the directional transfer of electrons from nZVI to the pollutant. Therefore, it is a common consideration of nZVI to be an electron donor.

Chlorinated organic compounds, include trichloroethylene (TCE), tetrachloroethylene, polychlorinated biphenyls, and numerous organochlorine pesticides such as 1,1,1-trichloro-2,2-bis(4-chlorophenyl) ethane (DDT), are known to be highly toxic to the human health and environment. For instance, this group of compounds is bonded strongly to our body fat and, therefore, accumulates in fatty tissues. In general, ZVI has high affinity to react with a wide range of this kind of chlorinated organic (R) compounds, which can be represented by the following reaction equation (Eq. (1.1)) [76]:

$$R - Cl + 2H^+ + 2e^- \xrightarrow{ZVI\ electron\ donor} R - H + HCl \tag{1.1}$$
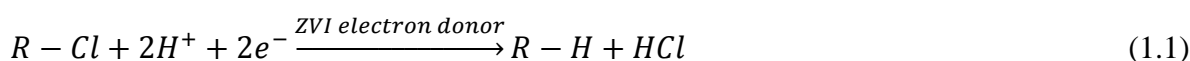
ZVIs was reported to dehalogen/degrade 1,4-chlorinated ethane, TCE, carbon tetrachloride, trichloroethane, vinyl chloride, carbon tetrachloride and γ-hexachlorocyclohexane (lindane) in various reports [1, 77-80]. More than that, nZVI particles are coupled with augmented techniques as microwave irritation and sonication that can enhanced the dehalogenations of COCs [81].
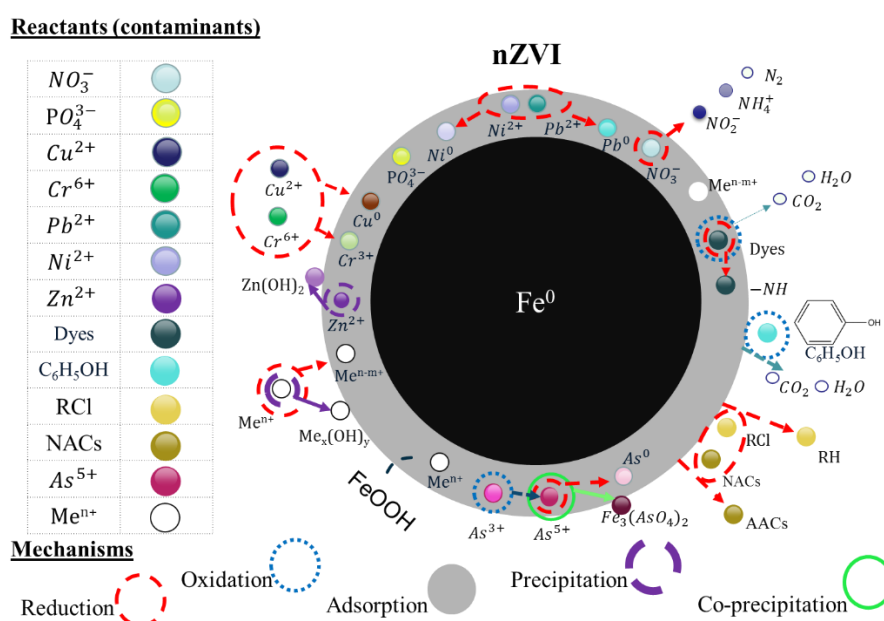
Fig. 1-1. Treatment of several contaminants using nZVI via different mechanisms.

Nitroaromatic compounds, including nitro benzene (NB), 2,4,6-trinitrotoluene (TNT), 2,4-dinitrotoluene, and 2,6-dinitrotoluene, are considered toxic and potential carcinogens at relatively low concentrations. ZVI can reduce nitro groups to produce aromatic amine compounds (AACs). Nitro benzene, for example, can be reduced to form aniline [82], and nZVI degraded the 2,4,6-trinitrotoluene in wastewater with up to 99% yield of amino aromatic product [83]. By the same analogy, Nitrate, one of the basic subjects of this thesis, is reduced in the same manner to form ammonia compounds [84-86]. The details of this process are explored elsewhere in chapter 3.

The nano iron can degrade a serious of organic compounds and oxidize them whenever the dissolved oxygen is present. This type of oxidation is known as Fenton oxidation reaction. The details of the oxidation reaction are provided below.

$$Fe^0 + O_2 + 2H^+ \rightarrow Fe^{2+} + H_2O_2 \tag{1.2}$$

$$Fe^0 + H_2O_2 + 2H^+ \rightarrow Fe^{2+} + 2H_2O \tag{1.3}$$

$$Fe^{2+} + H_2O_2 \rightarrow Fe^{3+} + OH^- + {}^\bullet OH \tag{1.4}$$

ZVI donates two electrons to O_2 in order to produce hydrogen peroxide (H_2O_2, Eq. (1.2)). Again, ZVI continues providing two electron to the produced peroxide to generate water molecule and ferrous ion (Eq. (1.3)). The combination of Fe^{2+} and H_2O_2 is the Fenton reaction (Eq. (1.4)) that produces ferric and hydroxyl ions, and, specifically, hydroxyl radicals (${}^\bullet OH$). These radicals are strong oxidizing agents and vital in degradation of several organic compounds [1, 70]. Integrated reductive nZVI with conventional Fenton-based oxidation (mixture of Fe^{2+} and H_2O_2) gain more power and effectiveness than every single sole process. In addition, Fenton-based oxidation reaction is combined with the basic Fenton oxidation reaction to form advanced Fenton process that can deal with phenol [1] and some types of dyes [79].

Heavy metals are found in the metallurgy, leather tanning, and electroplating industries. The mechanism of heavy metal removal strongly depends on the activity of heavy metal compared to iron. If the heavy metal is more noble (less active) than iron, the dominant mechanism is reduction of heavy metal ions (Cu^{2+}, Cr^{6+}, Ni^{2+}, etc.) to less toxic ions or elements (Cu, Cr^{3+}, Ni, etc.) accompanied with (co)precipitation. Or the heavy metal (e.g., Zn) is more active than iron, which, in that case, sorption and (co)precipitation are the incentive mechanisms [87]. Most studies focused on the removal of Cr(VI) [65, 88]. The

reaction mechanism involves instantaneous adsorption of Cr(VI) on the surface of nZVI, followed by chemical reduction of Cr(VI), and then precipitation of mixed Cr and Fe hydroxides in high pH caused by nZVI dissolution in water.

Arsenic is actually a natural-occurring mineral that is used in lots of everyday items like pesticides and car batteries. Small doses of arsenic can cause jaundice and a skin rash, but if given in a higher dose, a victim will experience intense pain, vomiting and diarrhea. Convulsions and a coma are not far behind, and within just few hours, circulatory failure will ultimately lead to death [5]. Nevertheless, arsenic poisoning does not happen in tales of murder and revenge. It is a threat that pursues humanity through drinking a cup of water contaminated with arsenic. Arsenic exists in two hazardous forms of arsenite (As(III) or As^{3+}) and arsenate (As(V) or As^{5+}). The mechanism of removal by nZVI is complex embracing different processes such as adsorption of arsenic complexes, oxidation of As^{3+} to As^{5+}, reduction to elementary As, surface precipitation, and coprecipitation with various iron corrosion products such as ferrous/ferric (hydr)oxides [89].

Regarding the rest of contaminants, the dominant reaction pathway or removal mechanism can take the form of reduction for some Me^{n+} (metal ions in Fig. 1-2) like for uranium ions as the reduction of U(VI) to U(IV) [90]. Particles of nZVI can also treat them via adsorption along with some other accompanying mechanisms as coprecipitation. More details are found in the next chapters (chapter 3 and 4) about phosphate adsorption.

1.3.3. Synthesis of nZVI

The fabrication techniques of nZVI is no different from complying with the previously recorded approaches used to manufacture nanomaterials, the top-down and bottom-up approaches. Another adopted classification is the physical methods and chemical methods. The physical methods comprise top-down approach methods such as grinding ball milling, lithography, abrasion and dry etching, and bottom-up approaches such as physical vapour deposition, atomic layer deposition, pulsed laser deposition and molecular beam epitaxy. The chemical method can belong to top-down approach like chemical etching, or to bottom-up approach if it is a sol-gel technique, chemical vapour deposition, or spray pyrolysis method [91]. Most of these physical or chemical methods were evolved as attempts to reduce the production costs of synthesis that will reflects on practice and in situ applications.

Promoting the Reactivity of nZVI for Water Treatment

From the methods to obtain nZVI physically, precision milling is a famous and reliable technique that diminishes the size of micro scale iron by grinding with a steel shot (balls) or a jet of flowing fluid in a high-speed rotary mill [92]. The process takes place in a short time, does not involve any toxic reagents compared to chemical methods and has strong eligibility to scale up. It can obtain nZVI sizes of range 10-50 nm with relatively high surface areas in the close proximity of 40 m^2/g. Apart from these qualities, the produced particles display a strong degree of agglomeration, and because of deformation and cracking with steel beads, their shapes are irregular and incoherent.

One of the most common methods to prepare nZVI is the chemical method featuring its deposition from a colloidal solution after chemical reduction of its ferric/ferrous salts by a strong reductant as sodium borohydride (or sodium tetrahydridoborate, $NaBH_4$). This technique is the foundation of synthesis in this dissertation, which is explained in details in the next (second) chapter. Mainly, this method is easy and simple to use in laboratories. But there is a possibility of attachment of some traces of toxic reducing agents after nZVI synthesis, therefore, it is recommended to make proper washing to the end product.

Other chemical preparations via reduction mechanisms, which are less common to use, can be spotted as well such as the reduction of iron (hydr)oxides compounds. For example, nano iron particles are produced by reduction of hematite (α-Fe_2O_3) and goethite (α-FeOOH) in an atmosphere of gaseous reducing agents (e.g., H_2, CO_2, or CO) at elevated temperatures [93]. Similarly, iron salts or oxides are carbo-thermally reduced by the same reducing gases that are produced from thermal decomposition (> 500 ^{o}C) of carbon-based substances (carbon nanoparticles, carbon black, or biochar) presented with the iron compounds as follows:

$$Fe(C_2H_3O_2)_2 + C \rightarrow Fe^0 + 2CH_2CO + CO + H_2O \tag{1.5}$$
$$Fe_3O_4 + 2C \rightarrow 3Fe^0 + 2CO_2 \tag{1.6}$$
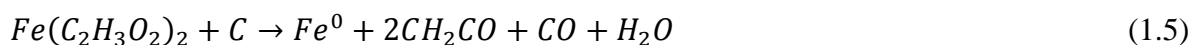
The carbon materials in the previous equations are cheap and available, which make this kind of methods cheap in their capital cost and quite inexpensive as a whole. However, the cost of operation, when applied in a large scale, is questionable. Regarding particle sizes and specific surface area of Fe^0/C produced, they are 20-150 nm in diameter with 130 m^2/g [94].

Some other methods to produce nZVI appeared, which are not common and still under

development, such as ultrasound-assisted method, green synthesis and electrochemical method.

The ultrasound-assisted method is a combination of a physical method, represented by utilization of ultrasound waves, and a chemical method as the borohydride reduction. This method with the ultrasound augmentation was able to produce smaller particle sizes (10 nm rather than 34 nm) and higher specific surface area (34-42 m^2/g) [95].

On another hand, green synthesis is a special kind, different from conventional ways, which involves the biosynthesis of nZVI by reducing iron ions in its solution by polyphenolic plant extracts [96]. This clean and eco-friendly synthesis is inexpensive for no high-energy requirements and scalable with ease, but this method has many drawbacks that requires efforts to deal with: a) there have been insufficient data about the performance of green synthesized nZVI in remediation or its physicochemical properties; b) the strong dependence on the type of plants used lead to various particle sizes of nZVI [80] and low values of surface areas (2.6-5.8 m^2/g) [97]; c) there is incomplete reduction of iron ions to nZVI; and, moreover, d) the destruction of plants occurs. The latter drawback can be partially solved by applying agrowaste such as eucalyptus waste and leaf Extracts from various residues (skin, albedo, flesh) of such fruits as mandarins, lemons, limes or oranges.

In another form, electrochemical synthesis of nZVI engages electrolysis to reduce solution containing ferrous or ferric ions at the cathode [98]. This method encompasses some advantages such as simplicity, fast kinetics, and cheap costs, but the produced particles exhibits high tendency of aggregation, which is only dissembled via ultrasonication using ultrasonic waves (20 kHz) and addition of a cationic surfactant as a stabilizing agent. The cathodic reaction can take the following form:

$$Fe^{3+} + 3e^- + stabilizer \rightarrow nFe^0 \tag{1.7}$$

As predicted, the effect of ultrasonication counteracted the aggregation phenomenon and resulted in forming 1-20 nm nZVI with around 25 m^2/g [80, 99].

1.3.4. Recent advances in nZVI

Unfortunately, nZVI has weaknesses including low stability, high rate of passivation of the material and restricted mobility of its particles. Most of advances and developments in nZVI are to counteract these weaknesses and can be categorized in the following sections.

Promoting the Reactivity of nZVI for Water Treatment

1.3.4.1. Improving reactivity of nZVI

Many attempts were performed to elevate the reactivity of nZVI to an upper level. One of the approved and widely acclaimed methods is the doping of nZVI with other transition noble metals such as silver (Ag), palladium (Pd), platinum (Pt), nickel (Ni), and copper (Cu). It was confirmed that this doping or coating operation enhances reduction process, whether it was reductive dehalogenation, denitrification, or else. The bimetallic materials tool up new features and mechanisms as the hydrogen catalysis speeds up the donation of electrons [1, 80]. The afforded reaction rate value depends on the coating material (with a reactivity order Cu<Pd<Pt). Nanoscale magnetic Pd/Fe particles succeeded in achieving > 99% removal of chlorinated hydrocarbons, such as 2,4-dichlorophenol [100], monochlorobenzene [101] and Pentachlorophenol [102] within few hours. Another bimetallic carboxymethyl cellulose (CMC)-stabilized nFe-Cu was coated with 0.5% metallic Cu/Fe (wt%) and added with a bimetal dose of 1g/L to degrade 88% of 1, 2, 4-trichlorobenzene (25 mg/L) within a day [80].

Much effort has been devoted to incorporate nZVI-carried noble metals into polymeric membranes for reductive degradation of polluting constituents, particularly chlorinated compounds [103, 104] . The reports show that nZVI serve as an electron donor while the noble metals catalyze kinetics of reaction.

1.3.4.2. Improving aqueous mobility of nZVI

In spite of being a very reactive material, nZVI has limited applications compared to mZVI and granular iron powders. The lack of stability, ease of agglomeration, and difficulty in separating tiny particles of nZVI are defects that led to such limitations. To solve these problems, it is preferential to immobilize nZVI particles onto solid porous supports such as activated carbon [105], Multi-walled carbon nanotubes (MWCNTs) [88], ordered mesoporous carbon (OMC) [106], ordered mesoporous silica [107], resin [108, 109], polystyrene resins [84], chitosan [110, 111], pillared clays [112], bentonite [113, 114], kaolinite [115], zeolite [116] and palygorskite [117]. Removal efficiency or adsorption capacity is estimated from batch experiments of known supporting material, contaminant and its initial conc., supported nZVI dose, optimum loading ratio (wt. nZVI/wt. support) and pH of aqueous contaminated solution. The previously mentioned supported nZVI dealt separately with contaminants such as arsenic, Cr(VI), nitrobenzene (NB), nitrate, Pb(II),

Cd(II), acid blue 113 dye, methyl orange dye and methyl blue dye. The supported materials achieved high adsorption capacities (for As^{3+} 121 mg/g and As^{5+} 125 mg/g in case of resin support) or high removal efficiencies (above~90% for the rest of contaminants based on the initial chosen concentrations) in a relatively short time. Supporting nZVI not only provides easy operation, facile mobility and stable slurry, but also it could improve reduction ability of nZVI as seen in the reduction of NB by nZVI/OMC.

Other methods were also applied to increase nZVI stability and mobility [80]. One of these methods is the surface coating of nZVI. However, in this case the coating targets change of surface charge of nZVI particles resulting in the prevention of electrostatic attraction or attaching large polymers to the surface that permits steric hindrance between particles. For this modification, a number of possible materials can be employed to nZVI surface such as polyacrylic acid (PAA), starch, CMC, guar gum and others. Another modification emulsifies nZVI to produce the type water-in oil-in water (W/O/W) or oil-in water (O/W). This technique used in W/O/W benefits from hydrophilicity of oil and separates nZVI particles in large droplets (sizes of 10–20 µm) that covers the surface of nanoparticle by two layers (water and oil) form inside to outside. The other kind of emulsion is O/W, which involves the placement of nZVI in a non-polar oil substance, e.g. soybean oil, which can offer oil droplets at sizes 1–2 µm embedding nZVI particles with high mobility in transportation. Unfortunately, these other methods of modifications like surface coating with stabilizers and emulsification often lead to passivation of nano iron material and lose of its reactivity.

1.3.5. Pricing of nZVI

Economics of nZVI determine on a potent role in the construction of practical applications and treatment facilities that utilizes the nanoparticles in the remediation of water. Therefore, the commercial cost of nZVI is an important aspect for practical applications. Table 1-1 lists some companies that are involved in mass production of nZVI. Actually, they are varying in nZVIs production according to their kind (particle size and specific surface area), their form (powder or suspension), modification type and price of product. The reported values in the following table are related to the powder form containing nanoparticles without applying any type of modification.

Promoting the Reactivity of nZVI for Water Treatment

Table 1-1. Commercially available companies of large-scale nZVI production [80].

Company name	Location	Particle size (nm)	Surface area (m^2/g)	Price ($/kg)
Toda Kogyo Corp.	Japan	70	30	27-35
Nano Iron	Czech Republic	20-100	20-25	129
Polyfon	USA, Florida	100-200	37-58	N.A.
Mknano	Canada	25	N.A.	1440
Sky Spring Nanomaterials, Inc	USA, Houston	20	40-60	3370
		40-60	6-13	2440
		60-80	7	2150
Nanostructured & Amorphous Materials, Inc.	USA, Houston	25	40-60	3300

N.A. – not available

It is observed in the previous table the variation of cost of nZVI. Mainly, this might be attributed to the applied synthesis technology, Fe^0 content (or quality, a very effective factor) and particle dimension. The cheaper value of cost could be an indication of the presence of greater content of iron oxides in nZVI or larger size. In addition, some companies as Nano Iron (Czech Republic) produces suspensions (20% dry mass) of nZVI.

As an example of a production for application, Toda America (owned subsidiary of Toda Kogyo Corporation) manufactures RNIPs (Reactive Nano-scale Iron Particles, Fe^0/Fe_3O_4) that participated in the first field-scale demonstration performed to assess the performance of emulsified nano-scale zero-valent iron (EZVI), which is surfactant-stabilized nZVI with (biodegradable) oil layer in water. EZVI was injected into the saturated in situ reaction zone to enhance dehalogenation of dense, non-aqueous phase liquids (DNAPLs) containing TCE [118].

The total cost of technology in a certain application depends on a serious of factors, which accounts for the difficulty of cost estimations. These factors are product type, amount ordered, transportation cost, additional laboratory and field experiments including geochemical and hydrogeological studies [80].

1.3.6. Potential application of ZVI

Here are some practical applications that nZVI found /can find its way to water treatment.

1.3.6.1. Permeable reactive barriers

One of the most promising and effective remediation technologies for the treatment of contaminated groundwater is the application of permeable reactive barriers (PRBs) filled with reactive material(s). This permeable wall is installed in the subsurface of ground that permits groundwater to pass through it and be treated during this flow, rendering compounds in water of low toxicity [1].

ZVI based permeable reactive barriers started in early 1990s as laboratory-scale PRBs or column studies [119, 120]. Particularly, the first commercial ZVI-PRB was constructed in the U.S. with granular iron metal to treat chlorinated hydrocarbon contamination, such as Trichloroethylene (TCE) and dichloroethylene (cis-DCE) and vinyl chloride (VC), as reported by Warner et al. (2005) after 10 years of operation [121]. Since that time of that successful implementation, more than 200 ZVI-PRBs were introduced at different contaminated sites, which made the U.S. Environmental Protection Agency (EPA) designate the ZVI-PRB as a standard remediation technology in 2002 [122, 123]. This kind of PRBs experienced the groundwater decontamination of COCs [124, 125], HMs [126, 127], arsenic [66] and nitrate (via a combined system of ZVI-PRB and biodegrading PRB [128]).

PRBs utilized nZVI supported on enhanced chitosan beads to remove heavy metals from wastewaters driven out of electroplating industry provided by First Chemical Reagent Manufactory (Tianjin, China) with decontamination rates 89.4%, 98.9%, 94.9% and 99.4% for Cr^{6+}, Cu^{2+}, Cd^{2+} and Pb^{2+}, respectively [111]. The increase in initial concentrations of Cu^{2+}, Cd^{2+} and Pb^{2+} contaminants and pH of media had a paramount effect on the removal rates by decreasing and increasing their values, respectively. On another hand, for Cr^{6+}, both increase in pH and initial concentration reduce removal efficiency. However, unfortunately, the aforementioned PRB was a laboratory-scale setup and not an in situ remediation application, but these kinds of laboratory-scale configuration are successful steps towards a scaled-up in situ process.

1.3.6.2. Pump-and-treat system

Mainly, pump-and-treat technology is functioning by withdrawing contaminated groundwater from subsurface (extraction well) to be pumped to treatment units of operations and chemical/bioremediation, then the treated water is injected again to the subsurface (recharge well) or to the surface lakes or rivers. According to Karn et al. 2009 [129], the predominant technology for addressing groundwater contamination was pump and treat until 1992. Because of its high cost in operation (for about 18 years in average [130]), this pump-and-treat method was replaced by PRB. And the number of public sites in the USA remediated by pump and treat has been reduced to less than 20% in 2005, and it could be expected that these (ex) situ remediation techniques will be phased out over next 20 years [6, 131]. However, pump-and-treat method can still be applied in groundwater remediation for shorter periods (<10 years), and it was effective and efficient recently when acted similar to conventional activated-sludge process in removing heavy metals from industrial wastewaters [87, 132].

1.3.6.3. Injection

The injection technology was developed in order to use nZVI in groundwater treatment as an alternative to the permeable reactive barrier technique using granular iron. It can be classified to: (1) injection of nZVI to form a reactive barrier and a treatment zone around injection wells, (2) injection of mobile nZVI to form a nZVI plume under injection wells, and (3) incorporation of nZVI into ground soil to adsorb or degrade pollutants [133].

There were some restrictions and limitations to widespread deployment of nZVI such as its fast agglomeration and sedimentation in colloidal suspensions, soils and sediments, which result in its limited mobility. This was depicted clearly when injecting nZVI into the groundwater and only 1.5% of it reached the remediation location at depth of 6 m [134] . Improvement strategies of subsurface transport of nZVI were suggested, which include coating with polyelectrolytes, polymers and surfactants or support on a suitable carrier (e.g., silica, carbon black, graphite, carbon mesosphere, and activated carbon). In a field investigation on transport of carbon-supported nano-scale zero-valent iron [135], CIC (Carbo-Iron Colloids) suspended with the polyanionic stabilizer carboxymethyl cellulose was introduced to the injection well at the contaminated site in the city of Leuna,

SaxonyAnhalt, Germany (downstream of Leuna works). The total particle and iron concentrations in samples were detected from the extraction well (5.3 m apart from injection well) indicating the Breakthrough of CIC (received 12% of the total amount Introduced).

As an example of application, ENZVI (E for emulsified) was injected into eight wells using a pressure pulse injection method over a five-day period in a demonstration test area within a larger DNAPL (dehalogenation of dense, non-aqueous phase liquids) source area at NASA's Launch Complex 34 (LC34) at Cape Canaveral Air Force Station, Florida, USA [118]. It was observed significant reductions in TCE soil concentrations (>80%) at four of the six soil sampling locations within 90 days of EZVI injection and significant reductions in TCE groundwater concentrations (57 to 100%) at all depths targeted with EZVI.

1.3.7. The impact of nZVI on living organisms and environment

Despite being applied in environmental remediation, nZVI could pose a considerable threat. Concerning nZVI environmental researches, the reports on its toxicity are relatively scarce. Most of reports focused on nZVI effects on microorganisms as Escherichia (E.) coli [136, 137] and on crustaceans, arthropods, annelids, fish larvae [138], plants [139], and infrequently mammalian cells [140]. Reports revealed the effects of nZVI including: a) enclosing nanoparticles to the cell membranes of bacteria followed by adsorption of nZVI, then penetration of these particles through these membranes, b) blockage of cellular ducts leading to structural changes in the membrane, or mobility and nutrient intake inhibition (leading to the death of bacteria), and c) formation of reactive oxygen species (ROS) as a result of iron oxidation (Eqs. (1.2) to (1.4)) [80], which may cause peroxidation of lipids and severe damage to DNA.

There are also some considerable points extracted from the literature about the degree of sensitivity of living things to nZVI [80]. Initially, the toxicity of nZVI towards microorganisms was focused mainly around E. Coli bacteria (sensitive to nZVI and Fe^{2+}), while Pseudomonas fluorescens, Bacillus subtilis, or Staphylococcus aureus shared lower sensitivity along with absence of negative effects on Vibrio fischeri and Psychrophilic bacteria, confirming the strong relation between the strain type and bactericidal sensitivity. For aquatic and soil organisms, Heterocypris incongruens in both aquatic and soil organisms has high sensitivity to CMC-nZVI, and larvae of Oryzias latipes was influenced by the toxic

effect of CMC-nZVI and oxidation products. CMC-nZVI and nZVI defected some earthworms (Eisenia fetida) and affected their reproduction, body mass and mortality at elevated concentrations above above 100 mg Fe/kg of soil. Some researchers explained that high toxicity of nZVI resulted from limited availability of oxygen due to its usage in the processes of its oxidation, and ROS (resulted from the oxidation of CMC–nZVI) affected the reproduction and mortality of soil organisms Folsomia candida.

Regarding plants, animals and humans, inhibiting effect of nZVI on the germination and growth could occur to some kinds of plants (Linum usitatissimum, Lolium perenne, Hordeum vulgare) with direct deposition and accumulation of nZVI particles on root surface, which led to the blocking of water and nutrient uptake by plant roots. The low solubility of nZVI allows its persistence in biological systems causing long-term effects (a mutagenic effect on organisms). In addition, boron (From nZVI synthesis) negatively affects the plant. So washing out BH_4^+ with water after nZVI synthesis can eliminate the boron contamination. But in some cases, nZVI (at low concentrations) stimulates the growth of Typha latifolia. In case of mammalian cells, iron again causes oxidative stress via redox cycling and ROS generation, resulting in lipid peroxidation and DNA damage. For animal, neurotoxic effects in rodent's neuron microglia was found. In case of man, nano iron dissolved in physiological saline caused human bronchial epithelium cells (responsible for the lubrication of the lungs and others) to die.

In order to control the impact on environment and reduce toxicity, coating nZVI with polymer-based materials and surfactants may reduce toxicity towards bacteria [141]. nZVI with a biodegradable polyaspartate coating increased bacterial populations by an order of magnitude relative to controls [142]. It causes stimulation growth of Gram (+) bacteria in soils. Moreover, enhanced microbial denitrification in the presence of nZVI occurred [143]. Toxicity of nZVI is reduced via coating with polyasparaginate, which limits direct contact of nanoparticles with cells [144]. It can be stated that a careful choice of nZVI concentrations (dose) and applying a suitable modification and method of synthesis minimize the toxic effects and remediate the environment.

1.4. Research objectives

The main objective of the purposed thesis is to promote the reactivity of nZVI that includes improvements in removal performance efficiency and kinetics. Dealing with numerous contaminants in water treatment to achieve this objective is beneficial and raises the confirmation level of enhancement in nZVI reactivity, but it is a time-consuming process, especially when you have a very restricted and limited time to finish the research work alongside with obtaining representative results and convincing conclusions. Based on this fact, this research decided on reaching its goals by the following strategy. Firstly, it has been planned to work on promoting the reactivity of nZVI concerning two major mechanisms, which are very common to take place for a whopping number of contaminants existing in water bodies (ground waters, surface waters, unconventional waters, etc.), and these mechanisms are chemical reduction and adsorption. Secondly, nitrate and phosphate were chosen for this study to represent these mechanisms, respectively. They are easy to prepare, handle, measure their concentrations and dispose. Technically, the rest of other non-dominant mechanisms like (co)precipitation, or simultaneous occurrence of adsorption and reduction, probably happens beside these types of processes. The improvement is expected to influence all mechanisms, especially the dominant remediation mechanisms. Thirdly, the promoting techniques of reactivity were suggested to follow the path of outcomes of literature survey, regarding bimetallic nZVI and supported nZVI on carriers as areas of interest. Until this point, the contribution of this work is ambiguous. Fourthly, the novelty of the thesis work, which is widely accepted as publications by esteemed journals [145-148], is about the technique of employing the modification on nZVI, methodology of work, analysis of data and providing solid evidences to back up hypotheses. Based on that, conclusive outputs are reached and the linkage of several research works of this dissertation is strengthened with a reasonable logic order. Here are the major objectives of this research covered in next points:

- Synthesize bare nZVI particles, fully characterize the synthesized particles, test the performance in nitrate and phosphate removal batch experiments under different conditions, scrutinize the mechanisms of removal by nZVI and provide the datum line of this work.

- Modify nZVI performance by addition of another contaminant during remediation processes, which can lead to simultaneous removal of coexisting contaminants, and obtain best conditions of promoting the reactivity of nZVI.

- Synthesize a novel composite of supported nZVI at optimum conditions of treatment and redo the same procedure performed on nZVI in order to compare performance.

- Investigate the degree of interference of common ions and organic matter with contaminants removal performance of nZVI-based reagents.

- Provide models of reaction kinetics of removal for most tested batch experiments by nZVI-based reagents.

- Regenerate the spent of nZVI and recycle.

- Apply nZVI-based reagent in a laboratory-scale application to evaluate performance and list pros and cons of this implementation for further amendments of design and operation in case of scale up.

- Report and publish the work to the scientific community to provide information, conclusions, recommendations and awareness, and receive feedbacks.

1.5. Dissertation framework

This dissertation has a framework composed of seven chapters that explains the way of promoting the reactivity of nZVI particles towards a suggested composite, backed up with a scientific background and theory related to nZVI, synthesis, characterizations, analyses, batch experiments, mechanisms, modeling, interference studies, recovery and regeneration, and practical application. Hence, the framework was organized as follows:

Chapter 1 gives information about the current situation of water pollution problems, the nature of contaminants investigated in this research, informative overview that encompasses nanotechnology in general and specifically in water treatment, and the role of nZVI in decontaminating a wide range of pollutants. The literature survey on nZVI covers most of its aspects especially synthesis techniques, modifications, treatment implementation and its environmental impact. Then the chapter identifies the goals of this research.

Chapter 2 presents the common materials and procedures performed prior and post conducting batch experiments of this research involving chemicals preparation, synthesizing method of pristine nZVI, characterization of properties of produced nanomaterials and

analytical inspections. Other non-common chemicals and steps are covered later in other chapters when needed.

Chapter 3 introduces the first suggested modification employed to nZVI surface during the remediation of eutrophication causing contaminants, nitrate and phosphorus, separately. The applied technique is a special one involving the addition of a certain contaminant of copper salt, which causes coating of nZVI surface rapidly throughout treatment. Batch experiments were carried out in different scenarios (conditions of pH, dissolved oxygen, higher contaminants concentrations and addition ratios of copper ions). The mechanisms of nitrate and phosphorus removal in addition to the promotion of nZVI reactivities were deeply discussed and explained. Kinetic models were proposed to describe reaction rates. This chapter also provides a technique for the recovery of phosphorus contaminant.

Chapter 4 suggests another modification that can increase both reactivity and mobility of nZVI particles. Different composites are produced of activated carbon supported nZVI under different synthesis and treatment conditions. The chapter shows the way of selecting the optimized composite from batch experimental studies against aqueous solutions of nitrate, phosphate and mixture of these contaminants, then discovers its properties and tests its performance in interference studies comprising organic matters and group of common ions at different compositions. The results of these tests are explained, compared to that of nZVI, plotted in well-fitted kinetic models that takes into account the passivation of nZVI due to interferences.

Chapter 5 presents the essential steps of handling a material used in a remediation process, the regeneration and recycle. The chapter manages to compare between different types of nZVIs. It shows the lack of stability of nZVI particles upon ordinary storage represented in an aged old-purchased nZVI, the effect of controlled acid treatment on this aged type of nZVI, and the potent influence of the regeneration process on a spent nZVI extracted from nitrate batch experiments with fresh prepared type. This presentation is demonstrated by methods of characterizations and batch experiments to compare performances of removal.

Chapter 6 displays the method of developing the application of nZVI reagent in a laboratory-scale continuous-flow system. It describes the importance of this procedure before

application on a large scale as it depicts the contemporary issues related to the remediation of a certain contaminant (nitrate) by a specific nZVI reagent in a type of design at certain operational conditions. Process and equipment designs are illustrated and performances are reported.

Finally, Chapter 7 lists the major findings included in this thesis and the anticipated future work. One of recommendations is suggested based on these findings that the combination of both modifications of copper salt addition and supporting nZVI on heat-modified activated carbon at optimum loading ratios and treatment condition (obtained from numerous investigations) forms a promising material that suits groundwater and wastewater treatment systems.

MATERIALS AND GENERAL PROCEDURES IN RESEARCH WORKS

Chapter 2 Materials and General Procedures in Research Works

This Chapter presents the common materials and procedures performed prior and post conducting batch experiments of this research involving chemicals preparation, synthesizing method of pristine nZVI, characterization of properties of produced nanomaterials and analytical inspections. Other non-common chemicals and steps are covered later in other chapters when needed.

2.1. Chemicals

Ferric chloride hexahydrate ($FeCl_3.6H_2O$, >99.0%, Junsei Chemical Co., Japan), sodium borohydride ($NaBH_4$, >98.0%, Sigma-Aldrich Inc., USA) and ethanol (C_2H_5OH, 99.5%, Wako Co., Japan) were purchased for nZVI synthesis. Activated carbon norit (steam activation, Sigma-Aldrich Inc., USA) was placed for supporting nZVI. Potassium nitrate (KNO_3, >99.0%, Wako Co., Japan) and potassium dihydrogen phosphate (KH_2PO_4, 99.5%, Kanto Chemical Co., Japan), were used to prepare reactant stock solutions, while pH buffer solution (Sansyo Co., Japan), hydrochloric acid (HCl, 35–37%, Wako Co., Japan) and sodium hydroxide (NaOH , 97%, Wako Co., Japan) were used for pH adjustments. Anhydrous copper (II) chloride ($CuCl_2$, 99.9%, Sigma-Aldrich Inc., USA) was added with specific amounts in the investigated modifying nZVI batch experiments. Sulfuric acid (H_2SO_4, Wako Co., Japan) and nitric acid (HNO_3, Wako Co., Japan) were used in washing and treatment processes of activated carbon or charcoal. Also anhydrous copper II chloride, cuprous chloride (CuCl, 99.0%, Junsei Chemical Co., Japan), lime stone ($CaCO_3$, 70%, Tawarayakobo Co., Japan), humic acid (Sigma-Aldrich Inc., USA) and sodium sulfate decahydrate ($NaSO_4.10H_2O$, 98%, Junsei Chemical Co., Japan) were utilized to produce common ions and organic matters in solutions to conduct interference studies. Domestic wastewater was brought from the screening chamber at Mikasagawa purification center, Hakata ward, Fukuoka prefecture, Japan. All solutions were prepared using deionized water

after deoxygenating by purging with nitrogen gas for 20 minutes. All chemicals were of analytical grade purity and were used as received without further purification.

2.2. Synthesis of bare nZVI

The bare nZVI was synthesized according to the bottom-up approach by the means of chemical reduction reaction described as follows.

$$4Fe^{3+} + 3BH_4^- + 9H_2O \rightarrow 4Fe^0 + 3H_2BO_3^- + 12H^+ + 6H_2 \qquad (2.1)$$
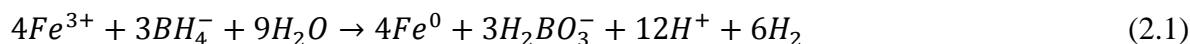
In this research work, the synthesis conditions were selected based on different optimizations of a previous research report [149]. Sodium borohydride (1.1472 M) was pumped into hydrated ferric chloride (0.1434 M) using a roller pump at a rate of 1 L/h with a volumetric ratio of 1:1 in 500 mL four-neck glass flask. Anaerobic condition was maintained by blowing a continuous flow of nitrogen gas. The synthesis mixture was stirred at 250 rpm, kept at 25 ± 1.5 °C in a water bath, and left 20 minutes for aging to complete the reaction. After completion of the chemical reduction process, the jet-black iron nanoparticles were rinsed with deoxygenized deionized water (DDW >100 ml/g) and anhydrous absolute ethanol three times each. The slurry was finally vacuum-filtered and anaerobically dried, then applied immediately in batch experiments. Fig. 2-1 summarizes the main stage of synthesis process and clearly depicts the configuration used in the production of nZVI (or nFe(0)).
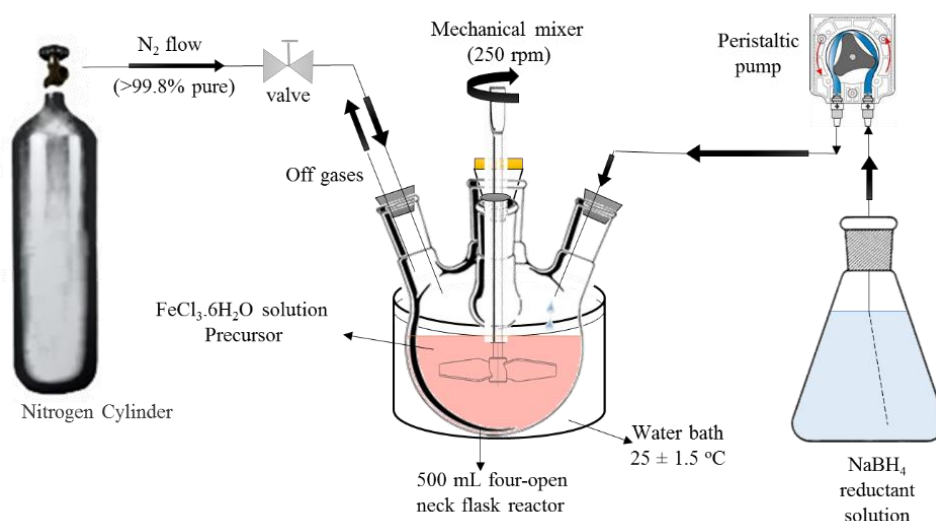
Fig. 2-1. The configuration of nZVI synthesis process.

2.3. Analytical investigations

The analyses are classified into two main types, analysis of material properties and quantitative analysis of contaminants found in aqueous solutions.

2.3.1. Material characterization

Nanoparticles of nZVI and their based derivative materials (fresh or spent state) were characterized to determine their physicochemical properties via transmission electron microscopy (TEM), laser-scattering particle size analyzer, X-ray diffraction (XRD) and surface characterization analyzer.

Surface morphologies of nano iron materials were recognized with TEM (JEM-ARM 200F, JEOL Co., Japan). The synthesized iron reagents were dispersed in ethanol with ultrasonication from which droplets of diluted suspensions were placed onto 300-mesh copper TEM support grids with carbon films and left to dry by volatilization of solvent prior to analysis. Another copper TEM support was used as a cover to prevent the loss of nZVI in the electromagnetic atmosphere inside TEM apparatus. Then samples for TEM analysis were observed at operating acceleration voltages of 200 kV.

Brunauer–Emmett–Teller specific surface area (BET SSA) of nanoparticles was gauged using a 3Flex surface characterization, Micromeritics, USA. For BET SSA analysis, the sample tubes were initially rinsed then dried at 110 $^{\circ}$C under vacuum for 1 h using VacPrep 061 degasser (Micromeritics, USA), followed by degassing of the samples placed in these tubes at 350 $^{\circ}$C for 2 h, and then the degassed solids were subjected to the nitrogen flow at 77 K. Dimensions of micropore volumes of nanoparticles were acquired in this test, whereas the aggregate particle size was determined by laser diffraction particle size analyzer (SALD-2300, Shimadzu Co., Japan).

Mineral compositions and crystallinity of iron products were analyzed using XRD (TTR, Rigaku, Tokyo, Japan) with Cu K$_{\alpha}$ radiation ($\lambda = 1.5418$ Å) emitted from Cu X-ray source operated at 200 mA and 40 kV at a continuous scanning range from 3° to 90° (2θ) with a scan rate of 2° (2θ) min^{-1}.

2.3.2. Spectrometric analyses

Quantitative analysis of investigated contaminants was acquired by following the procedures described in Hach methods [150] and standard methods for the examination of water and wastewater [151, 152].

Concentrations of nitrogen components in solution samples were colorimetrically determined by using an UV–Vis spectrophotometer (DR 3900, Hach Co., USA) in which nitrate, nitrite and ammonia were analyzed using dimethylphenol method at 345 nm, USEPA diazotization method at 515 nm and salicylate method at 690 nm, respectively. In addition, nitrate and nitrite concentrations were also inspected using autoanalyzer (SwAAn, BLTEC, Japan).

Concentration of phosphate (in terms of phosphorus) was obtained via USEPA PhosVer 3 (Ascorbic acid method) at 880 nm. Ferrous and total iron concentrations were obtained using 1,10-phenanthroline method at 510 nm and TPTZ method (2,4,6-tri(2-pyridinyl)-1,3,5-triazine) at 590 nm, respectively.

Finally, in order to continue further checking on the quality of the treated water, copper content was inspected using Bathocuproine method at 478 nm.

MODIFYING NZVI BY COPPER SALT ADDITION

Chapter 3 Modifying nZVI by Copper Salt Addition

This chapter introduces the first suggested modification employed to nZVI surface during the remediation of eutrophication causing contaminants, nitrate and phosphorus, separately. The applied technique is a special one involving the addition of a certain contaminant of copper salt, which causes coating of nZVI surface rapidly throughout treatment. In the following introduction section, the chapter presents a literature survey on nitrate and phosphorus removal performances by (n)ZVI and possible modifications used to enhance them, followed by the objectives of this study conducted in this chapter.

3.1. Introduction

There is an increasing interest on using zero valent iron (ZVI) for the removal of nitrate from groundwater and wastewater. During the last two decades, numerous researches were carried out on chemical reduction of nitrate by zero valent iron [85, 153-156]. The first use of zero valent iron, for treatment of nitrate pollution in a controlled laboratory experiment, was studied by Young et al. [157] who used Fe^0 to remove nitrate via reduction process. Then, during the last two decades, numerous researches were carried out on chemical reduction of nitrate by zero valent iron [13, 85, 153-156, 158]. Reports have shown the reaction pathways of nitrate reduction by ZVI [13, 155, 159-161]. Iron reduces nitrate to ammonia, nitrite and nitrogen with relative amounts according to the reaction conditions. The nanoscale (n) ZVI has proven its high efficacy and efficiency in nitrate reduction from wastewater in several reports [85, 154, 155]. Thus, nZVI is considered reliable to employ in wastewater treatment systems because of its high cost effectiveness, high reactivity, easy operation and low dosage [162].

The search for methods to improve the removal efficiency of nitrate and its kinetic reduction rate by ZVI is unstoppable. Efforts were made at first to explain the reduction kinetics and mechanism of nitrate by zero valent iron [153, 163]. To increase the denitrification rate of ZVI, Xu et al. [164] added ferrous ions and magnetite with micro size iron powder, which accelerated corrosion rate of iron and acted as good conductors of

electron transfer. In this case, the adsorption of nitrate on the iron surface increased along with a higher conductivity and transfer rate of electrons. Some other researchers were concerned about the effect of pH in promoting or inhibiting the denitrification rate using nZVI, proving that nitrate reduction by nZVI is an acid-driven surface-mediated process [155, 165]. Then, during the last decade, numerous reports focused on three main methods to enhance nitrate reduction efficiency (conversion) and kinetics: using a supported nZVI [112], dispersed nZVI by surfactant [166] and bimetallic nZVI particles [154, 167].

Every one of the above-mentioned methods developed nitrate reduction using roughly similar mechanisms. Carrying zero valent iron particles on an inert supporter accelerates the reduction rate as the supporter adsorbs nitrate, which improves the mass transfer of contaminants to iron surface, and the supporter breaks down the necklace-like structure of nZVI particles which results from agglomeration. Previous reports, using supporters as clinoptilolite [168], pillared clay [112], porous silica [169], and graphite [170] , revealed (in most cases) higher reduction efficiency and improved kinetic rate, and the relative increase in efficiency was about 65 % at low nitrate concentrations under anoxic condition. Particles of nZVI have aggregated structures that can be dispersed in synthesis process by adding surfactants. Surfactants contribute to decreasing the size of iron particles, reducing zeta (ζ) potential for high stable dispersion, shifting isoelectric point to acidic medium, and decreasing sedimentation and agglomeration through steric and electrostatic stabilization. However, the research efforts are low in nitrate reduction and removal from wastewater, and the presence of surfactant sometimes decreased the contamination removal via decreasing contaminant adsorption and blocking active sites (in case of adding polyvinyl alcohol-co-vinyl acetate-co-itaconic acid (PV3A) to treat trichloroethene [166]).

Coating nZVI particles with other metal has proven to improve the kinetics of nitrate reduction and the removal of other contaminants. Through some researches [154, 167, 171-173], which used different types of metals, such as Ag, Cu, Ni, Pd and Pt, to treat nitrate contaminant and others, the results showed higher reactivity of platinum due to fast electrode reaction kinetics with proton (H^+) reduction. Platinum, however, has high cost compared to copper. And, in general, although bimetallic nanoparticles exhibit lower agglomeration and aggregation behavior [174], but they suffer shorter lifetime and possible toxicity, and their

catalytic efficiency decreases with time due to iron hydroxide formation on iron surface which prevents the continuation of nitrate reduction [154].

Recently, contaminant removal was processed in the presence of other contaminants in which ZVI nanoparticles were capable of removing both contaminants with higher rate and efficiency than treating each contaminant solely. Sue et al. (2014) [156] reported removal of cadmium and nitrate simultaneously via nitrate addition/presence. A benefit of high pH value (caused in the course of nitrate reduction) was embraced to increase cadmium hydrolysis and precipitation. In this study of current chapter, the same basic principle could be employed to increase nitrate reduction rate with different mechanisms. When adding an optimized amount of copper salt to nZVI and nitrate suspension mixture (instead of coating nZVI with copper during synthesis), two electrochemical reactions occur one after another, which greatly boost reaction kinetics and removal efficiency. In addition, copper salt addition cures some of the nZVI defects in nitrate reduction reaction, which appear in its dependence on pH and dissolved oxygen.

Regarding phosphorus, recent reports about its adsorption [175] showed that nano-bimetal ferrites could remove phosphorus from water. The results indicated that the maximum phosphorus adsorption capacity was 13.5 mg/g at initial pH 2.64. Another study [75] reported that using nZVI as adsorbent could efficiently increase the maximum phosphorus adsorption capacity to 24.38 mg/g at initial pH 4.0. However, to the best of the author's knowledge, most of studies focused on removal of heavy metals by nZVI and very few of reports investigated on removal of phosphorus by nZVI [75, 176], and, there has been no literature on phosphorus removal by nZVI in the presence of noble metal salt (e.g., copper chloride) till 2016 [146].

Based on previously mentioned, this chapter investigates the effect of adding different amounts of copper chloride ($CuCl_2$) and its impact on nitrate reduction and phosphorus/phosphate removal by nZVI from water without intoxicating it. Furthermore, the other objective of this work is to monitor the influence of this addition on removing high nitrate or phosphorus concentrations by nZVI in presence/addition and absence/without addition of $CuCl_2$ (as the research on high concentrations of nitrate is poor). Additionally, the present research studies the effect of different conditions on nitrate reduction and phosphorus sorption by nZVI with and without copper chloride addition. Batch experiments

were conducted at different nitrate or phosphorus concentrations by adding different amounts of copper chloride to nZVI to investigate the optimal ratio of copper chloride to nZVI, and they were performed under anoxic and aerobic conditions and at different pH values. Also this pH effect on adsorption and the recovery of phosphorus were further investigated. Finally, kinetics of removal were carefully analyzed and studied.

3.2. Experimental setup

3.2.1. Batch experiments concerned with nitrate removal

Batch experiments were conducted to investigate the effect of copper chloride addition and acquire the optimum addition ratio of $CuCl_2$ to nZVI among different values (0, 0.02, 0.05 and 0.25 g salt/g iron). These experiments were anoxically carried out in 500 mL four-neck glass flask using 50 and 100 mg/L of nitrate solution with adding one gram of nZVI plus the corresponding amount of $CuCl_2$. Before adding nZVI sample, nitrate solution was purged with a nitrogen stream for 20 min, and its initial pH was adjusted at 7. The resulting mixture was stirred with a mechanical stirrer at 200 rpm and kept at 25 ± 0.5 ºC using a water bath for 60 min. The anoxic condition was maintained by continuous blowing of nitrogen gas into the reactor. At specific given time intervals, 5 mL of solution sample was withdrawn and filtered through a 0.22 μm membrane for the analysis of nitrate, nitrite, ammonium, ferrous, total iron and total nitrogen. The off-gas was absorbed in 100 mL acidic solution for analysis of ammonia gas. The general schematic installation is shown in Fig. 3-1.
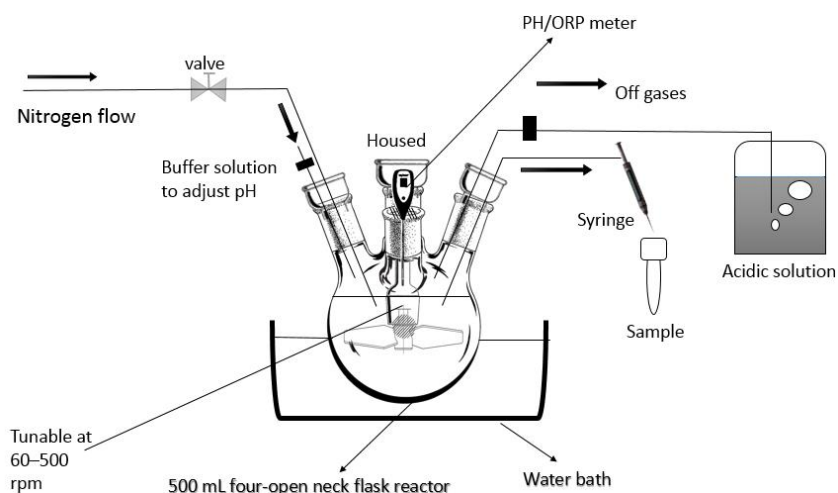
Fig. 3-1. General schematic installation of batch experiment of nitrate removal.

In order to study the effect of different parameters as pH and dissolved oxygen, the same experimental setup was used with only changing the variable parameter. Batch experiments were carried out under anoxic condition at different initial pH, acidic (pH 1.5), neutral (pH 7) and alkaline (pH 9) solutions, without pH control. These experiments were performed on 100 mg/L nitrate solution using one gram of iron with and without optimum amount of CuCl$_2$ (best ratio CuCl$_2$/nZVI). Other batch experiments were made under anoxic and aerobic conditions in 100 mg/L nitrate solution (initial pH 7) using one gram of iron with and without optimum amount of CuCl$_2$. Concerning the effect of chloride ions, its evaluation was discarded in this study.

Nitrate reduction at different nitrate concentrations (50, 100, 200, 300 and 500 mg/L) was demonstrated using the same batch installation under anoxic condition in neutral medium. The optimum amount of CuCl$_2$ was introduced along with one gram of iron in this set of batch experiments.

To test the reproducibility of results, batch experiments were replicated for at least two times. Average values were used in the representation of graphs and tables, and deviations were negligible.

3.2.2. Batch experiments investigated phosphate removal

Several batch experiments were executed to study adsorption of phosphorus and pursue kinetics of phosphorus removal on nZVI with or without addition of anhydrous copper chloride. 250 mg of nZVI were introduced to 300 mL conical flask filled with 250 mL of phosphorus solution (50 mg PO_4^{3-}-P/L as initial concentration). The flasks were tightly capped and mixed on orbital shaker (NS-LR, As One Co., Japan) at 200 rpm and 25 °C. A set of batch experiments was conducted under anoxic conditions with or without the addition of different amounts of copper chloride (10, 12.5, 25 and 100 mg). Anoxic state was achieved by deoxygenating the solutions with flowing nitrogen for 20 minutes prior to initiating experiments. The performance of nZVI was also tested for phosphorus adsorption without deoxygenating of deionized water (under oxic conditions). 5 ml of solution was periodically withdrawn to analyze phosphorus content. The optimum amount of copper chloride with nZVI, which made a compromise between achieving reliable results in phosphorus adsorption, cost-effectiveness and environmental safe measures, was used with 250 mg nZVI

on the removal of 250 mL of phosphorus solution (1, 5, 10 and 50 mg/L) at the same conditions previously mentioned in absence of air.

To investigate the effect of pH on adsorption of phosphorus by nZVI, Batch experiments were anoxically carried out on the removal of phosphorus of 250 mL solution (50 mg PO_4^{3-}-P/L) at three different pH mediums (acidic pH 2, neutral pH 7 and alkaline pH 12). These experiments were performed with or without addition of designated copper chloride amount to investigate its influence on adsorption process in different pH media as well. Concentrations of both phosphorus and total iron were inspected at certain periods of time on the withdrawn 5-mL samples.

In order to recover phosphorus from previously-performed batch experiments, the spent adsorbents from batch experiments that investigated the influence of pH were placed in high alkaline solutions (250 mL of pH 12) in conical flasks (300 mL capacity) and left on the shaker for two hours. Samples (5 mL each) were periodically collected at specific intervals of time to analyze phosphorus concentrations. In addition, the recovery of phosphorus was carried out in various sodium hydroxide solutions of different molarities (0.04, 0.1, 0.25, 0.4 and 1 M) to investigate the effect of molarity on the recovery percentage.

To achieve a satisfied quality control, all experiments were tested in triplicates during our study to check on the reproducibility of work and accuracy of results.

3.3. Characterization of nZVI

The TEM investigated the microscopic morphologies of nZVI prepared in this study, and its images are displayed in Figs. 3-2. These images identify clearly necklace-like aggregate structure of bare nZVI particles as observed in other researches [112]. The dark color in TEM images indicates heaver atomic mass particles whereas brighter zones contain lighter masses. Therefore, it is shown apparently that there is a narrow layer of iron oxide/hydroxide on the surface of nZVI particles. The narrow layer is important in the essence of treatment as it adsorbs nitrate, and Figs. 3-2 gives a rough indication of particle size obtained from different magnification powers in which particle size of nZVI appeared smaller than 50 nm.

The size of these particles was estimated according to various taken TEM images to be about 40 nm in average. This estimated value was emphasized (in case of excessive sonication of samples) using particle size analyzer by which a close result was obtained about

particle size distribution of nZVI ranging from 15-60 nm, while more than 80% by weight of nZVI particles have diameters less than 50 nm. However, in absence of adequate sonication of sample particles, huge aggregates were formed with a distribution presented in Fig. 3-3. The median, modal and mean diameters were 4.379, 2.834 and 6.560 µm along with a standard deviation of 0.58 µm.

Results of surface characterizations for nZVI showed a high BET surface area per unit mass (61 m^2/g) in two of the lab investigations. Even higher than any reported specific surface area in other research works as the BET specific surface area (SSA) values reported in literature are 25 m^2/g [177], 33.5 m^2/g [112], 36.5 m^2/g [178] and 46.27 m^2/g [85]. However, in different other investigations on nZVI particles, the BET SSA was found to be 16.3, 27 and 34 m^2/g. These results may not contradict with each other and with the highest detected surface area, because the SSA varies with the degree of oxidation, agglomeration and drying of nZVI particles [179, 180] in addition to the synthesis conditions of nZVI, which are fixed. The SSA is an important factor for characterization, but the reactivity and removal efficiency tested in batch experiments are way more important criteria for evaluating nZVI performance [149, 181], especially if the oxidized layer depicts more SSA and agglomerated particles provide lower SSA.

The XRD analysis confirmed the formation of zero valent iron (Fe^0) with its major deflection at 44.8^o (2θ) which was shown on nZVI pattern (refer to Fig. 3-4a). Iron oxides were not detected in XRD pattern of nZVI, which could be due to their relatively small amounts. Fig. 3-4b describes XRD pattern of spent nZVI reacted with nitrate in batch experiment under certain conditions (500 mL of 100 mg/L nitrate solution, CuCl$_2$/Fe mass ratio of 0.05, anoxic state and neutral media). There was found some unreacted nZVI at 44.8^o, copper ferrite (CuFe$_2$O$_4$.Fe$_3$O$_4$) clearly at least at around 35° and 63°, and magnetite (Fe$_3$O$_4$) at 30.26^o, 57.08^o and others. Magnetite was formed as a result of iron conversion to its oxides in the overall nitrate reduction reaction equation:

$$NO_3^- + 3Fe^0 + 3H_2O \rightarrow Fe_3O_4 + NH_4^+ + 2OH^- \tag{3.1}$$
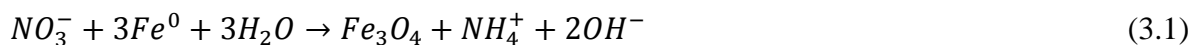
Meanwhile, copper ions were reduced to copper (Eq. (3.2)) then some were precipitated and some were oxidized and reacted with iron oxides to produce copper ferrite spinel (Eq. (3.5)) according to the following reactions [182]:

$$Cu^{2+} + 2e^- \rightarrow Cu \tag{3.2}$$

$$2Cu + H_2O \rightarrow Cu_2O + 2H^+ \tag{3.3}$$

$$Cu_2O + H_2O \rightarrow 2CuO + 2H^+ \tag{3.4}$$

$$CuO + Fe_2O_3 + Fe_3O_4 \rightarrow CuFe_2O_4.Fe_3O_4 \tag{3.5}$$

where it is noticed the release of protons (H^{+}) from Eqs. (3.3) and (3.4), which would be one of the reasons for reduced final-reached pH value of treated nitrate solution in the presence of copper ions. Furthermore, protons are essential for nitrate reduction as shown in further discussions.

Regarding phosphorus adsorption, copper ferrite compounds (CuFe$_2$O$_4$.Fe$_3$O$_4$) also appears in the XRD pattern of the spent CuCl$_2$/nZVI (1:10 wt/wt), shown in Fig. 3-5. These compounds are the key components of the adsorption process of phosphorus as discussed further in this chapter. It is noticed the presence of iron and phosphorus compounds indicating occurrence of chemisorption and coprecipitation [176, 183] side by side with physisorption [75].
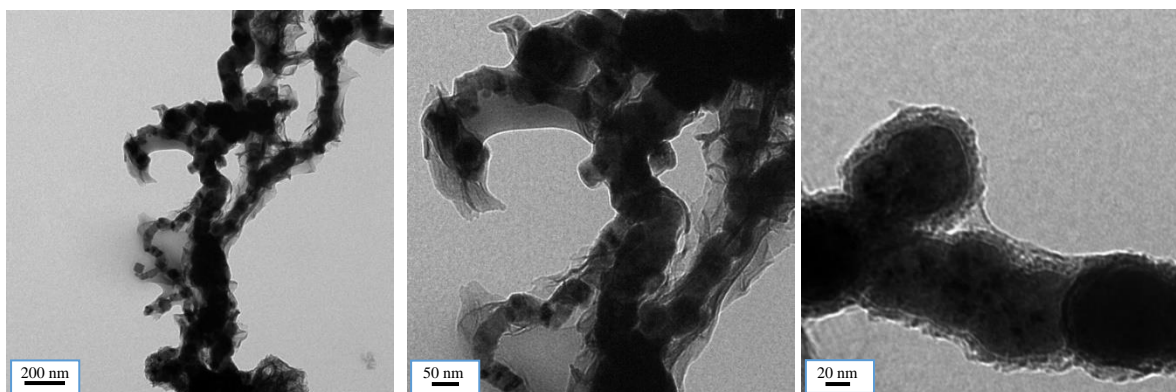
Fig. 3-2. TEM images of nZVI at resolutions of 200, 50 nm and 20 nm, respectively.
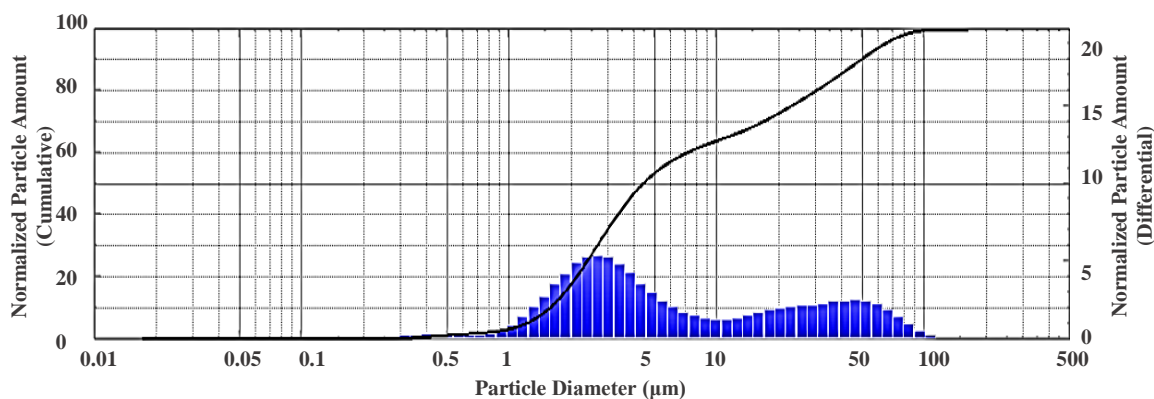
Fig. 3-3. Particle size distribution of nZVI (by laser-scattering particle analyzer).
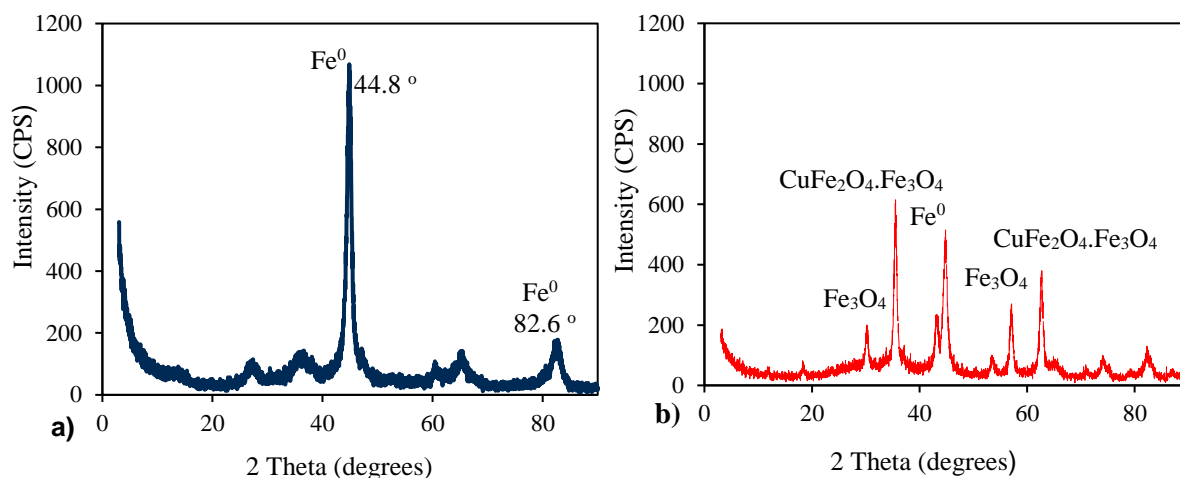
Fig. 3-4. XRD patterns of a) fresh nZVI and b) spent $CuCl_2$/nZVI from nitrate batch experiment.
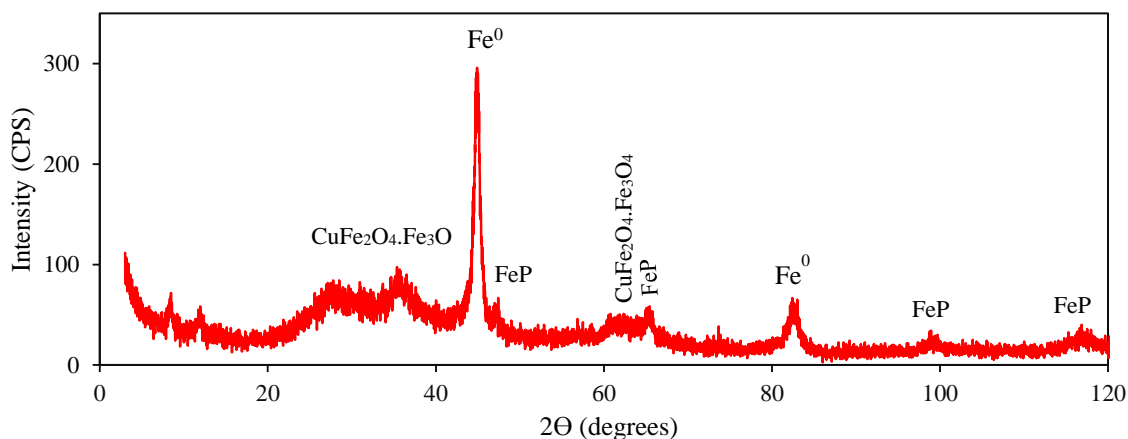
Fig. 3-5. XRD patterns of spent $CuCl_2$/nZVI with prominent peaks for iron, copper and phosphorus products.

3.4. Mechanisms of removal

Every contaminant has its specific mechanism of removal by nZVI shown as follows.

3.4.1. Nitrate reduction reaction pathways

The fate of nitrate, nitrite, ammonia and total nitrogen in the solution medium was investigated for 100 mg/L of nitrate without and with copper salt addition (Figs. 3-6 & 3-7). Tracing nitrite concentration indicates the reduction of nitrate to nitrite, so the nitrite concentration increases at the beginning of time. Meanwhile, nitrite is consumed in side reactions to produce ammonia and with a lesser amount, nitrogen.
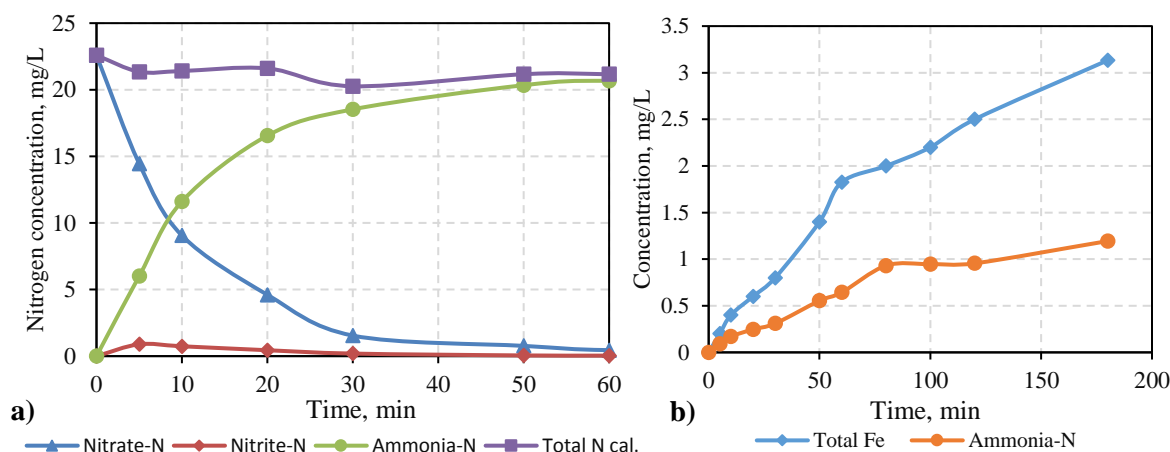
Fig. 3-6. Concentrations of (a) various nitrogen species during the nitrate reduction (100 mg/L) by nZVI and (b) total iron in reaction mixture and ammonia in acidic solution
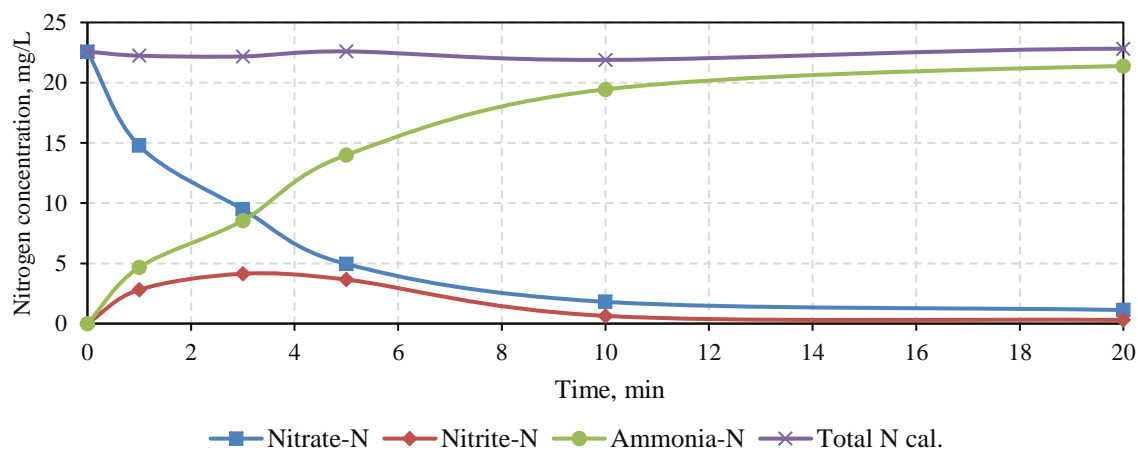
Fig. 3-7. Concentrations of various nitrogen species during the nitrate reduction (100 mg/L) by CuCl2/nZVI (0.05:1 wt/wt)

The reaction between iron and nitrate can take these following reaction pathways [155]:

$$4Fe^0 + NO_3^- + 10H^+ \rightarrow 4Fe^{2+} + NH_4^+ + 3H_2O \tag{3.6}$$

$$Fe^0 + NO_3^- + 2H^+ \rightarrow Fe^{2+} + H_2O + NO_2^- \tag{3.7}$$

$$3Fe^0 + NO_2^- + 8H^+ \rightarrow 3Fe^{2+} + 2H_2O + NH_4^+ \tag{3.8}$$

$$3Fe^0 + 2NO_2^- + 8H^+ \rightarrow 3Fe^{2+} + 4H_2O + N_{2\,(g)} \tag{3.9}$$
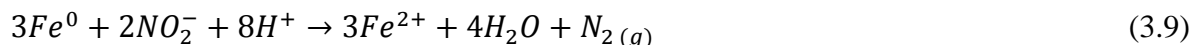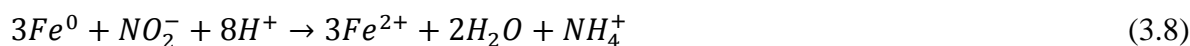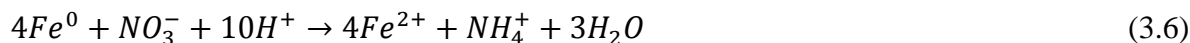
Nitrate is reduced in the presence of protons, which are found in the aqueous medium (Eqs. (3.6) and (3.7)). This is indicated in the graphs of Figs. 3-6 and 3-7 in which nitrate concentration decreases by the time. Nitrite is produced, and it increases in concentration to reach a peak then decreases as it participates in other reactions to give ammonia and nitrogen

(as in Eqs. (3.8) and (3.9)). It is obvious that nitrite and nitrogen are produced in small amounts, and ammonia is the main product. Ammonia is stripped from nitrate solution as a vapor at high pH (pH>9.5) then absorbed in an acidic medium, and its concentrations are shown in Fig. 3-6b. The theoretical total nitrogen amount of 100 mg/L nitrate solution corresponds to about 22.58 mg nitrogen per liter. However, due to nitrogen gas and ammonia vapor evolution, the calculated total nitrogen (emphasized by analysis as well) is a bit less than the original amount in Fig. 3-6a using nZVI (~ 21 mg/L), while it is slightly less than original amount of nitrogen using $CuCl_2$/nZVI at the optimum addition ratio in Fig. 3-7 (~ 21.9 mg/L). Ammonia vapor was absorbed in an acid solution for both batch experiments. In case of treatment using $CuCl_2$/nZVI, the final pH value of the treated solution was not as high as the pH of the solution treated with nZVI only, and especially the final pH value was about 9.5 causing no ammonia stripping. The pH and ORP monitoring for both batch experiments appears in Fig. 3-8. For both nitrate reductions via nZVI (Fig. 3-8a) and $CuCl_2$/nZVI (Fig. 3-8b), pH increased as H^+ ions were consumed from water in Eqs. (3.6) to (3.9) so that it reached pH 10 in Fig. 3-8a. However, this value of pH slightly decreased (pH 9.5) in case of using $CuCl_2$/nZVI at Fig. 3-8b resulted from the release of H^+ ions in Eqs. (3.3) and (3.4). The ORP value for both batch experiments decreased due to the pH increase, consumption of oxidative NO_3^- and generation of reductive NH_4^+ and Fe^{2+}.
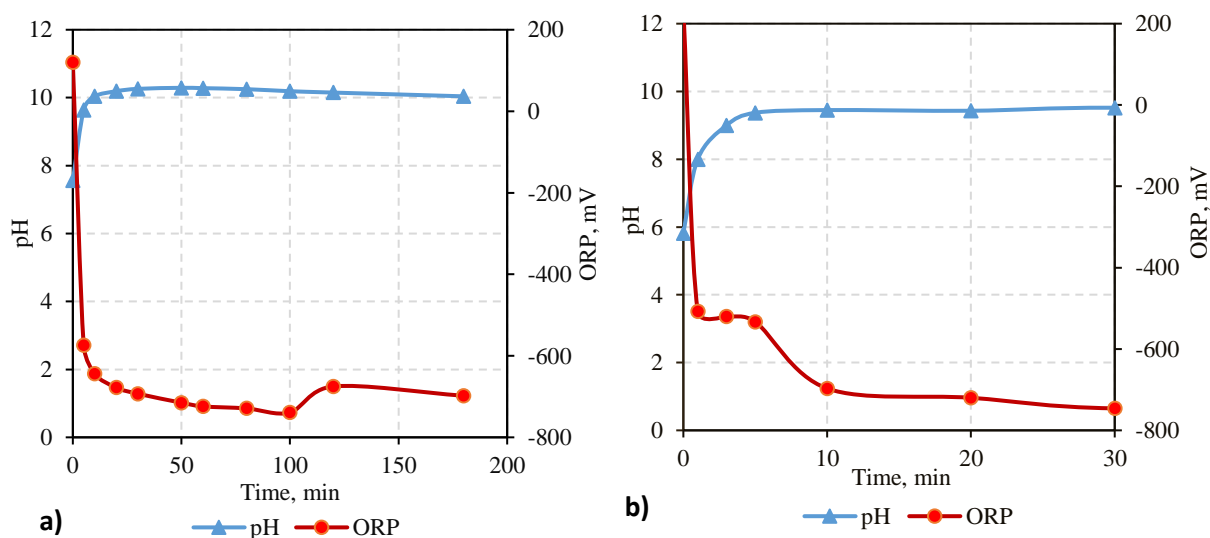
Fig. 3-8. pH and ORP monitoring during the nitrate reduction (100 mg/L) by a) nZVI and b) $CuCl_2$ /nZVI (0.05:1 wt/wt).

3.4.2. Phosphorus removal

A series of batch experiments was carried out to investigate different effects of copper chloride load values, initial pH value, and dissolved oxygen on phosphorus removal by nZVI. The performance of phosphorus removal by nZVI with addition of a specific amount of $CuCl_2$ (25 mg, 1:10 of $CuCl_2$/nZVI mass ratio) was compared against phosphorus removal by nZVI. Fig. 3-9 shows the phosphorus removal profiles for nZVI in different cases (with anoxic condition, aerobic condition and addition of copper chloride mass). The removal efficiency of the phosphorus by nZVI provided with $CuCl_2$ addition is around two times more than that by nZVI at the same time of 30 minutes and three times faster in overall (to reach a certain value at both of them). The kinetics of phosphorus removal under aerobic condition seems to be faster at the beginning than that under anoxic condition then they both reach the same equilibrium value. Aerobic atmosphere offered more iron corrosion to nanoscale iron surface which in turn helped in more phosphorus adsorption as ferric (hydr)oxides are good sorbents for contaminants [75, 184-186]. Generally, the adsorption capacity of nZVI in these experiments was 28 mg $PO_4^{3-} - P$/g Fe that was enhanced at least 1.7 times more than its original value by adding small amount of copper chloride (25 mg). Thus, a complete removal had occurred by nZVI/$CuCl_2$ within 30 minutes. By reviewing different sorption capacities of iron-based compounds illustrated by Almeelbi et al. [75], the obtained sorption capacity in this study was the highest among others (at this maximum equilibrium value of phosphorus obtained in this chapter) as presented in the graph of Fig. 3-10 (see Table 3-1 for further illustration).
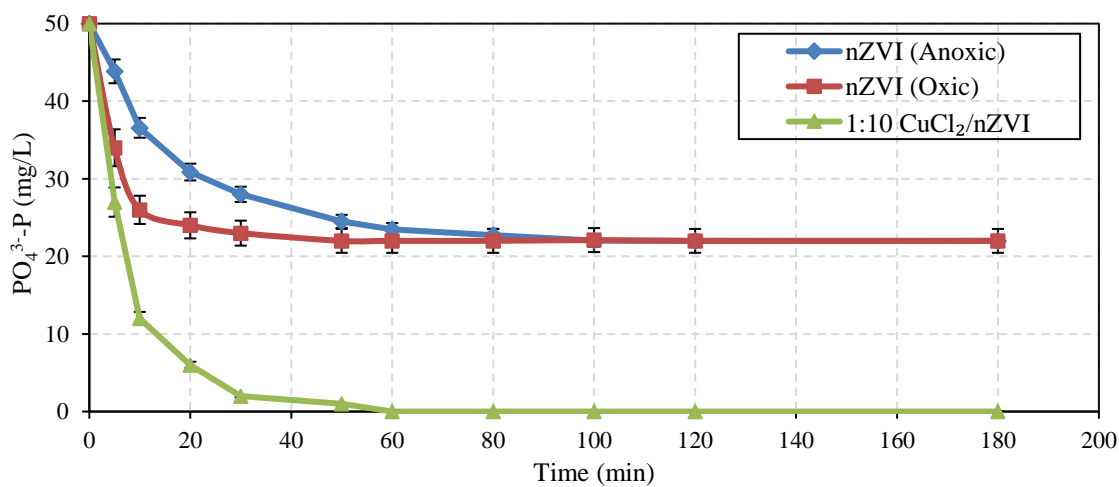
Fig. 3-9. Effect of copper chloride addition and oxic conditions on phosphorus adsorption by nZVI.
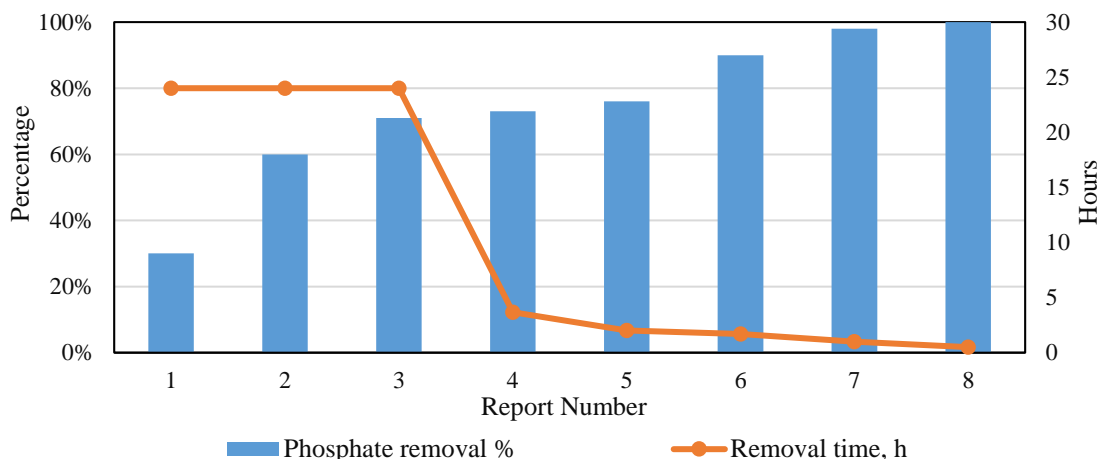
Fig. 3-10. Adsorption of phosphorus by iron-based materials based on several reports (refer to Table 3-1 for further illustrations).

Table 3-1. Adsorption of phosphate by iron-based materials based on several reports.

Report number	Iron-based material	Treated water	Phosphate material	Adsorption capacity, P mg/g	Reference
1	Akaganeite	Sea water	NaH_2PO_4	4	[184]
2	Synthetic Goethite	Sea water	NaH_2PO_4	7.9	[184]
3	Iron oxide tailing	Deionized water	KH_2PO_4	6	[185]
4	Iron hydroxide– eggshell waste	Distilled water	KH_2PO_4	9	[28]
5	Steel slag	Distilled water	KH_2PO_4	5.3	[187]
6	Hydroxy-iron	Deionized water	KH_2PO_4	4.84	[188]
7	nZVI	Deionized water	KH_2PO_4	24.38	[75]
8	nZVI/$CuCl_2$	Deionized water	KH_2PO_4	50	Present

3.5. Promotion of removal kinetics via copper salt addition

3.5.1. Effect of copper chloride addition on nitrate reduction

The performance and kinetics of reduction using nZVI in copper salt presence is higher than using nZVI alone. Nitrate was completely removed in 20 minutes using nZVI/copper salt while it took about an hour to reduce all nitrate amount using ordinary nZVI. The reason for high reaction kinetics was attributed to two electrochemical reactions that can take place. The first electrochemical reaction occurred spontaneously via reducing copper ion with electrons given from iron oxidation as follows [189]

$$\text{Fe} \rightarrow Fe^{2+} + 2e^-, \ E^o = -0.44 \text{ V} \tag{3.10}$$

$$Cu^{2+} + 2e^- \rightarrow Cu, \ E^o = 0.34 \text{ V} \tag{3.11}$$

where E^o is the reduction potential of half-cell reaction, and the potential of the two redox reactions is 0.78 V which indicates galvanic spontaneous reaction [190]. The presence of copper ions stimulates iron to corrode in higher amounts and faster rates giving more electrons, which can take part in nitrate reduction. Furthermore, the formation of copper ferrites leads to increasing protons concentration in the reaction medium, which favors nitrate reduction (Eqs. (3.2) to (3.5)). The previous explanation is similar to the same effect posed by acid action on nZVI [155, 191]. Also, this electrochemical reaction increases initial ferrous concentration, and a higher initial ferrous ions (Fe^{2+}) concentration indicates an easier iron corrosion, increases nitrate adsorption on iron surface and enhances nitrate reduction [164].

Another reason for high kinetic rate and greater performance is attributed to the catalytic effect of copper. Copper and its compounds act as an inert electrode or a catalytic surface on which indirect electron transfer could occur. Fig. 3-11 depicts this mechanism along with the original direct electron transfer mechanism that happens meanwhile between nZVI and nitrate. E_1^o and E_2^o are the cell potentials of two overall electrochemical reactions of direct and indirect electron transfer, respectively. Hydrogen is formed from proton reduction then reduces nitrate. So the catalytic effect of copper is shown when the adsorbed (ad.) hydrogen rapidly reduced the adsorbed nitrate from aqueous (aq.) solution. The hydrogen reduction was proved to be a more powerful reducing species than electron transfer [192].

To the best of author's knowledge, the obtained nitrate reduction results from copper salt addition indicate higher kinetic rate than any other reported values using either a supported nZVI, dispersed nZVI by surfactant or bimetallic nZVI particles [1]. Even though the technique used in this method is different, bimetallic method could be considered the closest to this technique. However, the speed of reaction in this study is more than two times faster than that by copper-coated nZVI particles [154, 167]. Moreover, although bimetallic nanoparticles exhibit lower agglomeration and aggregation behavior [174], but they suffer shorter lifetime and possible toxicity, and their catalytic efficiency decreases with time due to iron hydroxide formation on iron surface which prevents the continuation of nitrate reduction [154].
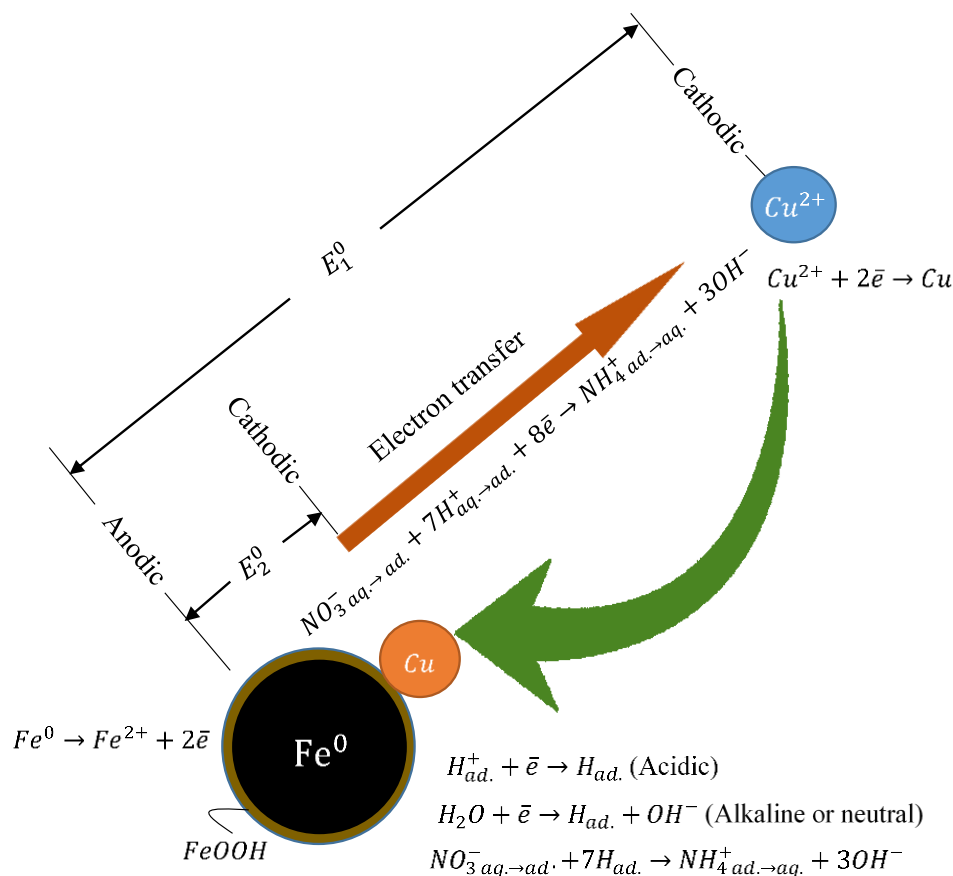
Fig. 3-11. The effect of copper ions presence on nitrate reduction by nZVI.

3.5.2. Effect of copper chloride addition on phosphorus removal

The addition of copper ions clearly modified and improved the speed of phosphorus sorption by nZVI. Fig. 3-9 elucidates this improvement in kinetics of removal. Copper chloride reaction with nZVI increased iron corrosion on the surface and provided its surface with copper and copper ferrite particles. These copper compounds increase electric conductivity of the surface and aid in sorption of phosphorus molecules by ferrites, ferrous hydr(oxides) and ferric hydr(oxides). Copper chloride itself was not capable of adsorbing phosphorus. A control test was performed on copper chloride of 25 mg load to discover that it did not remove any phosphorus (Fig. 3-12). Thus, the key components of the adsorption process are copper ferrite compounds ($CuFe_2O_4.Fe_3O_4$), which appear in the XRD pattern of the spent $CuCl_2$/nZVI (1:10 wt/wt), shown in Fig. 3-5, at deflection angles 2θ around 35° and 63°. Copper ferrite compounds could have been formed by the same mechanism discussed previously in Eqs. (3.2) and (3.5) [145]. These compounds have the ability to adsorb

phosphorus, and their adsorption capacity for phosphorus can reach 13.5 mg/g at pH 2.64 [175]. They can also speed up the rate of adsorption as shown in this study. However, the presence of iron oxides (Fe_2O_3 and Fe_3O_4) on the shell of nZVI particles with Cuprospinel ($CuFe_2O_4$) compounds ended up increasing the rate of adsorption, which is observed in Fig. 3-9 when applying oxic condition with phosphorus adsorption by nZVI, a higher rate was obtained. And the probability of Iron oxides existence was higher under aerobic condition as follows [155]:

$$Fe^0 + \frac{1}{2}O_2 + H_2O \rightarrow Fe^{2+} + 2OH^- \tag{3.12}$$
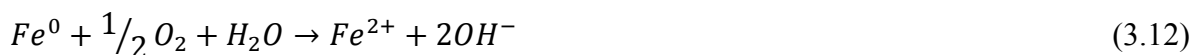
Also as indicated by the previous reports (Table 3-1), iron oxide hydroxides were usually the main constituents of adsorbents for phosphorus compounds.

3.6. Optimizing different copper salt loads

3.6.1. Optimization of load in nitrate decontamination

Batch experiments were set up to investigate the effect of different loads of copper chloride on nitrate reduction. Different loads of $CuCl_2$/nZVI mass ratios (0, 0.02, 0.05 and 0.25) were examined to find the optimum load in this case that provides the highest nitrate reduction performance. As shown in Figures 3-12a, the performance of the three profiles ($CuCl_2$ present) is roughly abreast. The quite near performance is due to the previously explained mechanism in which slightly higher amounts of copper ions would not act negatively on nitrate reduction. However, there is a slightly better performance exhibited by $CuCl_2$/nZVI of 0.05 g/g. Also, it can be intuited from the concentration of ferrous ions for different loads of copper chloride, shown in Fig. 3-13, that high load of copper ions resulted in higher concentrations of ferrous ions compared to that of lower loads. High ferrous concentration could increase the toxicity of the treated water, so using a large portion of copper chloride salts is not recommended, and for the reason that copper compounds are also hazardous contaminants.

3.6.2. Optimization of load in phosphate decontamination

Different loads of copper chloride (10, 12.5, 25 and 100 mg) were added during phosphorus removal (50 mg PO_4^{3-}-P/L) by 250 mg of nZVI from 250 mL solution accounting for different

CuCl$_2$ to nZVI mass ratios (1:25, 1:20, 1:10 and 1:2.5, respectively). Fig. 3-12b describes the difference in performance of nZVI towards the removal of phosphorus via varying copper chloride loads. It was found that adding a load of 5 mg CuCl$_2$ removed phosphorus within 100 minutes followed by removal in 80 minutes for 12.5 mg CuCl$_2$ load, and then phosphorus was removed in 30 minutes by adding 25 mg of CuCl$_2$. Finally, when 100 mg CuCl$_2$ was applied, phosphorus was removed by nZVI in 10 minutes. By increasing the amount of CuCl$_2$, the kinetics of adsorption becomes faster, and adsorption capacity of nZVI increased by this addition. In case of CuCl$_2$-free nZVI, the adsorption capacity was the lowest with 22 mg PO$_4^{3-}$-P/ g nZVI.
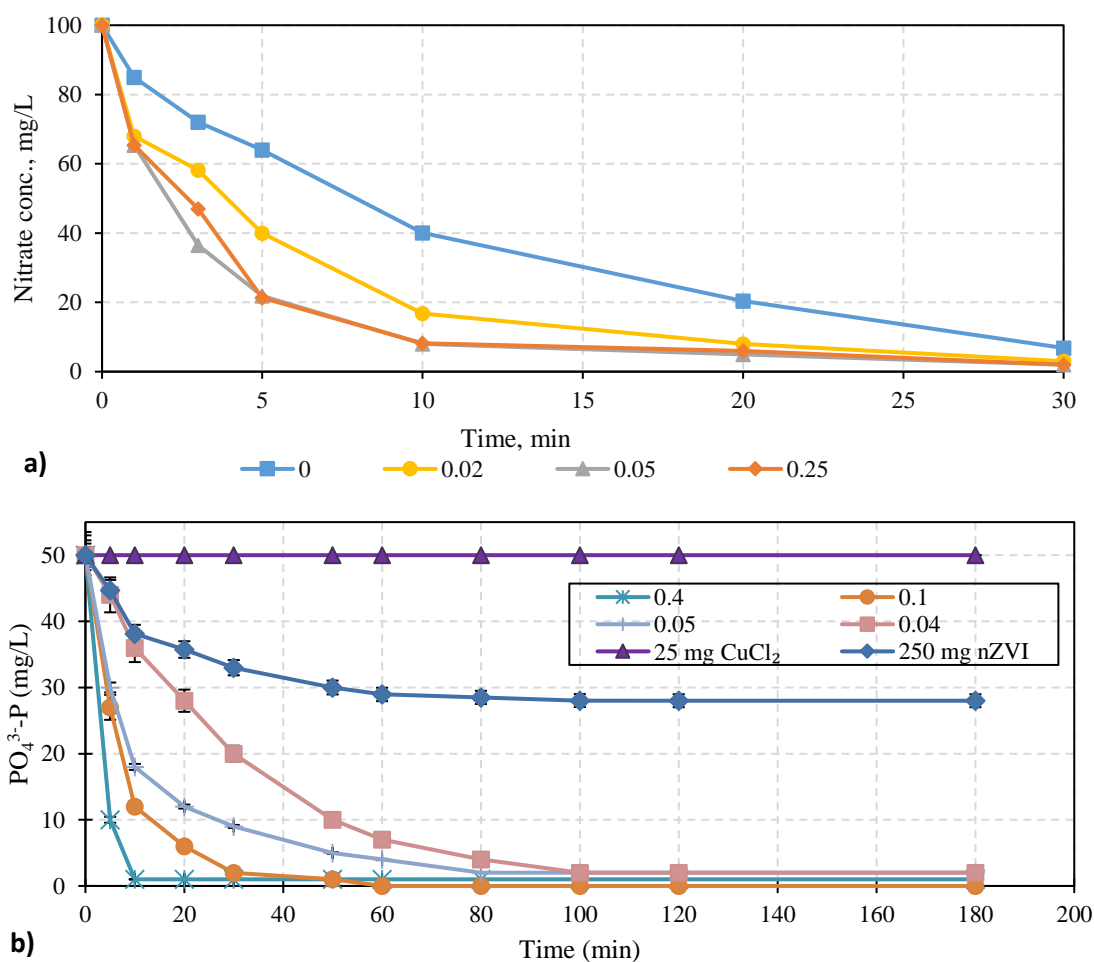
Fig. 3-12. a) Nitrate reduction and b) phosphate removal by nZVI under different loads of CuCl$_2$ to nZVI mass ratios.
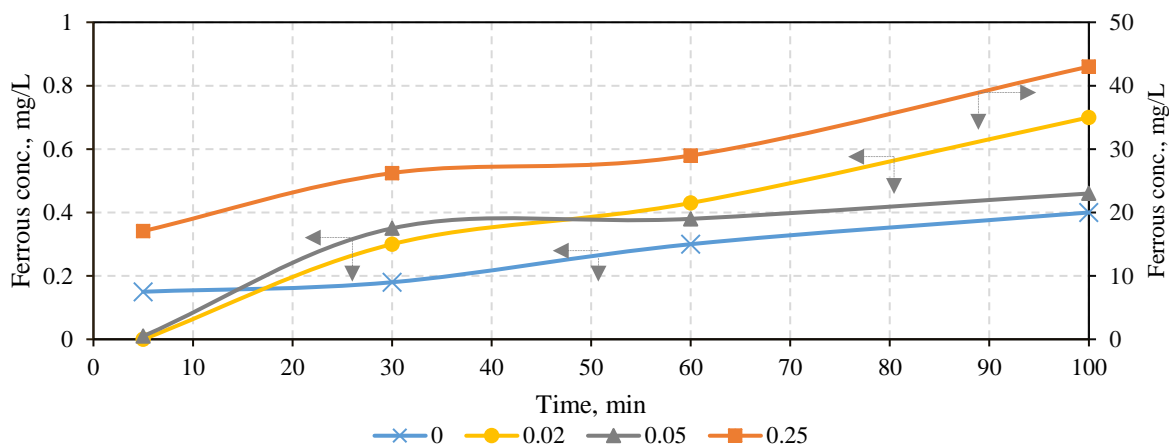
Fig. 3-13. Effect of CuCl$_2$ / nZVI mass ratio concentration on ferrous release from 50-mg/L nitrate solution.

3.7. Effect of pH value

It is commonly known from previous reports the fact that nitrate reduction favors acidic medium. It is an acid-driven surface-mediated process as previously mentioned. Low pH medium dissolves the oxide hydroxide layer of iron surface (FeOOH) and clears it for further reactions. Therefore, the reaction proceeds at a higher rate than that of neural-medium reaction. Fig. 3-14a shows the reduction of 100 mg/L of nitrate using nZVI and nZVI in presence of copper chloride, at optimum ratio of 0.05 (CuCl$_2$ to nZVI mass ratio), in acidic, neutral and alkaline medium, initially adjusted at pH 1.5, 7 and 9, respectively. For simplicity, copper-chloride-added nZVI is denoted as C-nZVI. The shown graph illustrates the greater performance of nZVI in acidic medium compared to other media, while nZVI presented the lowest kinetic performance in the alkaline medium. However, the presence of copper chloride (in all different pH mediums) greatly enhanced the reaction rate compared to others (without CuCl$_2$). As indicated by Fig. 3-14a, nitrate reduction profiles of nZVI in acidic medium and C-nZVI in all three mediums lie in the same vicinity showing roughly close performance. To take a close look at the performance of the competitive profiles, for those who removed more than 90% of nitrate within 10 minutes, Fig. 3-14b focuses on the kinetic profiles of acidic nitrate reduction using nZVI and other nitrate reductions in three different mediums (acidic, neutral and alkaline) using C-nZVI. The figure illustrates the higher stability and reliability of C-nZVI in all media than that of nZVI. It shows that the kinetics of C-nZVI in neutral medium are close to kinetics of nZVI in acidic medium. In addition, both performances of

nitrate reduction of C-nZVI in acidic and alkaline medium are slightly higher. This reliability of C-nZVI in all pH mediums is maintained as the mechanism, previously suggested with Eqs. (3.2) to (3.5), showed the production of protons in case of alkaline or neutral medium to produce copper ferrite. Also, it is commonly known that the electrochemical reactions (caused by $CuCl_2$ addition) are improved in alkaline or acidic mediums due to high electric conductivity of these mediums which facilitates movement of ions [193].

The results of batch experiments concerning phosphorus removal under different pH media using nZVI revealed its dependency on pH. Fig. 3-15 depicts the adsorption of phosphorus using nZVI under pH 2, pH 7 and pH 9, and the same investigation under the same acidic, neutral, and alkaline mediums using nZVI with addition of copper chloride. The results show that the adsorption of phosphorus increases with decreasing pH value. In case of using nZVI solely, there was no adsorption in alkaline medium, while the adsorption kinetics of phosphorus increased from that in neutral to acidic medium. The time necessary for removal of phosphorus was the indicator for kinetics enhancement, which decreased from 60 minutes at pH 7 to 20 minutes at pH 2. On contrary, addition of copper chloride enhanced adsorption in alkaline medium to approximately the same trend as adsorption of phosphorus using nZVI only in a neutral medium. Also, the added copper chloride improved nZVI adsorption to phosphorus in neutral medium, and its adsorption profile is close to that of acidic nZVI as shown in Fig. 3-15. However, addition of copper chloride failed to improve kinetic performance in acidic medium. It is proved from total iron analysis (illustrated by Fig. 3-16) that the concentration of corroded iron, indicated by total iron, increases by either decreasing the pH value or adding copper chloride. This result is clearly shown when comparing the profiles of total iron concentration of phosphorus adsorption using nZVI with and without copper chloride addition in the neutral and acidic media in Fig. 3-16. However, the relative increase in concentration of total iron released to the solution resulted from copper chloride addition in neutral medium (70-48 mg/L) is much less than that generated by acidic action (247-48 mg/L). To sum it up, copper chloride plays a role close to acidic action in increasing iron corrosion, speeding up electron transfer rate and providing iron (hydr)oxide layer which aid in phosphorus adsorption. Moreover, copper compounds formed at the surface of nanoscale iron particles seemed to catalyze the adsorption of phosphorus.
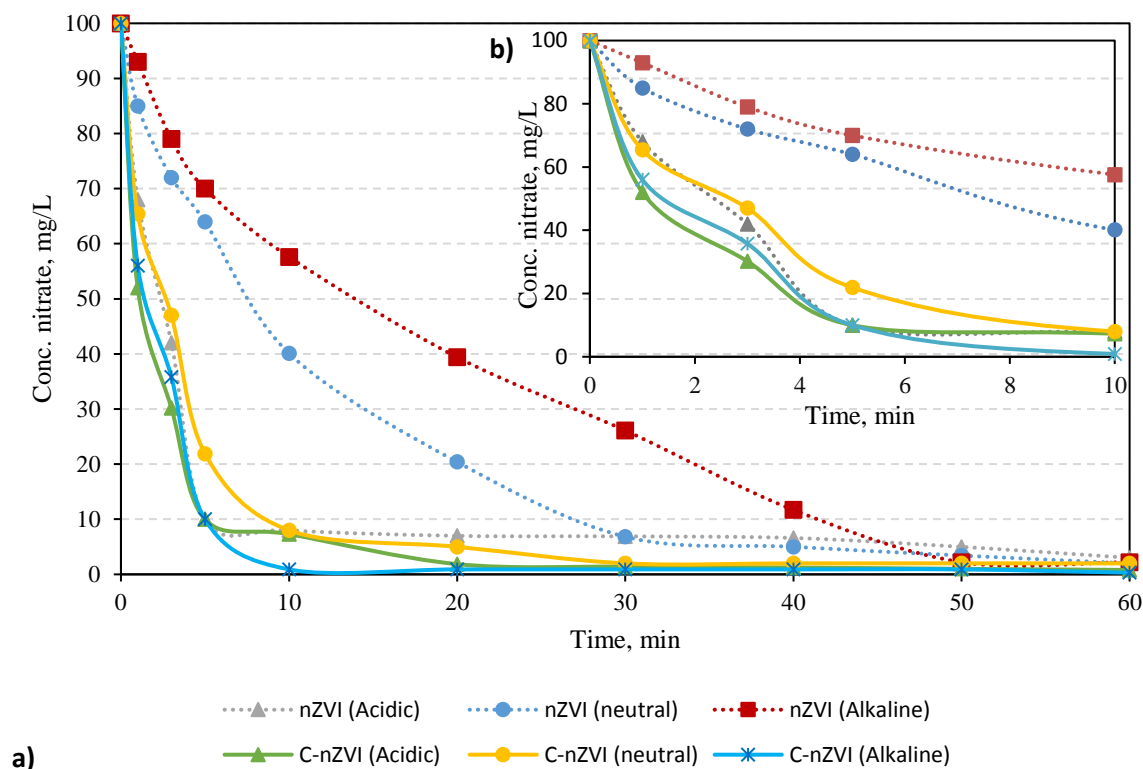
Fig. 3-14. Effect of pH on nitrate reduction of 100 mg/L using nZVI and C-nZVI.
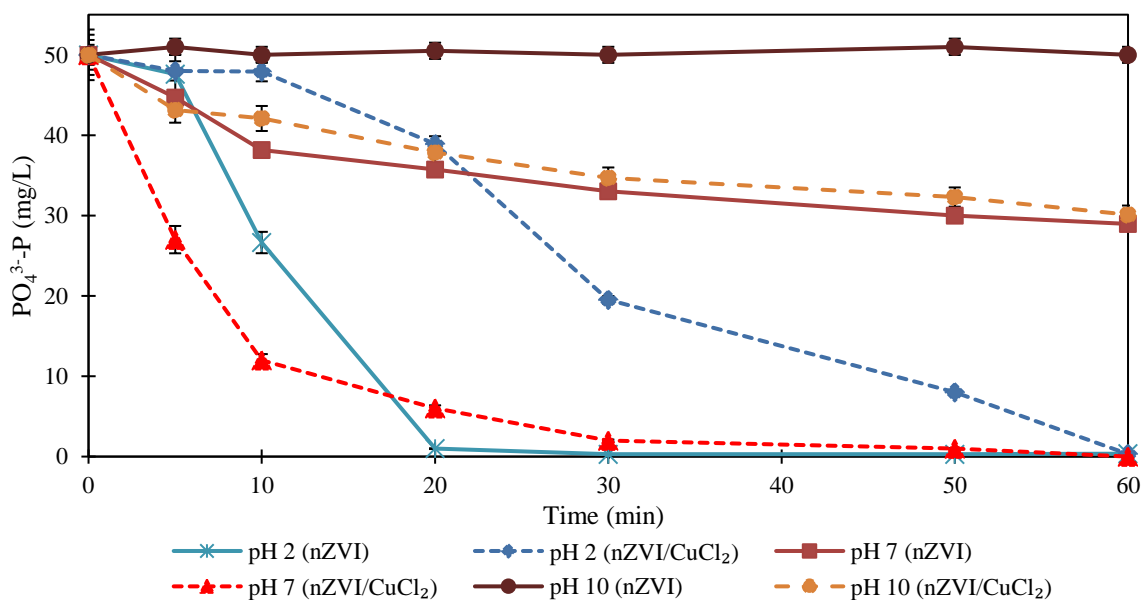
Fig. 3-15. Effect of pH on phosphorus adsorption (reaction conditions: 50 mg/L PO_4^{3-}-P solution treated using 250 mg nZVI; and using 1:10 mass ratio of $CuCl_2$/nZVI in case of addition).
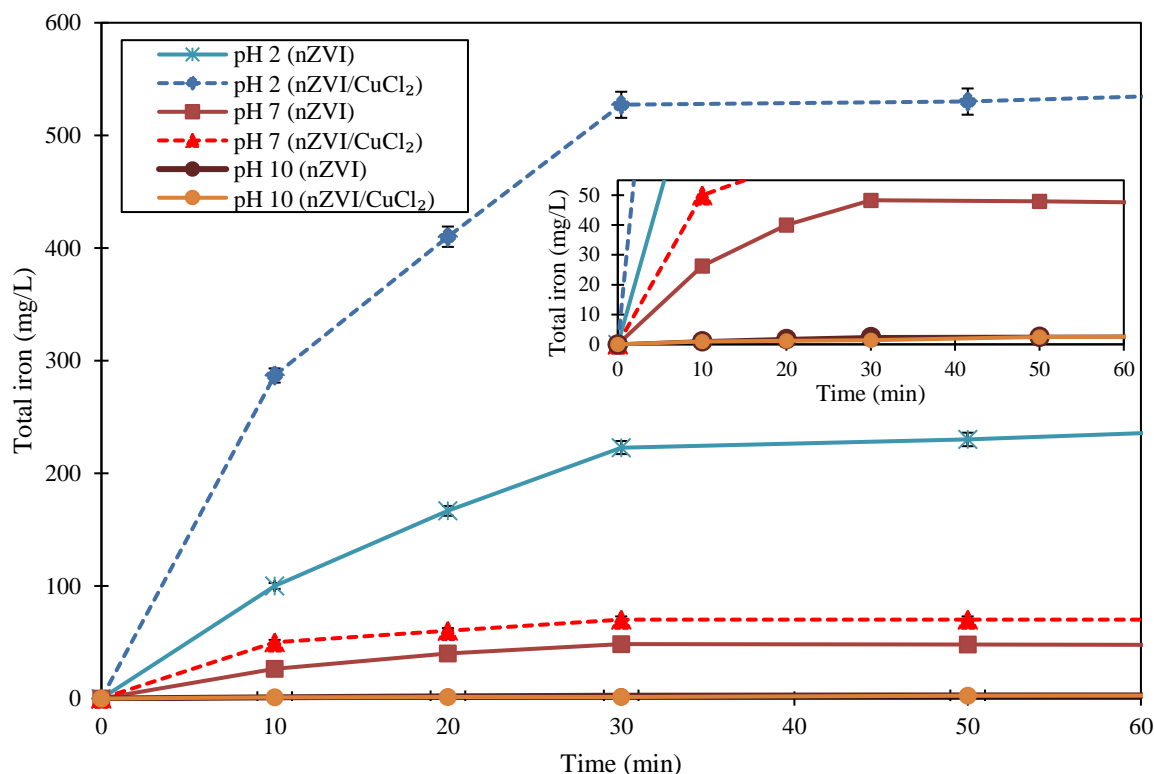
Fig. 3-16. Total iron concentration versus time of phosphorus batch experiments that studied pH effect.

3.8. Removal of high contaminant concentrations

The high rate of kinetics could be observed in treatment of high concentrations (200, 300 and 500 mg/L). The performance of nitrate reduction with different nitrate concentrations using nZVI in the presence of $CuCl_2$ at an addition ratio of 0.05 g $CuCl_2$ per one gram nZVI is shown in Fig. 3-17a. For initial concentrations 50, 100 and 200 mg/L, nitrate was totally removed in 5, 20 and 30 minutes, respectively. For higher concentrations of nitrate, 300 mg/L of nitrate was removed within 60 minutes, while nitrate concentration of 500 mg/L solution was lowered until approaching the standard allowable limit of 50 mg/L within the same period. The high kinetic rate of nitrate reduction led to driving the treatment into safe legal regulations within one hour.

The kinetic profiles of phosphorus removal with $CuCl_2$/nZVI are shown in Fig. 3-17b, which presents the removal of 1 to 10 mg PO_4^{3-}-P/ L only in 5 minutes. A complete removal of phosphorus concentration of higher initial concentration (50 mg PO_4^{3-}-P/ L) occurred within half an hour.
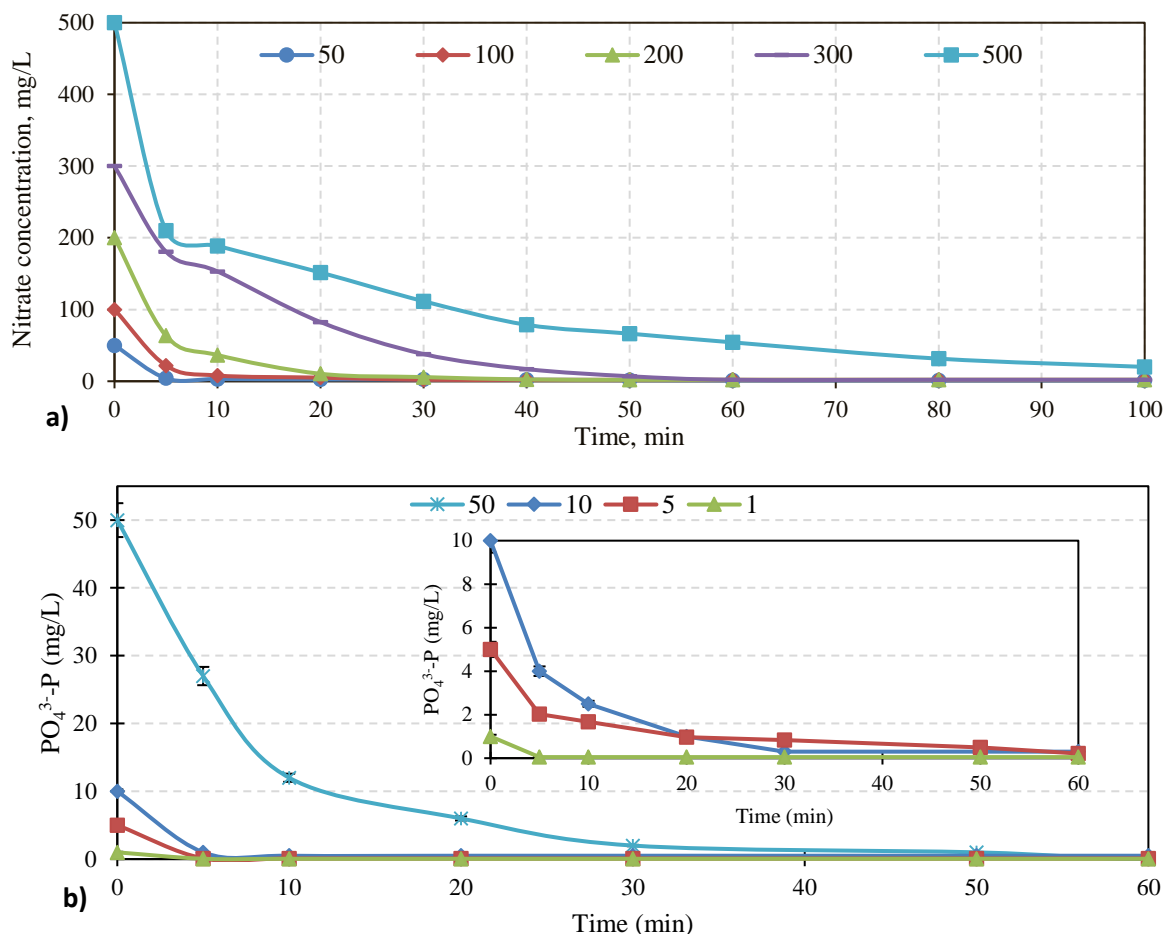
Fig. 3-17. Effect of CuCl$_2$ addition on a) different nitrate concentrations in mg/L (0.05 g CuCl$_2$/g nZVI) and b) phosphorus removal of different initial concentrations (mg/L) by CuCl$_2$/nZVI (1:10 wt/wt) and nZVI (Inserted chart).

3.9. Effect of dissolved oxygen

Nitrate reduction by nZVI is known for instability and weak performance in the presence of dissolved oxygen (DO). In most of nitrate reduction experiments carried out under aerobic conditions, removal efficiency decreased about 40% compared to that of those experiments that were carried out under anoxic condition or on ground water (low DO) [112]. The same behavior was noticed for treatment of other contaminants [194], indicating poor air stability of nZVI due to its high surface reactivity (towards oxidation with air). However, this appears to be no problem for nitrate removal using copper-chloride-added nZVI (0.05 g CuCl$_2$/g nZVI mass ratio). As observed in Fig. 3-18, the performance of nitrate reduction (Initially 100 mg/L conc.) under aerobic condition by nZVI varies than that of nZVI under anoxic condition by 40% lower removal efficiency at the equilibrium state (about 90 minutes).
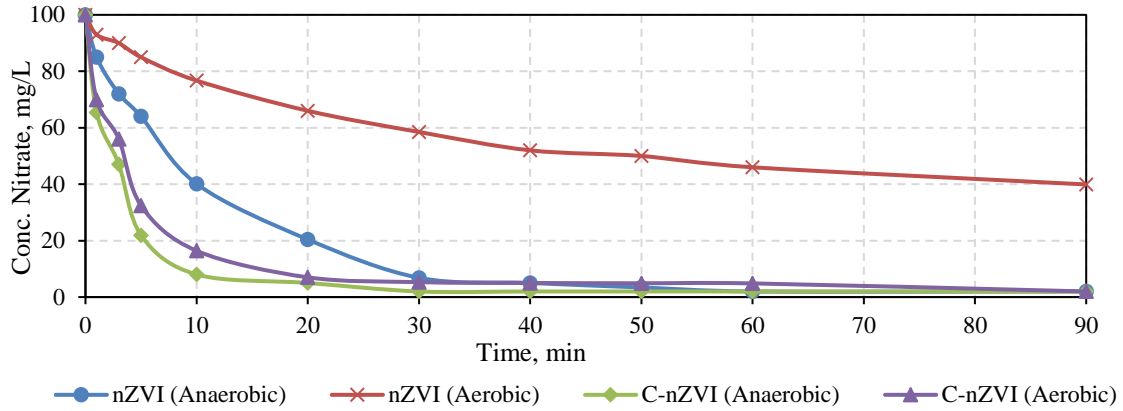
Fig. 3-18. Effect of dissolved oxygen on nitrate removal by nZVI and C-nZVI

On another hand, the performance of nitrate reduction by nZVI in CuCl$_2$ presence (C-nZVI) is roughly the same in all cases. The high rate of electrochemical reaction dominates, compared to the reaction kinetics of iron with water and oxygen, shown in Eq. (3.12).

Aerobic reduction profile of nitrate using C-nZVI outperforms nitrate reduction using bare nZVI, especially at the beginning. And reduction under aerobic condition by C-nZVI experiences close performance in kinetic rate and removal efficiency to the same reduction under anoxic condition. The same trend was observed in case of phosphorus with bare nZVI as discussed before in section 3.4.2 .

3.10. Reaction kinetics

3.10.1. Nitrate reaction kinetics

Table 3-2 documents the reaction kinetic constants for most of batch experiments processed in our study, fitting the available data with different kinetic equations (first and second order rate equations, and Langmuir-Hinshelwood (LH) equation). These models were employed for describing non-catalytic and surface-catalyzed reactions and investigating the kinetics of nitrate reduction by ZVI [191, 195], shown as follows:

first-order rate equation: $\frac{dC}{dt} = -KC,$ (3.13)

and its linear form: $C = C_i e^{-Kt},$ (3.14)

second-order rate equation: $\frac{dC}{dt} = -k_{N1}C^2,$ (3.15)

and its linear form: $\frac{1}{C} = k_{N2}t + \frac{1}{C_i}$, (3.16)

Langmuir-Hinshelwood equation: $\frac{1}{r} = \frac{1}{k_{N3}k_{N4}} \cdot \frac{1}{C} + \frac{1}{k_{N5}}$, (3.17)

where C is nitrate concentration at time (t), while C_i is the initial concentration of nitrate. K, k_{N1}, k_{N2}, k_{N3}, k_{N4} and k_{N5} are reaction rate constants, and r is the rate of reaction.

MAKHA stochastic global optimization algorithm [196] was used to obtain the optimum minimum least square error and correlation coefficient (R^2) for the curve fitting with linearized/nonlinear rate equations, as it is required to distinguish between different kinetic rate equations, and to determine the most accurate equation that fits the present data. Table 3-2 shows the results of implementing kinetic models on investigated results of batch experiments, and it describes their correlation coefficient and first-order rate constant (K). Previous reports concluded that nitrate reduction kinetics followed first-order reaction [85, 191] and others showed that LH equation was the best fit [112]. In our study, efforts were applied to find out the best model from these equations, and, as expected, three rate equations were competing in Table 3-2, especially the first-order and LH equations. However, if the average values of R^2 are considered along with assuming that R^2 of an equation rate of an experiment of value less than 0.9 means that the experiment's profile does not probably match the rate equation, so first-order rate equation (average R^2 value of 0.94, 3 experiments of kinetics nondescript by the equation) showed more applicability than LH equation (0.9, 5) and second-order equation (0.89, 7). Thus, most profiles obeyed first-order reaction kinetics, while reactions under aerobic conditions seemed to follow second-order rate equation. However, first-order reaction model failed to describe nitrate removal at low pH values (experiments # 9 and 12), and the same applies to other kinetic models. The reason could be accounted to the description of the original rate equation from reaction kinetics [197]:

$$\frac{d[NO_3^-]}{dt} = -k[H^+]^n[NO_3^-]$$ (3.18)

where the component enclosed by square brackets indicates its concentration in aqueous solution, k is the reaction rate constant, and n is a stoichiometric coefficient parameter. While at high concentrations of protons along with its high consumption, it is difficult to neglect large variations in H^+ concentration and its influence on the rate equation. Also data of experiment # 19 did not fit first-order reaction kinetics as high concentration of nitrate increased significantly the initial rates in the beginning.

Promoting the Reactivity of nZVI for Water Treatment

Regarding reaction rate constant, it is noticed that kinetics of nZVI in the presence of copper chloride salt is boosted about 3.7 times than the kinetics of nZVI without copper chloride addition (at the same category, see the ratios of reaction constants at Table 3-3). Table 3-3 was constructed based on choosing reference experiments and comparing the first-order rate constants of other experiments with that of the reference experiment. It is also extracted from the same table that the addition of copper chloride enhanced reaction kinetics by 9.9 times in the presence of dissolved oxygen contained in the reaction medium (see comparison between experiments # 21 and 23).

Table 3-2. Implementation of kinetic rate equations on investigated results of batch experiments.

Experiment category	#	$CuCl_2:Fe^0$ (wt/wt)	Initial nitrate conc.	Initial pH	Aerobic /Anoxic	First order (R^2)	Second Order (R^2)	LH (R^2)	K, h^{-1}
Cu salt loads	1	0	50	7	Anoxic	0.98	0.90	0.99	5.1
Cu salt loads	2	0.02	50	7	Anoxic	0.95	0.81	0.95	27.2
Cu salt loads	3	0.05	50	7	Anoxic	0.96	0.82	0.94	27.7
Cu salt loads	4	0.25	50	7	Anoxic	0.95	0.83	0.91	24.7
Cu salt loads	5	0	100	7	Anoxic	0.97	0.90	0.92	4.3
Cu salt loads	6	0.02	100	7	Anoxic	0.95	0.91	0.94	7.5
Cu salt loads	7	0.05	100	7	Anoxic	0.97	0.95	0.92	16.1
Cu salt loads	8	0.25	100	7	Anoxic	0.96	0.95	0.9	15.6
pH effect	9	0	100	1.5	Anoxic	0.83	0.88	0.73	17.7
pH effect	10	0	100	7	Anoxic	0.98	0.92	0.92	4.5
pH effect	11	0	100	9	Anoxic	0.94	0.58	0.70	3.7
pH effect	12	0.05	100	1.5	Anoxic	0.80	0.93	0.79	18.6
pH effect	13	0.05	100	7	Anoxic	0.98	0.95	0.92	15.8
pH effect	14	0.05	100	9	Anoxic	0.99	0.82	0.98	27.7
High $C_{NO_3^-}$	15	0.05	50	7	Anoxic	0.96	0.97	0.94	27.7
High $C_{NO_3^-}$	16	0.05	100	7	Anoxic	0.97	0.95	0.93	15.0
High $C_{NO_3^-}$	17	0.05	200	7	Anoxic	0.92	0.88	0.88	7.2
High $C_{NO_3^-}$	18	0.05	300	7	Anoxic	0.98	0.76	0.93	4.6
High $C_{NO_3^-}$	19	0.05	500	7	Anoxic	0.8	0.94	0.95	2.2
DO effect	20	0	100	7	Anoxic	0.99	0.91	0.9	4.2
DO effect	21	0	100	7	Aerobic	0.90	0.98	0.65	0.9
DO effect	22	0.05	100	7	Anoxic	0.99	0.94	0.93	15.8
DO effect	23	0.05	100	7	Aerobic	0.92	0.97	0.97	8.9

Table 3-3. Comparing reaction rate constants of investigated reactions.

Experiment category	Reference experiment #	Related experiment #	Rate constant ratio (Related/reference)
Cu salt loads	1	2	5.3
Cu salt loads	1	3	5.4
Cu salt loads	1	4	4.8
Cu salt loads	5	6	1.7
Cu salt loads	5	7	3.7
Cu salt loads	5	8	3.6
pH effect	10	9	3.9
pH effect	10	11	0.8
pH effect	13	12	1.2
pH effect	13	14	1.8
pH effect	9	12	1.1
pH effect	11	14	7.5
DO effect	20	21	0.2
DO effect	22	23	0.6
DO effect	21	23	9.9

3.10.2. Phosphorus adsorption kinetics

The XRD pattern of spent $CuCl_2$/NZVI (1:10 wt/wt, Figure 3-5) shows the presence of iron phosphide, which indicates that a chemical adsorption could have been occurred. So two common adsorption reaction models were used to depict such adsorption cases and fit the data. They were as follows:

Pseudo-first-order rate equation [198]:

$$\frac{dq_t}{dt} = k_1(q_e - q_t) \tag{3.19}$$

with linear form:

$$\ln(q_e - q_t) = \ln q_e - k_1 t \tag{3.20}$$

and Pseudo-second-order rate equation [199]:

$$\frac{dq_t}{dt} = k_2(q_e - q_t)^2 \tag{3.21}$$

with linear form:

$$\frac{t}{q_t} = \frac{1}{k_2 q_e^2} + \frac{t}{q_e} \tag{3.22}$$

where q_e and q_t are adsorption capacities (mg adsorbate/g adsorbent) at equilibrium and time t (h), respectively; k_1 is pseudo-first-order rate constant (h^{-1}); and k_2 is pseudo-second-order rate constant g/(mg.h). Adsorption capacity at any time t (q_t) can be obtained from Eq. (3.24):

$$q_t = \frac{(C_o - C_t)V}{m} \tag{3.24}$$

where C_o and C_t are phosphorus concentration in liquid phase at initial and at time t (mg/L), respectively; m is the mass of adsorbent (g); and V is the volume of phosphorus solution used in adsorption batch experiments.

Table 3-4 shows the results of data fitting using the indicated models, and the results suggested that the adsorption process using both under-investigated adsorbents followed the pseudo-first-order reaction model with high correlation coefficient (R^2). The results agreed with the previous discussion. Adsorption of P using nZVI in acidic medium had the highest reaction rate (k_1=10.56 h^{-1}, Table 3-4, Fig. 3-15), but a close rate could be achieved using NZVI with added CuCl$_2$ (k_1=6.24 h^{-1}, Table 3-4, Fig. 3-15). It is noticed that the kinetic rates were higher for NZVI/CuCl$_2$ especially in neutral and alkaline mediums.

Table 3-4. Kinetic values for pseudo first and second order models.

pH (Materials)	C_o (mg/l)	C_e (mg/l)	RE (%)	q_e (mg/l)	Pseudo first order		Pseudo second order	
					k_1 (h^{-1})	R^2	k_2 (g/mg.h)	R^2
pH 2 (nZVI)	50	0.3	99.4	49.7	10.56	0.89	0.0378	0.73
pH 7 (nZVI)	50	28	44	22	2.94	0.99	0.282	0.99
pH 10 (nZVI)	50	50	0	0	0	0	0	0
pH 2 (nZVI/CuCl$_2$)	50	0.23	99.54	49.77	2.34	0.94	0.00168	0.08
pH 7 (nZVI/CuCl$_2$)	50	0	100	50	6.24	0.99	0.468	0.99
pH 10 (nZVI/CuCl$_2$)	50	26.8	46.4	23.2	1.74	0.98	0.156	0.99

3.11. Recovery of contaminants

Phosphorus was recovered by desorption process at high pH (12) from the spent nZVI and nZVI/CuCl$_2$ resulted from batch experiments investigating pH effect. The spent solids that

resulted from examining the influence of acidic medium pH 2 and alkaline medium pH 10 are denoted as SpH 2 and SpH 10, respectively. Their kinetic profiles are shown in Fig. 3-19a in which the maximum recovery percentage achieved by spent particles was around 60 % (30 out of 50 mg PO_4^{3-}-P/L) from nZVI/CuCl$_2$. The original equilibrium adsorption time was roughly 60 min while the recovery (desorption) time was about the same value. The recovery of phosphorus in case of spent nZVI/CuCl$_2$ was in general slightly higher than that of spent nZVI, pointing out to a higher desorption equilibrium values and kinetics. It is noticeable that the recovery of phosphorus was low (about 41.5 %, 8.3 released out of 20 mg P/L originally adsorbed) from spent nZVI/CuCl$_2$ resulted from batch experiment operated at pH 10. It could be the formation of copper hydroxide compounds on the surface of nZVI prevented desorption of a part of phosphorus in the recovery process.

The recovery of phosphorus from spent nZVI or nZVI/CuCl$_2$ can reach 100% at higher basic medium (1 M NaOH). When operating on the recovery of phosphorus from spent nZVI or nZVI/CuCl$_2$ (resulted from batch experiments with neutral medium at initial P concentration 50 mg/L) using sodium hydroxide solutions of different molarities (0.04, 0.1, 0.25, 0.4 and 1 M), the results appeared in Figure 3-19b showed the effect of molarity of NaOH on the recovery percentage. The recovery of both spent irons were relatively close to each other, so the results were plotted together with mean values. It is obvious that the more alkaline the solution was, a better recovery was gained.
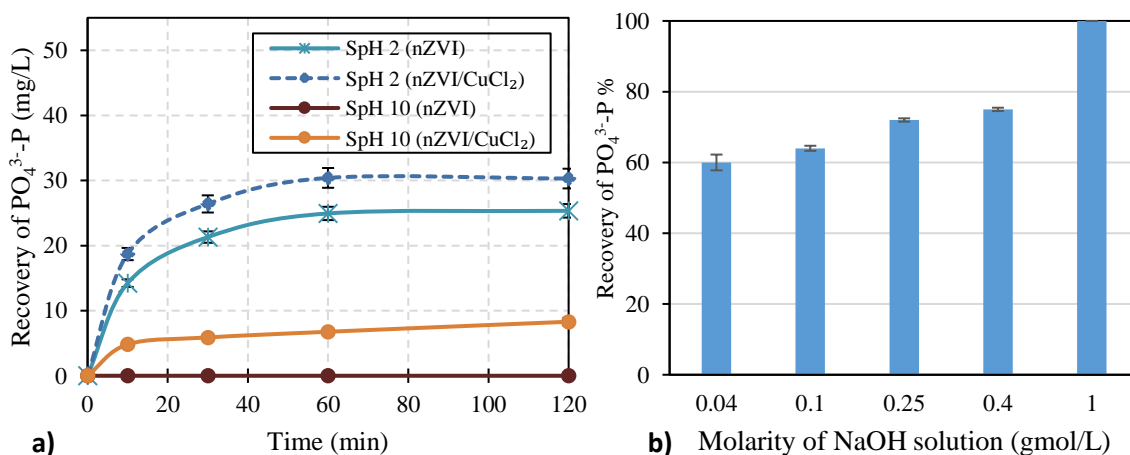
Fig. 3-19. a) Recovery of phosphorus from spent iron in alkaline medium of pH 12, and b) Recovery of phosphorus from spent nZVI or nZVI/CuCl$_2$ in alkaline medium of NaOH at different molarities (both spent irons extracted from batch experiments on neutral phosphorus solution of initial concentration 50 mg/L PO_4^{3-}-P).

3.12. Conclusions

In this chapter, nanoscale zero valent iron was synthesized to decontaminate nitrate from water. Via analysis and characterization, the obtained nZVI had a high surface area to unit mass (61 m^2/g), small nano size (39 nm), homogenous morphology and high reactivity which agreed with other nano-Fe^0 in previous reports. It was suitable enough to give a representative adsorption capacity of 28 mg PO_4^{3-}-P/ g nZVI in neutral conditions, similar to previous reports worked on the same issue. Copper chloride salt was added during nitrate reduction and phosphorus adsorption by nZVI to promote nitrate and phosphorus removal efficiency and their kinetics.

Concerning the effect on nitrate removal, the electrochemical and catalytic effects of copper ions enhanced nitrate removal kinetics around 3.5 times more than that by ordinary pristine nZVI solely and shortened time of removal by more than 67%. Hence, in a series of batch experiments under various conditions, copper-salt-added nZVI removed nitrate in alkaline and acidic mediums with relatively close efficiencies. Dissolved oxygen had only a little influence on nitrate removal in the presence of $CuCl_2$. With copper chloride addition, nitrate was reduced to safe regular limits for high concentration (500 mg/L) in an hour, while it was completely removed for lower concentrations in much shorter time. Kinetics of nitrate removal by nZVI with and without $CuCl_2$ addition followed first-order kinetic reaction model, while the second-order rate model could suit better reactions under aerobic condition. This research work demonstrated adding another type of contaminant as one of methods to promote reaction kinetics for nitrate remediation.

Concerning the effect on phosphorus removal, the adsorption capacity increased by copper chloride action via addition up to 50 mg PO_4^{3-}-P/ g nZVI and a complete removal was shortened to half of its original time (60 min). Increasing copper chloride load led to enhancing kinetics of removal, but it is important to select a load, which provides satisfactory results without endangering environment or wasting money. A ratio of 1:10 of $CuCl_2$/nZVI was previously selected in most of batch experiments especially on 50 mg PO_4^{3-}-P/L to clearly show kinetic profiles. These processes, such as increased corrosion rate, the formation of iron hydroxides that aided in phosphorus adsorption and production of copper ferrite compounds that catalysed the adsorption intake, played an important role in providing higher adsorption

capacities and kinetics for phosphorus removal via nZVI with copper chloride load. Investigating pH effect on phosphorus adsorption showed its influence on the adsorption process as the amount of adsorbed phosphorus incubated using nZVI increased along with decreasing pH value. The best performance carried out using acidic nZVI was closely resembled by adsorption using nZVI/CuCl$_2$ in a neutral medium. Also, addition of CuCl$_2$ increased adsorption capacity of nZVI for phosphorus from zero to 20 mg PO$_4^{3-}$ $-$ P/L in alkaline medium. In addition, the amount of recovered phosphorus was slightly higher when released from spent nZVI/CuCl$_2$ than that of ordinary nZVI. There was a direct relation between the degree of alkalinity of the basic solution used in phosphorus recovery and the amount of phosphorus recovered. A complete recovery was achieved in an alkaline solution of 1 M sodium hydroxide solution.

IMMOBILIZATION OF NZVI ONTO THERMAL-TREATED GRANULAR ACTIVATED CARBON

Chapter 4 Immobilization of nZVI onto Thermal-treated Granular Activated Carbon

This chapter suggests another modification that can increase both reactivity and mobility of nZVI particles. Different composites are produced of activated carbon supported nZVI under different synthesis and treatment conditions. The chapter shows the way of selecting the optimized composite from batch experimental studies against aqueous solutions of nitrate, phosphate and mixture of these contaminants, then discovers its properties and test its performance in interference studies comprising organic matters and group of common ions at different compositions. The results of these tests are explained, compared to that of nZVI, plotted in well-fitted kinetic models that takes into account the passivation of nZVI due to interferences.

4.1. Introduction

Despite its low dosage, high reactivity, easy operation and high cost effectiveness, nZVI has some concerns about its reliability in environmental applications. The nZVI particles are fine powders, which tend to agglomerate with each other forming necklace-like structures that hinder some active sites from participating in the decontamination process. These particles cannot also be utilized in fixed-bed columns unless they have granular shape. Other environmental pollution issues, such as iron pollution and rapid loss of nZVI in drinking water, may occur as a result of applying nZVI in a water treatment process [105]. Direct application of nZVI in a water treatment process, for example, a conventional treatment process, requires fast and total separation of nZVI via gravitational settling in order to recover, reuse and improve the effluent quality [132, 200]. Hence, nZVI should be carried onto supporting materials to overcome clumping aggregation of nanoparticles and to enhance their separation and hydraulic conductivity. The immobilization of nZVI by a supporter can be accomplished by trapping inside its pores or fixing of nZVI on its surface [201]. The idea is based on the distribution of nano-sized particles on the porous support material with a

larger surface area. Thus, this will provide more active sites leading to a higher reactivity [202].

Supported nanoscale zero valent iron showed higher efficacy and applicability in terms of mobility and packability than bare nanoscale zero valent iron in groundwater and wastewater treatment technologies [80, 203-205]. According to the type of application, the major restrictions of the widespread implementation of nZVI are summarized as: limited mobility and fast agglomeration as in nZVI injection in groundwater [203], the rapid loss of nZVI and its tiny non-granular particle shape as limitations in fixed-bed columns and permeable reactive barriers [105], or low settling rates of its tiny particles as a restriction to its deployment in conventional wastewater treatment process [200]. The supporting material can be designed with certain size and characteristics and controlled to overcome these restrictions for water remediation technologies.

Nano-scale zero-valent iron supported on activated carbon can provide an effective treatment for nitrate, phosphate or both of them co-existing with each other. In some reports [75, 145, 146, 165], unsupported nZVI proved its high efficacy in nitrate or phosphate removal from water. However, due to the agglomeration, sorbent separation and other problems, which were formerly mentioned, nZVI may not be completely suitable for direct application in wastewater treatment. The support, activated carbon, is environmentally-benign non-expensive material, and it can adsorb nitrate and phosphate. However, the presence of graphite or activated carbon with iron can act as electron accepting cathodes and promote iron corrosion [206, 207]. Cho et al. studied the effect of loading ratios of AC to nZVI on nitrate removal [208]. The study revealed that nZVI/AC is more susceptible to deactivation by oxidation compared to the unsupported Fe^0 nanoparticles and subjected to the mass transport limitation resulted from the thick layering of nZVI on porous AC. This led to the decreased reactivity of the supported material.

This chapter studied the best technique to support nano-scale zero-valent iron (nZVI) on granular activated carbon (GAC) through a detailed study to maximize its removal efficiency and kinetic rates of nitrate reduction and phosphate adsorption. A new technique of heat treatment before supporting nZVI was introduced and investigated for its promoting effect on the decontamination process. GAC and nZVI are important materials for water treatment [80, 209] , and this field would benefit of finding the best combination of them and

treatment method to achieve the best remediation results. Adding that researches related to simultaneous interference and removal of nitrate and phosphorus from water and, also, phosphorus removal by supported nZVI are scarce [210].

The objectives of this chapter are to investigate the effect of mass ratios of nZVI to ordinary/treated AC on removal efficiencies and kinetics of nitrate, phosphate or both coexisting contaminants in water and wastewater. Treatments of AC, such as thermal treatment [211, 212], acid treatment [213], acid-thermal treatment [214] and addition of ethanol, might reduce corrosion of iron and modify textural structure and surface chemistry of AC to attract phosphate and nitrate, adding that the increase of AC tendency to adsorb contaminants suits nitrate reduction by nZVI as a surface-mediated process [112]. This chapter also investigates the effect of the presence of Cu_2Cl_2, $CuCl_2$, $CaCO_3$ (hardness), humic acid and contaminants of domestic wastewater on the removal efficiency of nitrate and phosphate contaminants.

4.2. Synthesis of AC-supported nZVI

Ordinary nZVI was prepared following up the instructions shown in chapter 2, section 2.2 [145]. In the synthesis procedure of nZVI/AC, N_2-purged ferric chloride hexahydrate solution ($FeCl_3.6H_2O$, 0.1434 M) was mixed with a specific mass of activated carbon for 1 h, then sodium borohydride solution ($NaBH_4$, 98%, 1.1472 M) was pumped into the suspension mixture using a roller pump at a rate of 1 L/h with a volumetric ratio of 1:1 in 500 mL four-neck glass flask. A continuous flow of nitrogen gas maintained an anaerobic condition in order to achieve the best performance of nZVI by reducing its susceptibility to oxidation. The other conditions of the synthesis mixture were fixed, same as nZVI synthesis, such as stirring at 250 rpm under temperature 25 ± 0.5 ℃ using a water bath, and the aging time was 20 minutes in order to complete the reaction. After reduction, the jet-black suspension was washed with deionized water (DW >100 mL/g, 10% ethanol) and rinsed with anhydrous ethanol three times. The nZVI/AC slurry was finally separated by vacuum-filtering, anaerobically dried, and then used immediately in batch experiments. All aqueous solutions were prepared from water purified by a Milli-Q system (18 MΩ.cm).

4.3. Treatment methods

Several methods were proposed in order to produce a supported nZVI that matches in performance with nZVI reactivity or exceeds it. One of the problems, which faced the production of nZVI/AC and appeared in previous researches, was the rapid oxidation (instability) of nZVI supported on AC [105, 208]. Some reports mentioned using ethanol during nZVI synthesis to reduce oxidation by minimizing the contact with water [177], which could be approved as one of the treatment methods. The suggested method was performed by dissolving $FeCl_3.6H_2O$ in a 4/1 or 1/4 (v/v) ethanol/distilled water mixture during the synthesis of AC-supported nZVI. Activated carbon was treated with different ways prior to its application in the synthesis process of the supported nZVI. Acid treatment was conducted to wash/oxidize AC surface and remove any ashes, residues, etc. AC was washed with a mixture of concentrated hydrochloric and sulfuric acids (to eliminate ash from inside the carbon), then soaked in 8 M nitric acid at temperature 60 ^{o}C for 24 h or 90 ^{o}C for 6 h (as mentioned in literature researches [105, 214]) to examine different conditions and their effect on supporting nZVI for nitrate and phosphate removal. Thermal treatment process can be implemented on activated carbon particles to modify its pore structure and surface chemistry. AC was degassed, loaded on a ceramic crucible with cover (to minimize air exposure) and heated at elevated temperatures (550, 750 and 950 ^{o}C) in a muffle furnace for varied periods of time (1, 2 and 4 h). Different combinations of acid and thermal treatment were used with a view to finding the optimum conditions of treatment.

4.4. Batch experiments

Batch experiments were classified into three main categories: batch experiments dealing with concentration of nitrate 200 mg NO_3^-/L, denoted as batch I; batch experiments for phosphate (PO_4^{3-}) decontamination of 50 mg PO_4^{3-}-P/L (represented as phosphorus) which are batch II; and batch III are batch experiments for treating both coexisting contaminants at 200 mg NO_3^-/L and 50 mg PO_4^{3-}-P/L. All solutions used in all batch experiments were initially purged by a continuous flow of nitrogen gas for 30 minutes, so that the reactions could undergo under anaerobic conditions in closed conical flasks with tightened caps. Batch experiments were

examined in duplicates during our study to acquire a quality control and check on the accuracy of results and reproducibility of work.

Batch experiments were conducted at room temperature (25 ± 2 ^{o}C) using nZVI, AC, or nZVI/AC (composites) against 200 mL solutions (initial pH 7) of batches I, II and III in 300 mL conical flasks under 200 rpm shaking. At defined time intervals, 2 mL of solution sample were withdrawn and filtered through a 0.22 μm membrane for the analysis of nitrate, phosphorus, nitrite and ammonium. Batch experiments I, II and III were mainly carried out with the same previously-referred-to configuration except for added composites. If the added composite contained iron, its iron content was initially fixed at 200 mg (i.e., 1g Fe /L conc., which was applied in most of batch experiments). Activated carbon was added to batches and examined solely with different masses (1 and 5 grams), and it was used as a supporter for nZVI with different amounts and ratios that prepared the composite during synthesis. Due to various applications of treatment methods, composites used for nitrate and phosphate batch experiments are best presented in Table 4-1 which depicts their materials, mass ratios, denotations, and treatment conditions, such as nitric-acid treatment process temperature (Θ_N) with its duration (t_N) and thermal treatment process temperature (Θ_T) with its duration (t_T). Acid washing and treatment preceded thermal treatment of activated carbon, which was then applied in nZVI/AC synthesis process. As far as the composites in Table 4-1 are concerned, most of them were applied in batch experiments I, II and III to examine their performances (removal efficiency and kinetics).

Sorption tests were performed with GAC by adding 1 gram of it in each 200 mL of 10, 30, 50, 80, 100 and 120 mg/L nitrate solution and another 1 gram of GAC in each 200 mL of 5, 10, 15, 25, 35 and 50 mg PO_4^{3-} − P /L phosphate solution. The tests were conducted at room temperature (25 ± 2 °C) for 24 h under constant shaking at 250 rpm. The amount of adsorbate adsorbed per unit mass of adsorbent at equilibrium (q_e, mg/g) and equilibrium concentration (C_e, mg/L) were determined from these tests.

Table 4-1. Composites of AC-supported nZVI under assorted treatment conditions of activated carbon.

#	Denotation of Composite	nZVI : AC mass ratio	Θ_N, ºC	t_N, h	Θ_T, ºC	t_T, h
1	A	0	0	0	0	0
2	AT_2^{550}	0	0	0	550	2
3	AT_2^{750}	0	0	0	750	2
4	AT_2^{950}	0	0	0	950	2
5	AT_4^{950}	0	0	0	950	4
6	AN_{24}^{60}	0	60	24	0	0
7	AN_2^{90}	0	90	2	0	0
8	$AN_6^{90}T_2^{550}$	0	90	6	550	2
9	$AN_{24}^{60}T_4^{950}$	0	60	24	950	4
10	$AN_6^{90}T_4^{950}$	0	90	6	950	4
11	F	nFe^0 only	0	0	0	0
12	F_5^1A	1:5	0	0	0	0
13	$F_5^1AT_2^{950}$	1:5	0	0	950	2
14	$F_5^1AN_{24}^{60}T_4^{950}$	1:5	60	24	950	4
15	F_2^1A	1:2	0	0	0	0
16	$F_2^1AT_2^{950}$	1:2	0	0	950	2
17	FA	1:1	0	0	0	0
18	FAT_2^{950}	1:1	0	0	950	2
19	$FAN_6^{90}T_4^{950}$	1:1	90	6	950	4
20	F_1^2A	1:0.5	0	0	0	0
21	$F_1^2AT_1^{950}$	1:0.5	0	0	950	1
22	$F_1^2AT_2^{950}$	1:0.5	0	0	950	2
23	$F_1^2AT_4^{950}$	1:0.5	0	0	950	4
24	$F_1^2AN_{24}^{60}T_2^{950}$	1:0.5	60	24	950	2
25	$F_1^4AT_2^{950}$	1:0.25	0	0	950	2

$F_{n_2}^{n_1}AN_{n_4}^{n_3}T_{n_6}^{n_5}$ was used as a term to express the composite composition and type of treatment it received, where F stands for n-Fe^0, A for activated carbon, n_1 and n_2 together represent the mass ratio between nZVI to AC (n_1/n_2, gm Fe/gm AC), N and T stands for nitric-acid and thermal treatment, respectively. n_3 is the nitric-acid treatment temperature, ºC , whereas n_4 is the nitric-acid treatment time period (duration, h). By the same analogy, n_5 is the thermal treatment temperature, ºC, while n_6 is the thermal treatment duration, h.

4.5. Properties of nZVI and nZVI/AC

4.5.1. TEM investigation

Nanoscale zero-valent iron particles have a magnetic property and electrostatically-charged surfaces that result in combining particles together forming agglomerates as shown in TEM images of nZVI in Figs. 4-1 (a, b and c). The aggregated structure can prevent some active sites from participating in reactions by blocking their access to face contaminants. The particle size of nZVI was estimated from numerous TEM images to be about 10 nm in average, some of them appear in Figs. 4-1 (d and e) after disaggregation with ultra-sonication for 10 minutes. However, AC-supported nZVI particles appear in Figs. 4-2 (a, c and d) where nZVI particles are supported on AC particle surface (illustrated in the inserted image of Fig. 4-2a), which aid in more efficient utilization of surface area of nZVI. It is suggested that the pores were also occupied with nZVI particles which agrees with scanning electron microscopy images (SEM) reported in different studies [105, 208]. In some cases of using high mass ratio of nZVI to AC, some unsupported nZVI particles could exist as in using F_1^2A and F_1^4A, seen in Fig. 4-2b.
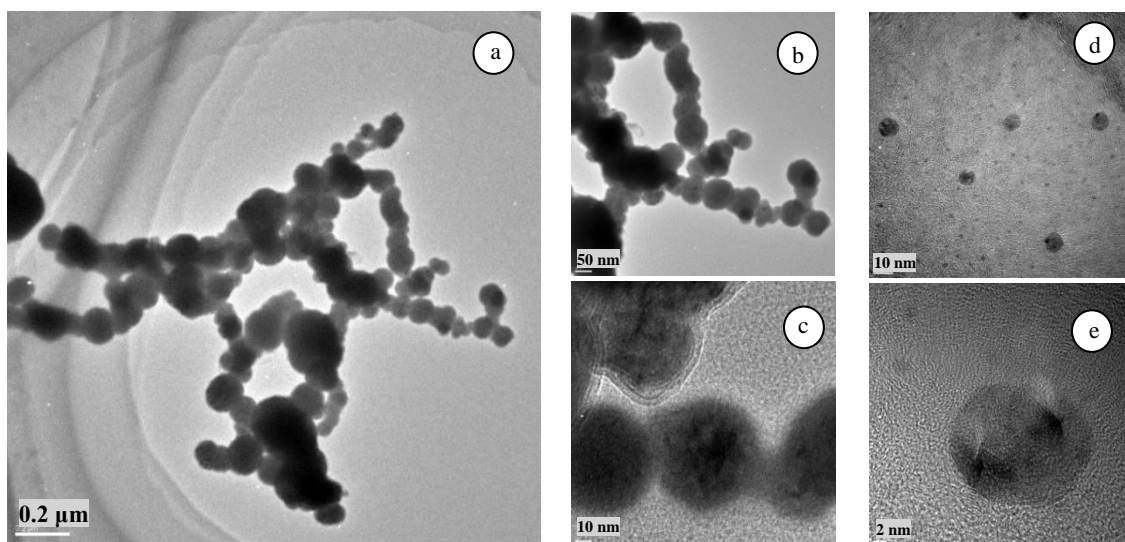
Fig. 4-1. Transmission electron microscopy (TEM) images of bare (unsupported) nZVI at resolutions of (a) 0.2 μm, (b) 50 nm and (c) 10 nm, and images of nZVI after ultrasonication at resolutions of (d) 10 nm and (e) 2 nm.
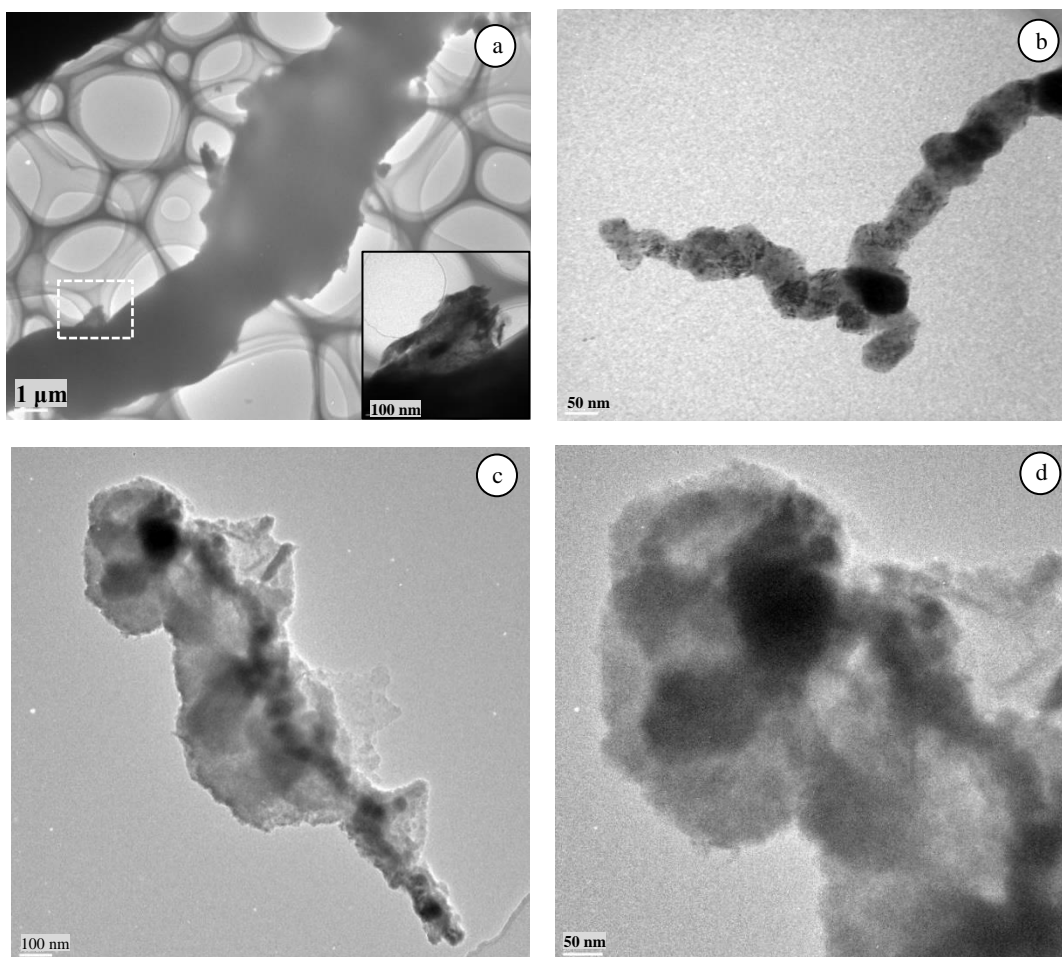
Fig. 4-2. TEM images of AC-supported nZVI at resolutions of (a) 1 μm and for inserted image of 100 nm, and (b) 50 nm (of free unsupported iron), (c) 100 nm and (d) 50 nm (more focus).

4.5.2. Size characterization

Table 4-2 presents the specific surface area and pore volume of nZVI and nZVI/AC at different mass ratios. As the mass ratio increased, the specific surface area decreased from 877 m^2/g (of activated carbon) in a relation close to the multiplication product of activated carbon mass fraction and BET specific surface area of AC. Therefore, by applying this relation, nZVI/AC at the mass ratio of 1:5 (F_5^1A) could have SSA of 730.8 m^2/g, and for F_2^1A and F_1^2A, BET SSA could be 584 and 292.3 m^2/g, respectively. Comparing these values with the analytical values in Table 4-2 indicates that nZVI covered AC surface according to its mass ratio, which is an important parameter to determine the degree of coverage to AC surface.

Pore volume is another important parameter that showed the location of nZVI on AC support. It was reduced 14.5% in case of supporting small portion of iron (F_5^1A, 16.6 wt% Fe). Also, it is added that the micropore (<2 nm) surface area of AC was 683 m²/g that accounted for more than 70% of its BET SSA, which was reduced, in case of F_5^1A, to 582 m²/g (14.8 % reduction). In case of F_2^1A (33.33 wt% Fe), the micropore surface area was 340 m²/g (~ 50.22% reduction) with a diminishing micropore volume of 0.1158 cm³/g (~ 65% reduction). This result indicated that increasing iron content led to the presence of more nZVI in the micropore area.

The average particle size of AC was 1 mm, and the aggregated particle size of nZVI was 6.56 μm. This result can also be deduced from the morphology of nZVI and its aggregates. The average particle size of AC-supported nZVI was within 0.6-1 mm range. However, at high amounts of nZVI (F_1^4A) in a composite, the unsupported part (nZVI) had aggregated particle size of 65 nm.

Table 4-2. General particle characterization of nZVI and nZVI/AC at different mass ratios.

Item	A	F	F_5^1A	F_2^1A	F_1^2A
BET SSA, m²/g	877	61	740	531	270
Micropore volume, cm³/g	0.33	0.0754	0.282	0.1158	0.05

4.5.3. XRD analyses

The XRD analysis pattern of nZVI/AC at ratio 1:5 (F_5^1A) is shown in Fig. 4-3. It describes that nZVI was found at its major reflection at 44.8° (2 theta), graphite clearly at 26.86°, and few of iron ferrite and iron carbide. The iron oxides were whether not determined or slightly detected, which could be due to their relatively small amounts. The latter result elucidated that if nZVI was more prone to oxidation by decreasing nZVI to AC ratio then more iron oxides should have been detected.

Phase name	Content %
iron high	25
Graphite-3R, syn	72
Iron Carbide	0.5
α-ferrite	2.5
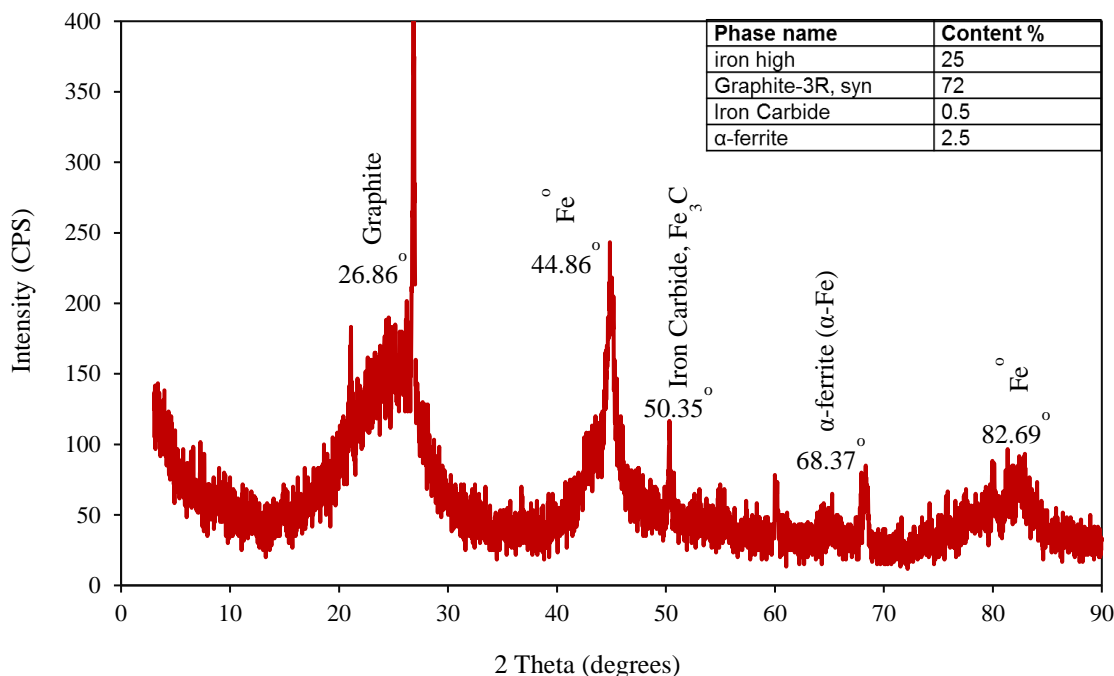
Fig. 4-3. X-ray diffraction analysis pattern of F^1_5A.

4.6. Optimizing best nZVI/AC ratio

Activated carbon carried nZVI at different mass ratios, their resulting composites were tested in batch experiments I and II, and their performance results are shown in Figs**.** 4-4 (a and b), respectively. Regarding batch experiments I, supporting with higher masses of AC led to lower equilibrium removal efficiencies (15 %, 28.5 % and 35% for F^1_5A, F^1_2A and *FA*, respectively). However, using lower masses of AC to support nZVI (F^2_1A) seemed to have slightly higher reduction ability (around 54%) than that of nZVI (41%). On another side, supported nZVI performed more efficient in adsorbing phosphate (> 60% removal) than nZVI (~45%). Again F^2_1A had the best removal efficiency among composites, and the same trend was noticed for the rest of composites. Although supporting on high surface area leads to higher chances of oxidation and corrosion [105, 208], besides ferrous and ferric ions can enhance adsorption process of phosphate [146], but this could not be the main explanation which did comply with nitrate reduction, however, it did not agree with the trend of phosphate adsorption among supported nZVIs. For example, F^1_5A should have the highest phosphate adsorption capacity as well as the lowest removal efficiency of nitrate, which was not the case. Adding that AC has a low adsorption capacity of phosphate (refer to Fig. 4-5b) and can

eliminate a part of nitrate (as in Fig. 4-5a) which increased significantly on applying 5 times of its original mass. The reaction rate depends on the probability of contacting each reactant with one another, so the higher the probability is, the higher the reaction rate is. Thus, increasing the mass and concentration of AC in the solution produced hindrance, which decreased the probability of contact between nZVI on the support and contaminants resulting in their lower performance.
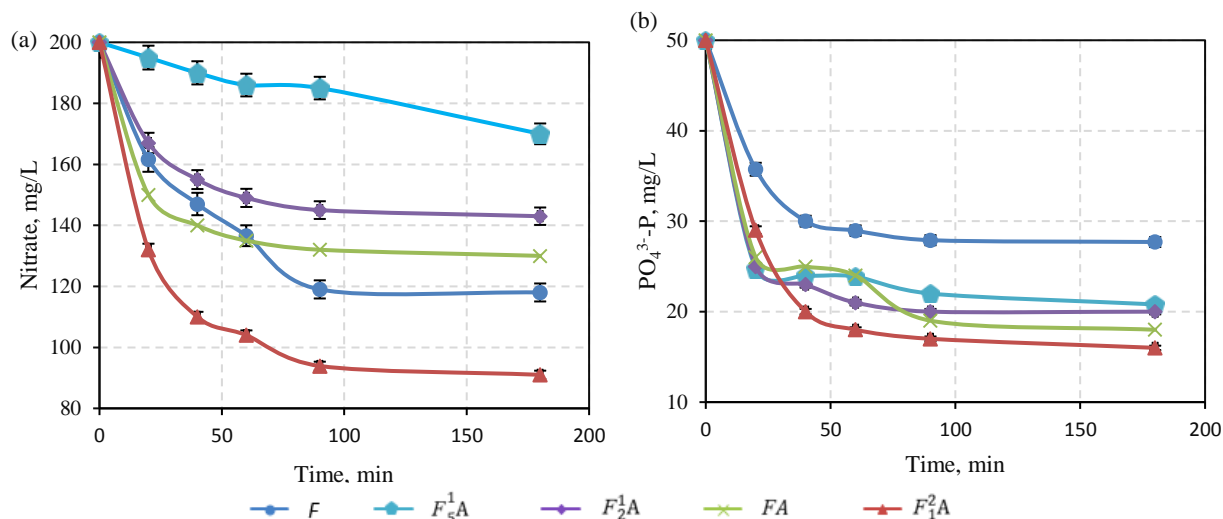
Fig. 4-4. Effect of supporting nZVI on AC at different mass ratios in (a) batch experiments I and (b) batch experiments II.
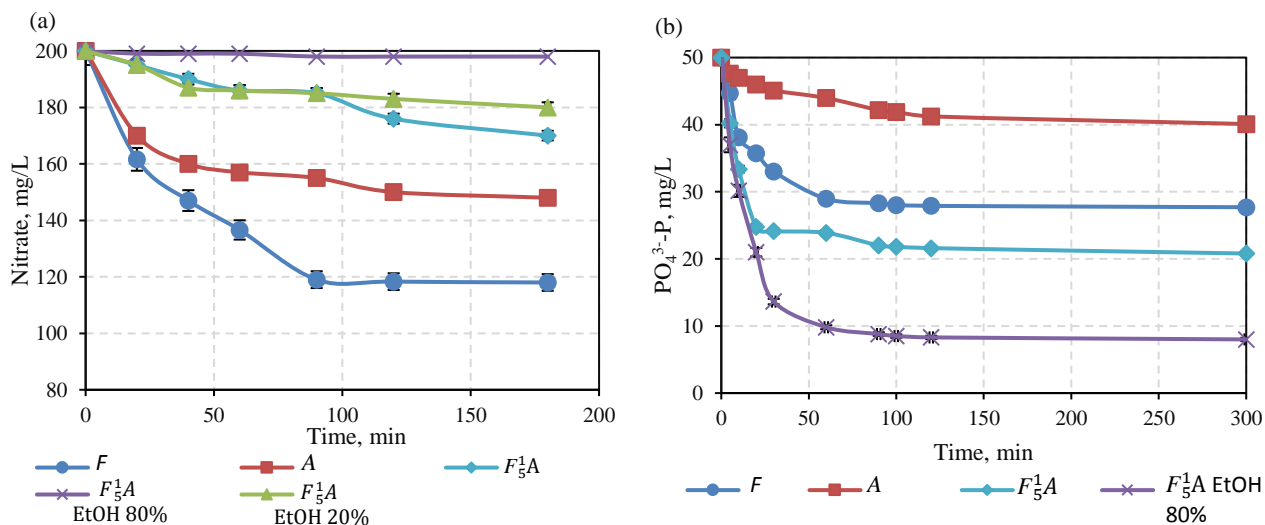
Fig. 4-5. The effect of using ethanol in the preparation of nZVI/AC (1:5) on (a) nitrate removal (batch I) and (b) phosphate removal (batch II).

4.7. Effect of treatment

Four kind of methods were studied that aim to produce enhanced AC-supported nZVI for nitrate and phosphate treatment purposes by overcoming oxidation of nZVI, modifying surface chemistry and charge to increase affinity towards these contaminants or by facilitating mass transport inside pores of activated carbon support.

4.7.1. Synthesis in ethanol-water medium

 In order to reduce oxidation, F_5^1A was synthesized in ethanol medium at two concentrations 20% and 80% by volume, consequently used in batch I and II experiments. The results, presented in Fig. 4-5, show the negative impact of using ethanol in the synthesis process of AC-supported nZVI. The removal percentage of nitrate, in batch experiments I, decreased along with increasing ethanol volume, it was reduced from 15% in pure distilled water medium to 10% and 1% at 20% and 80% ethanol by volume, respectively. On contrary, the phosphate removal for F_5^1A was enhanced from 60% to 84 % when prepared originally in ethanol medium of 80% composition by volume and the rest was distilled water. To explain these results, XRD analysis was carried out on a sample of F_5^1A EtOH 80%, from which the pattern was obtained in Fig. 4-6. Apart from some elements and compounds were found the same as identified in Fig. 4-3 (showing XRD pattern of F_5^1A that detected Graphite and Fe^0), some other iron oxides (FeO, Fe_2O_3) appeared, such as wustite and hematite, in high amount (ca. 35% wt) which states the oxidation of nZVI and agrees with other reports [105, 208, 213]. Activated carbon has affinity to adsorb ethanol [215] which might have occupied the micro porous structure leaving the majority of nZVI on the outer surface with higher probability of oxidation.

4.7.2. Action of treating activated carbon with three treatment methods

Activated carbon, originally, presents significant sorption capacities of nitrate and phosphate contaminants [216-218]. Individual nitrate and phosphate adsorption tests were conducted using activated carbon. Figs. 4-7(a and b) show the experimental and estimated results obtained from Langmuir model for the nitrate and phosphate sorption process using AC. Among some tested mathematical sorption models, Langmuir adsorption isotherm model was

the best fit to the existing experimental data. This sorption ability exhibited by AC can be affected by the treatment method which in turn can affect the supporting process of nZVI.

Nitric-acid treatment, thermal modification\treatment and nitric-acid thermal treatment were applied on AC for batch experiments I (as seen in Fig. 4-8). Nitrate sorption favored high temperatures of thermal treatment for moderate durations, as shown in Fig. 4-8a. Among different treatment temperatures and durations, nitrate sorption capacity was increased for optimized conditions of thermal treatment of AC at 950 °C and 2 hours.

The higher intake of nitrate might evidently prove the expansion of pores of AC, which can take a part in modifying the performance of AC-supported nZVI. However, Zhang et al. provided proofs on the expansion of the microcrystalline structure of AC by the modification temperature ranging from 700 to 1100 °C, subsequently the pore morphology was slightly degraded and collapsed resulting in a decrease in BET SSA and pore volume along with increasing pore diameter and external surface area [165]. It was inferred that the surface chemistry property of AC exhibited a major role in attracting nitrate groups (negatively charged groups in general). The thermal treatment/modification decreased the total amount of oxygen-containing functional groups (carboxyl, lactonic and phenolic groups) to minimum at 900 °C, which favored nitrate adsorption.

Fig. 4-8b demonstrates the effect of nitric acid treatment on AC. As it is shown that the nitrate sorption dramatically decreased, and the sorption of nitric acid prior to the batch experiment might be the reason for the poor sorption. However, if thermal treatment was applied after nitric acid treatment process, the sorption of nitrate was promoted. Nitric-acid treatment process targets oxidation of AC surface, and then by heat action, oxygen-containing groups were decomposed leaving basic groups on the surface. According to Ota et al., the surface charge of AC became positive which attracted nitrate with high affinity [214]. In general, composite AT_2^{950} was the best performer in nitrate removal followed by $AN_{24}^{60}T_4^{950}$ for the same mass of AC (1 g). For further confirmation on the promoting effect of treatment, results describing treatment action on composites of different nZVI:AC ratios are shown in the upcoming section.

Phase name	Content %
Wustite, syn	24
β``-Fe$_2$O$_3$	0.5
Iron Oxide a	6
Hematite	4
iron high	16
Graphite-3R	28
Carbon	21
Iron Oxide b	0.5
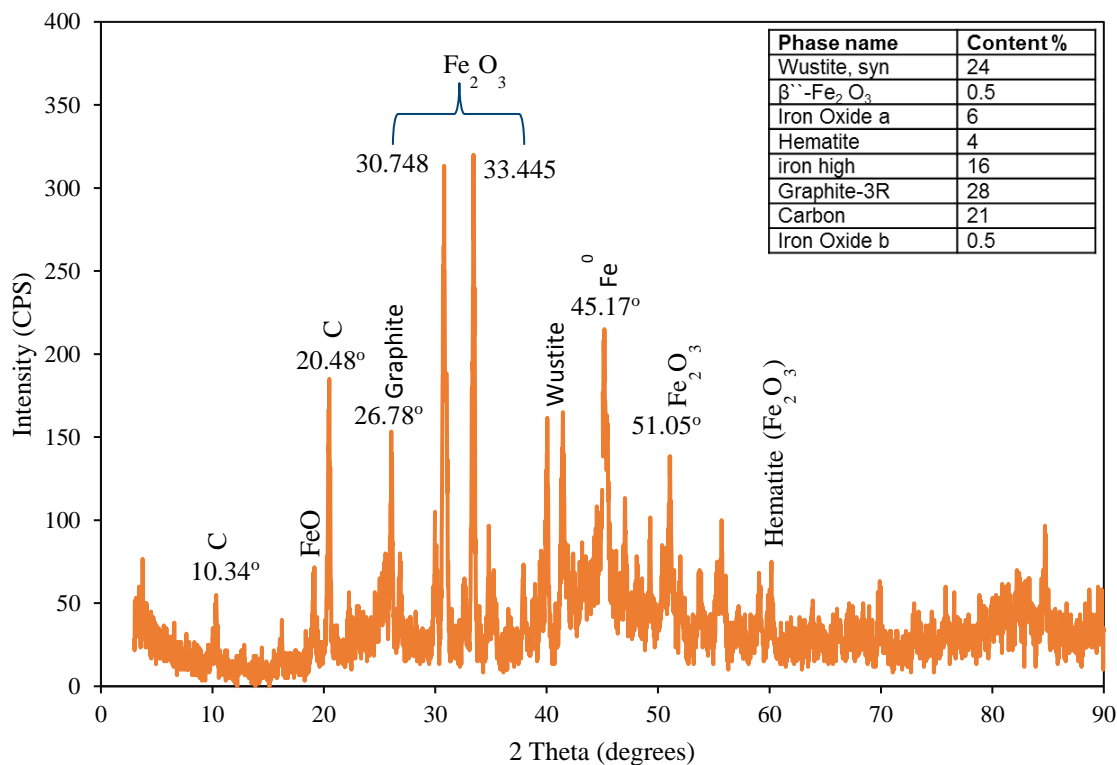
Fig. 4-6. The XRD diffractogram of $F^1{}_5A$ EtOH 80%.
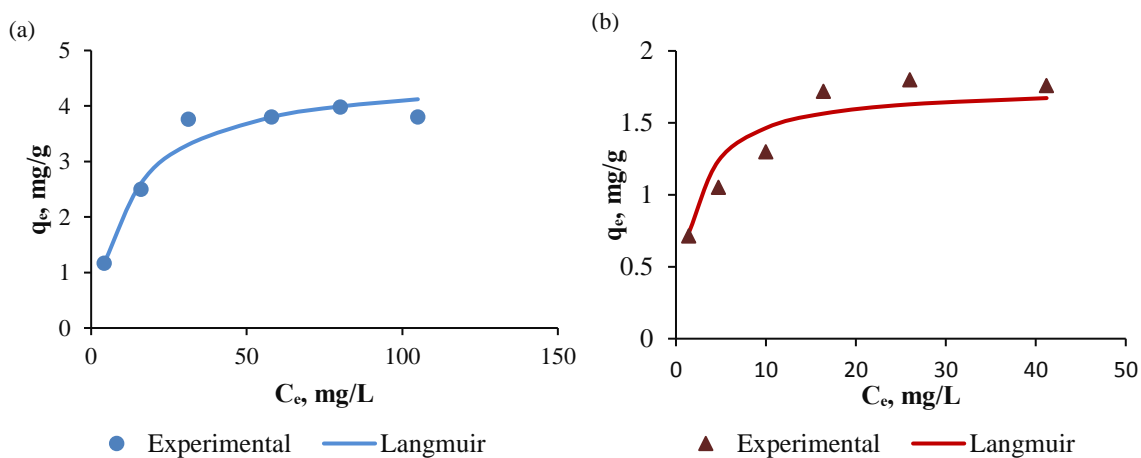
Fig. 4-7. Adsorption isotherm of (a) nitrate and (b) phosphate using AC best described by Langmuir equilibrium isotherms ($q_e = q_mK_LC_e/(1+K_LC_e)$), where K_L (the constant of surface energy) = (a) 0.0813 L/mg and (b) 0.5085 L/mg, and q_m (the maximum capacity of sorption) = (a) 4.6 mg/g and (b) 1.75 mg/g.
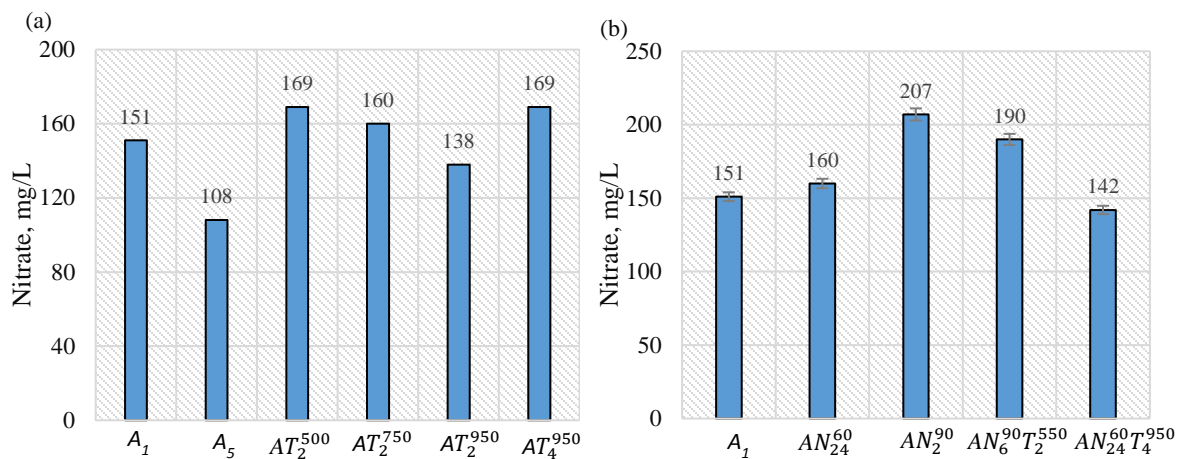
Fig. 4-8. Effect of (a) thermal treatment and (b) nitric-acid thermal treatment on AC (Batch experiments I).

4.7.3. Treatment action on composites of different nZVI:AC ratios

At mass ratio nZVI to AC of 1:5 (F_5^1A), as previously observed, the performance of untreated F_5^1A was weak in nitrate removal, which was lower than nano iron itself. However, if the treatment was applied to AC before synthesis of F_5^1A, nitrate removal was enhanced up to the same performance of nZVI as in case of $F_5^1AT_2^{950}$ (refer to Fig. 4-9a). This composite adsorbed phosphate with ca. 75% removal efficiency within 100 min compared to that of nZVI with ca. 45% as shown in Fig. 4-9b.

Thermal treatment seemed to produce reasonable enhancement at ratio 1:5 (F_5^1A), so it was applied to another ratio 1:2 (F_2^1A). Fig. 4-10 depicted the effect of this application on batch experiments I and II. In this case, the untreated F_2^1A performed lower than nZVI (F) in nitrate removal, but thermal treated F_2^1A, especially $F_2^1AT_2^{950}$, outperformed the untreated composite and nZVI as in Fig. 4-10a. Not only the outperformance did occur in nitrate removal experiments, but also it happened with phosphate removal (Fig. 4-10b).

The composite of equal amounts of nZVI and AC (FA) was examined with thermal treatment and acid thermal treatment, and the results of application in batch I and II experiments are found in Fig. 4-11. As presented in Fig. 4-11a, $FAN_6^{90}T_4^{950}$ acquired nearly the same removal efficiency of nitrate by nZVI but with a higher kinetic rate. FAT_2^{950} had a higher performance to remove nitrate (ca. 59%) and reliable performance to treat phosphate (ca. 86%) separately in batches I and II as noticed in Figs. 4-11(a and b), respectively. These

experiments were still confirming up until this point the enhancing additional value of the thermal treatment process.

The composite of optimum mass ratio of nZVI/AC (F_1^2A) was studied under intensive investigation to acquire the optimum conditions for a treatment in Figs. 4-12 and 4-13. Regarding thermal treatment, activated carbon of composite F_1^2A was thermally treated at 950 ℃ and at different periods (1, 2 and 4 h) in Fig. 4-12a. The composite $F_1^2AT_2^{950}$ succeeded in removing nitrate with a removal efficiency (ca. 67.5%) 1.5 times more than that of iron (ca. 45%) and more than 25% increase in nitrate removal than untreated F_1^2A. The 1-h period began the slight improvement then the optimum thermal treatment period was 2 h among tested time periods. On contrary, treating in 4 h made a reverse effect on nitrate removal performance, turned out to a quite similar nitrate removal profile to that of untreated F_1^2A. The phosphate adsorption removal profiles were almost the same for thermally-treated composites with a high intake of (ca. 85%) leaving untreated F_1^2A with ca. 68% and nZVI with ca. 45%. Also, the nitric acid-thermal treated composite was tested as in Fig. 4-13, which showed that it had a very close performance to that of $F_1^2AT_2^{950}$ in both contaminants removal.
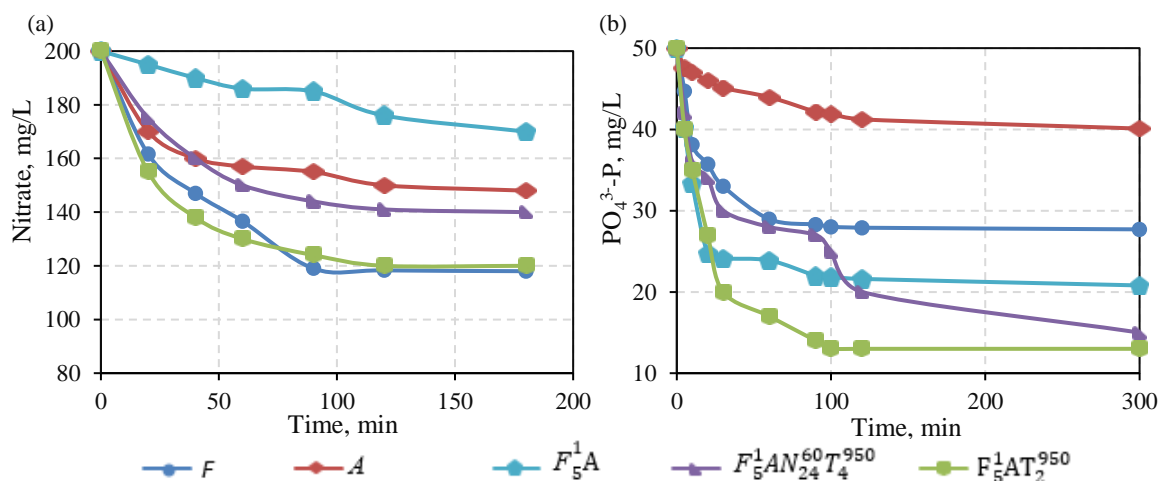
Fig. 4-9. Nitrate reduction profiles for treated composite nZVI/AC at ratio 1:5 in Batch experiments (a) I and (b) II.
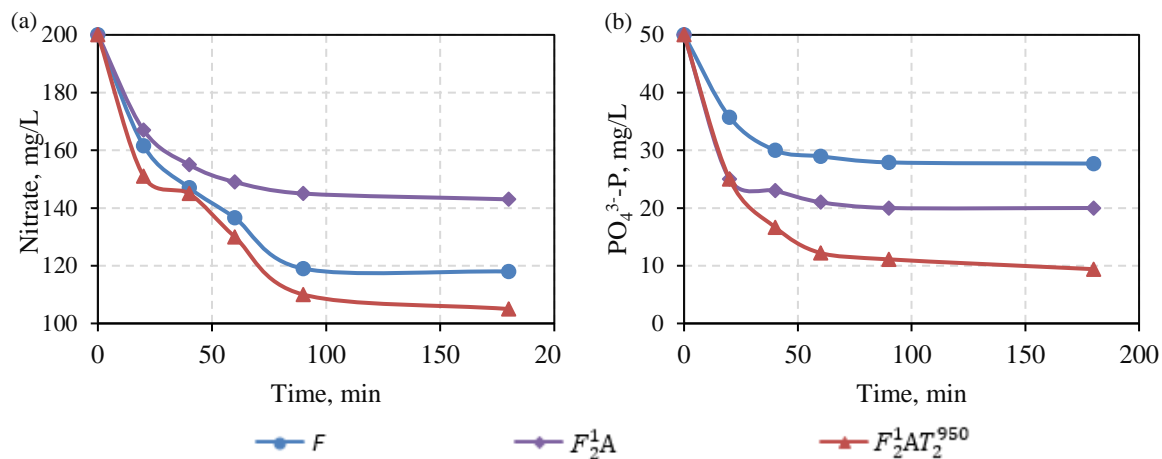
Fig. 4-10. The effect of thermal treatment on (a) nitrate reduction in batch I and (b) phosphate removal in batch II by nZVI/AC (1:2).
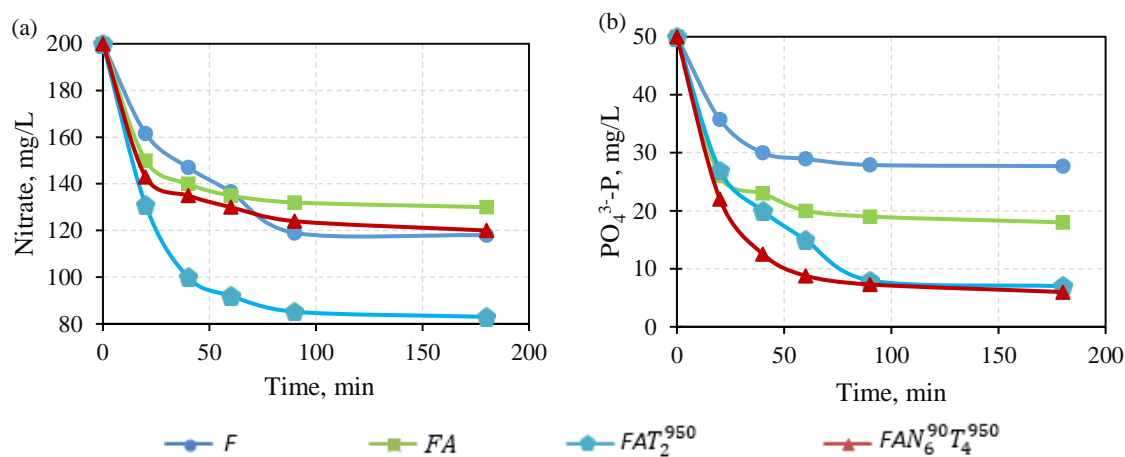
Fig. 4-11. Thermal or/and nitric-acid treatment for nZVI/AC (1:1) in (a) batch experiments I and (b) batch experiments II.
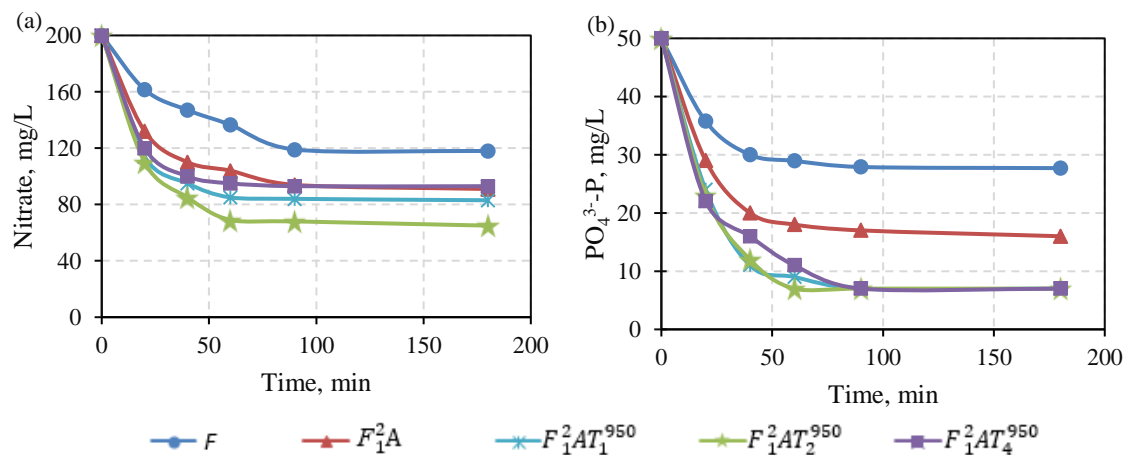
Fig. 4-12. The influence of thermal treatment duration on removal performance of F^2_1A in experiments (a) I and (b) II.
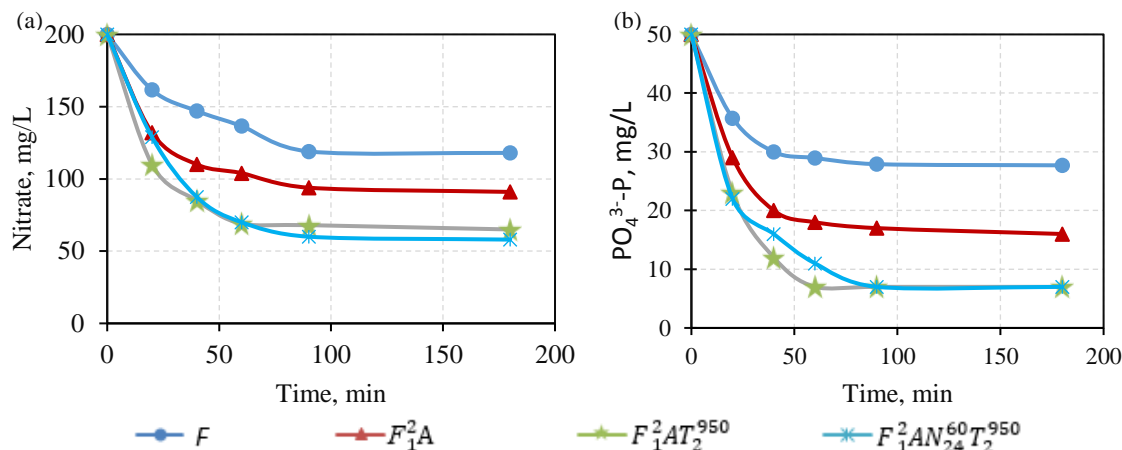
Fig. 4-13. The performance of nitric-acid thermal treated $F^2_1AN^{60}_{24}T^{950}_2$ in batch experiments (a) I and (b) II.

4.7.4. Performance in batch experiments III

Nitrate (200 mg/L) and phosphate (50 mg/L as P) solution in batch experiments III was subjected to some of the aforementioned composites and nZVI in separate experiments. Using nZVI, the presence of high concentration of phosphate led to a dramatic decrease in nitrate removal efficiency (15%) compared to phosphate-free nitrate solution (ca. 40%), while, on the other hand, phosphate removal efficiency was elevated from ca. 45% (for nitrate-free phosphate solution) to about 95%. Performance curves are shown in Fig. 4-14 in which all batch experiments of nZVI are presented in order to compare profiles. From the graph, it is shown that phosphate removal kinetics was greater than the reduction kinetics of nitrate in batch III, and it seemed that phosphate adsorption occurred rapidly at first which left the nitrate contaminant to the spent iron. Adding that nitrate reduction by nZVI resulted in the formation of iron I and II (hydr)oxides that can promote phosphate adsorption capacity and kinetics [145, 146].

The composites passed through performance investigations in these batch experiments III. Starting with composite *FA*, nitrate and phosphate removal kinetics of thermally treated *FA* had a close resemblance to that of nZVI, while untreated *FA* had the lowest efficiency, as shown in Fig. 4-15. The performance of composite F^2_1A and its treated derivatives are depicted in Fig. 4-16. $F^2_1AT^{950}_2$ had the highest removal efficiency (ca. 43% for nitrate and 90 % for phosphate) within 1h of treatment. Most of composites outperformed nZVI in nitrate removal treatment experiments, and they showed close performances in the

vicinity of nZVI results of phosphate removal. The high performance of $F_1^2 AT_2^{950}$ in batch experiments III might be attributed to the porous structure of AC which prevents the quick consumption of nZVI by either one of contaminants on the behalf of another, because the kinetics of reaction relies on mass transfer step and diffusion resistance through pores, so there would be some amount of non-spent nZVI at the pores at which the reduction reaction or adsorption could occur.
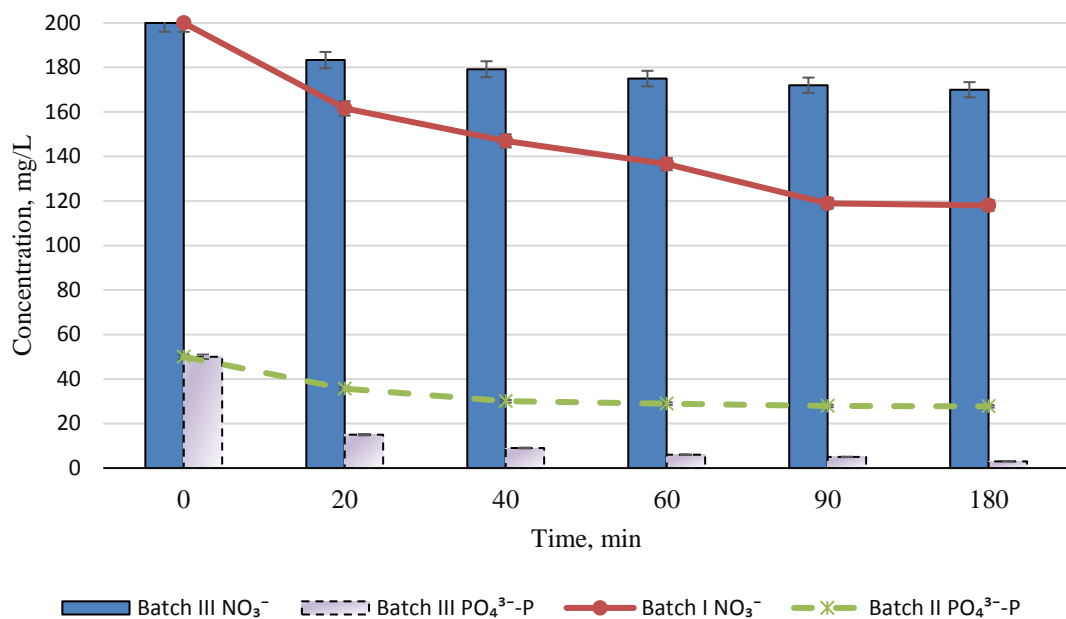
Fig. 4-14. Performance of nZVI in batch experiments I, II and III.
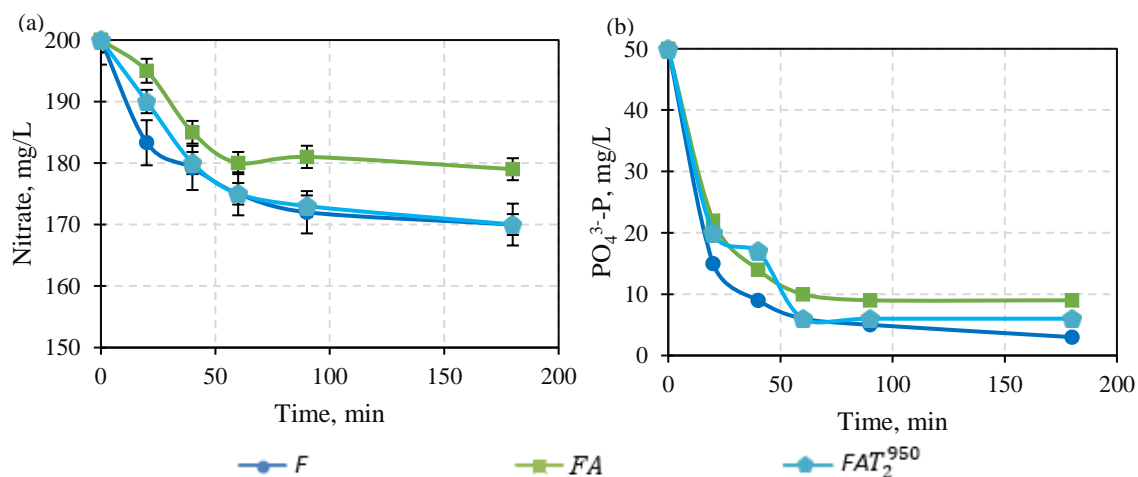
Fig. 4-15. Thermal or/and nitric-acid treatment for nZVI/AC (1:1) in batch experiment III presenting (a) nitrate and (b) phosphate removal.
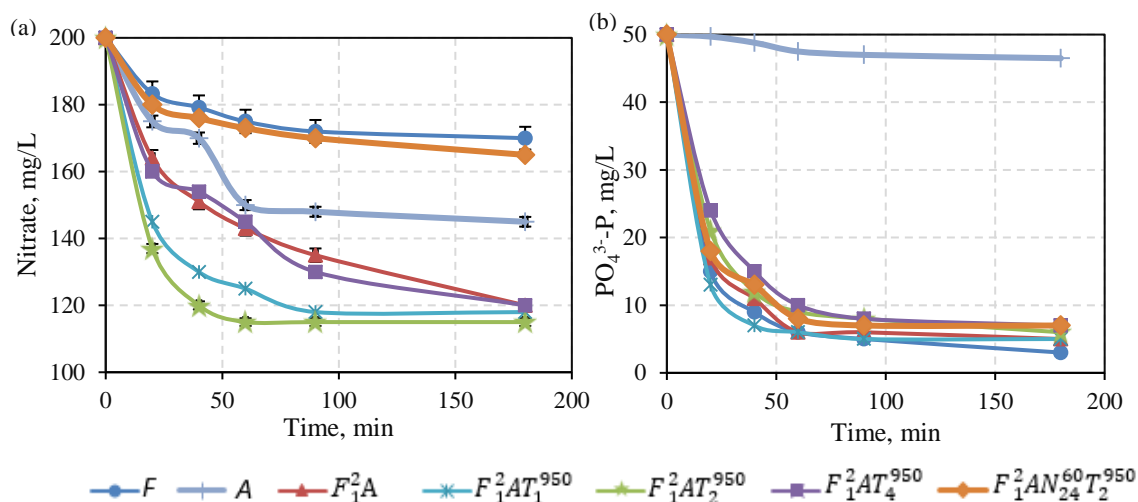
Fig. 4-16. The removal of (a) nitrate and (b) phosphate by treated composites F^2_1A in batch experiments III.

4.8. Obtaining composite of optimum treatment conditions

4.8.1. Obtaining optimum composite from nitrate and phosphorus profiles

A thermally treated composite $F^2_1AT^{950}_2$ proved to be the best performer so far with the optimum treatment conditions in decontamination of nitrate and phosphate solutions and mixtures. Yet it was still needed to confirm the optimum mass ratio of nZVI to AC. Hence, larger mass of nZVI was used when testing $F^4_1AT^{950}_2$ at its optimum treatment conditions of AC. The results, revealed in Fig. 4-17, made a comparison between AC-supported nZVI at several mass ratios and optimum treatment conditions for nitrate removal purpose in batch experiment I. By tracking nitrate removal curves in Fig. 4-17a and removal efficiencies of those composites after a period of 90 min in Fig. 4-17b, it was confirmed that $F^2_1AT^{950}_2$ had the highest performance, whereas $F^4_1AT^{950}_2$ performed in almost the same way as nZVI. The lower mass of AC compared to nZVI reduced the supporting effect of AC on nZVI, so both profiles of nZVI (F) and $F^4_1AT^{950}_2$ were almost close to each other. $F^2_1AT^{950}_2$ might have the optimum mass ratio among tested composites which almost support most of nZVI particles. In this research study, $F^2_1AT^{950}_2$ was assigned to be the best composite with optimum treatment conditions based on the collected data, designated as O-Fe^0/AC. However, due to low mass of AC and slightly inhomogeneous mixing in the synthesis process, $F^2_1AT^{950}_2$ could

have some small amounts of unsupported nZVI, as shown in TEM images in Fig. 4-2b. This issue can be solved by increasing the homogeneity inside the reactor during synthesis process and/or by slightly increasing the mass of AC. Even if the mass ratio of 1:1 (FAT_2^{950}) is used in the conventional treatment process in wastewater treatment plant, it has higher performance than nZVI with anticipated higher settling rates and lower iron loss then it can be separated easily in the clarifier. It can be also successfully applied in packed columns and permeable reactive barriers for contaminant removal purposes. In addition, it can be used in groundwater treatment via injection wells with controlled mobility (according to supporter's size) that enables the composite to propagate easily to the desired remediation location.

The reduction and adsorption processes of contaminants by nZVI can be improved when the contaminant directly contacts nano iron surface in a surface-mediated process. Thermal treatment changed textural properties of AC support through increasing pore size and external surface area and decreasing pore volume and total specific surface area. When nZVI particles filled the contracted volume of the pores of AC, they might come closer to the external surface, and then mass transport could be facilitated. But, according to previously stated in thermal modification reports, the surface chemistry has changed by decaying carboxyl, lactonic and phenolic groups, and the basic groups remained to provide surface of AC support with positive charge. This was capable of attracting NO_3^- to the surface of AC, which could mediate between nitrate contaminant, and nZVI surface. Phosphate (PO_4^{3-}) has a higher negative charge which means more attraction towards AC surface, and which explains its higher removal efficiency than that of nitrate.
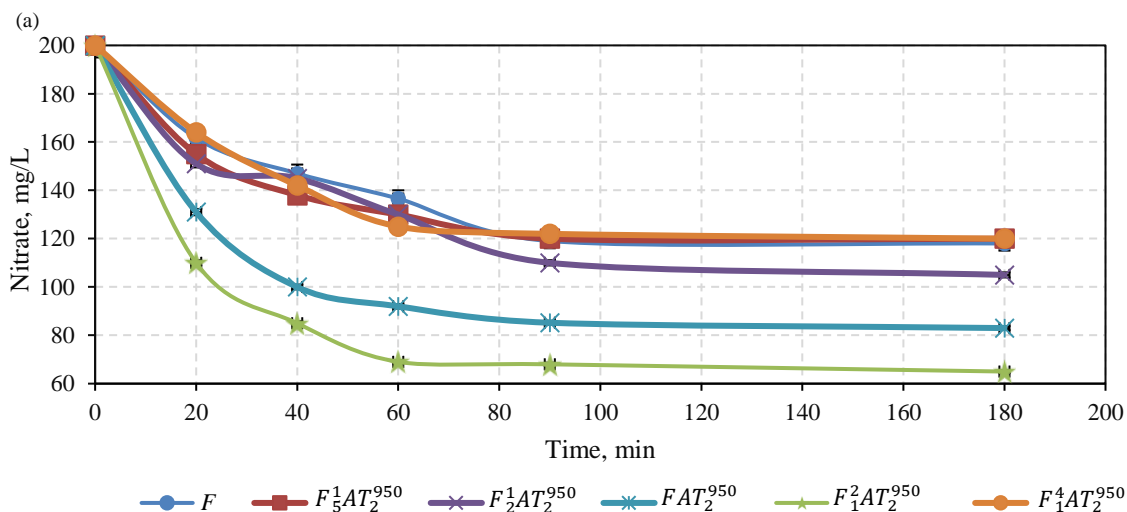
(a)
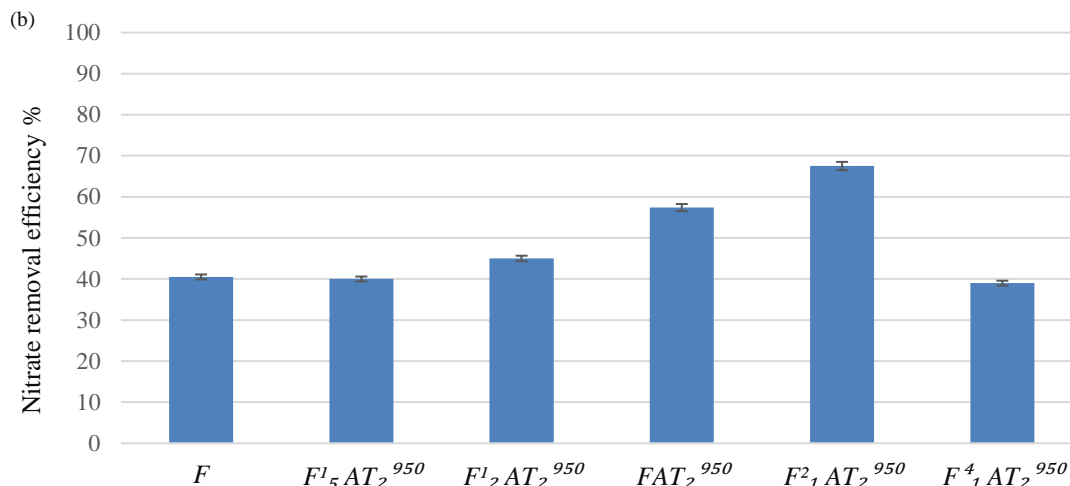
Fig. 4-17. (a) The removal profiles of nitrate and (b) their removal efficiency at 90 min by thermal treated composites of nZVI/AC at different mass ratios in batch experiments I.

4.8.2. Nitrite, ammonia and nitrogen profiles

Nitrate (NO_3^-) was reduced by nZVI or nZVI/AC to produce nitrite (NO_2^-), ammonia (NH_4^+) and nitrogen gas [85, 145]. Nitrite was involved again in a reduction reaction by nZVI particles to form ammonia and nitrogen gas. To study the influence of AC (as predicted to be a support and inert material), nitrite, ammonia and evolved nitrogen (calculated from subtracting total nitrogen concentration from initial nitrogen concentration) were monitored for some examples of composites (F_1^2A, $F_1^2AN_{24}^{60}T_2^{950}$ and $F_2^1AT_2^{950}$) in batch experiments I. Figs. 4-18(a, b and c) describe these profiles of nitrate reduction to nitrite, ammonia and evolved nitrogen (expressed as mg/L), respectively. Nitrite concentrations generated from all composites were higher than that produced from nano iron with being that of treated composites the highest. However, nitrite concentrations decreased to lower values after more than 5 h of treatment. Ammonia was produced in large quantities for the nitric-acid washed/treated of the optimum composite ($F_1^2AN_{24}^{60}T_2^{950}$), and ammonia release was usually an indication for high removal efficiency of nitrate, and it is worth mentioning here that AC is a weak adsorber of ammonia [219]. $F_1^2AN_{24}^{60}T_2^{950}$ production of ammonia reached 29.4 mg/L at 90 min compared to 16.7 mg/L from nZVI at the same time. Regarding evolved nitrogen, high amount was produced from untreated F_1^2A which compensated for its lower ammonia production (observed in Figs. 4-18 (b and c)). In this case, nitrate reduction process favored nitrogen over ammonia production. However, high ammonia release is not a series

problem (in case of composites with treated AC) as more than 90% of ammonia can be stripped within several hours from experiment's solution using flowing air in alkaline medium, especially the solution pH was already high (>10).
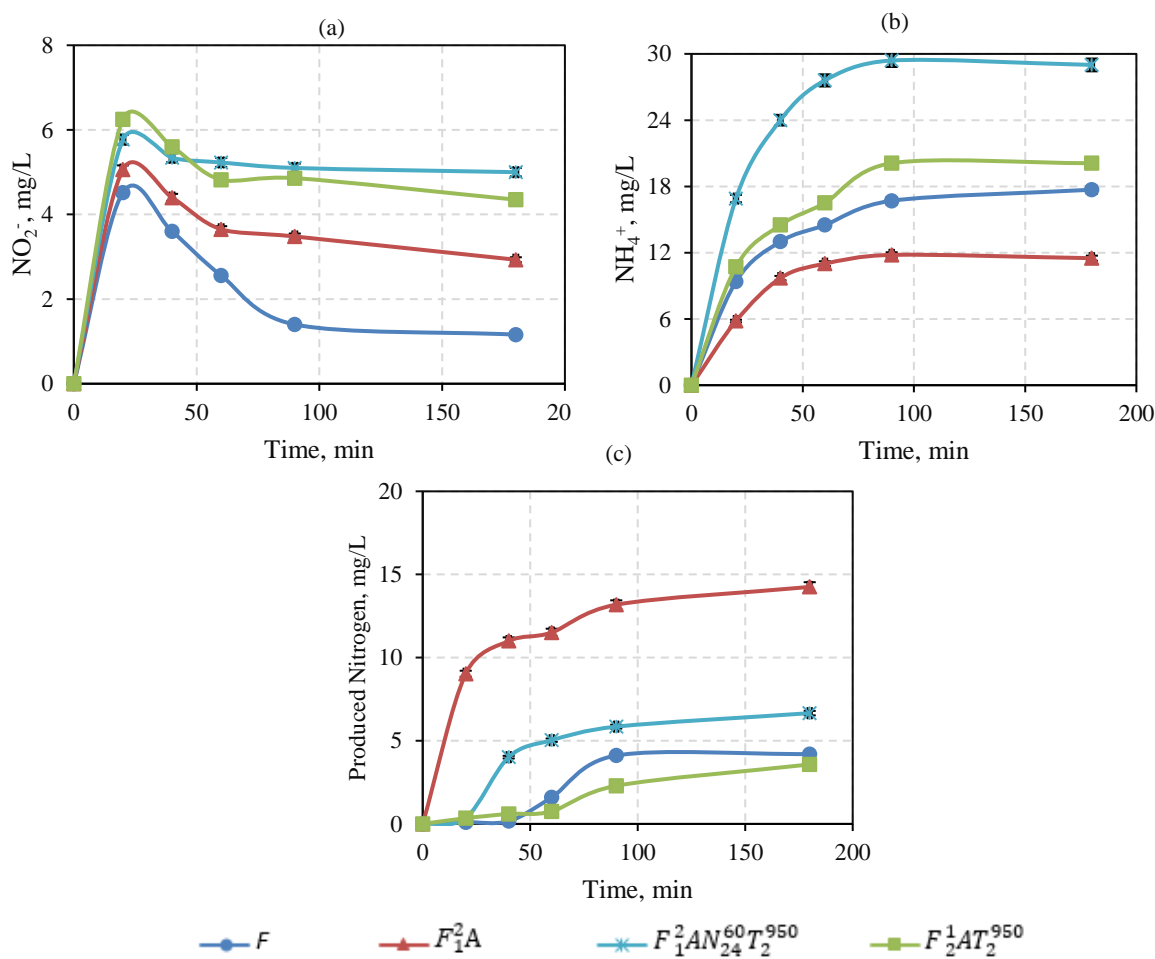
Fig. 4-18. (a) Nitrite, (b) ammonia and (c) evolved nitrogen profiles for nZVI and AC-supported nZVI in batch experiments I.

4.9. Interference studies

4.9.1. Introduction

It is well known form the literature that nZVI particle can undergo treatment process for each contaminant via different mechanisms, and the kinetic rate may differ in each mechanism. In spite of its advantageous properties, though, the major defect of nZVI is its prospective sensitivity to the presence of intervening matters. The existence of minerals, organic matters and other components greatly affects the kinetic rate and efficiency of the remediation

process. The problem exacerbates more if more than one pollutant exists among these intervening matters which requires simultaneous removal of contaminants.

The interference effect occurs when more than one substance coexists in the solution whether this interfering substance is a hazardous pollutant exceeding conventional thresholds or contaminant under safe guideline limits. The presence of this or these interfering substance(s) intervene with the efficiency and performance of the chemical reagent (nZVI) to treat the target contaminant that requires elimination to the extent of safe regulation. This situation of numerous components presenting all together in one medium (water body) is the actual case of treatment. Usually different water bodies contain diverse compositions of different concentrations, but for the same category, the water bodies contain some substances in common. For example, Natural waters (sea water, ground water and river water) contain organic matter as humic acid and minerals including dissolved cations of calcium, sodium, potassium, magnesium, and other elements, along with anions of bicarbonates, sulfates, chlorides and others [220]. If the water body is contaminated with a certain hazardous pollutant, precautions should be engaged in design of treatment equipment determination of the number of operating units (pre-treatment, primary, advanced, etc.) and the calculation of dosage amounts of treating reagent as the existence of these minerals, organic matters and other components greatly affects kinetic rates and efficiencies of remediation process. The problem exacerbates more if more than one pollutant exists among these intervening matters, which requires simultaneous removal of contaminants.

A few numbers of studies chose during their original investigations to inspect interference impact on the removal efficiency of a certain contaminant using nZVI and its counterparts [156, 176, 221]. Other reports extensively studied the effect of substance interference and characteristics of water bodies on the effectiveness of nanoscale or microscale ZVI for contaminant sequestration [222-227]. It was reported that phosphate uptake by nZVI was neither affected by ionic strength of the solution nor by the presence of coexisting ions, except for the carbonate ion [176]. The latter ion decreased the phosphate removal by more than 80%. These results confirmed another older report within the same subject and reached to close observations and concluded the low impact of coexisting common ions of natural waters and wastewaters on phosphate adsorption [228]. A complete nitrate removal was conducted by Su et al. when Cd ions coexisted within a certain value

and, depending on this value, the composition of nitrate reduction products changed [156]. In addition, nitrate ions enhanced Cd precipitation and increased the removal capacity of Cd (II) by nZVI greater than four times the original capacity. Simulated Cd and nitrate contaminated groundwater (Santa Barbara, California, USA) was the medium for some of their experiments to test the efficacy of bimetallic nZVI-Au in actual cases. After that, in another report, bare nZVI and sulfide-modified iron (S-nZVI) were tested in different water matrices contaminated with Cd [221]. Cd removal efficiencies of both nZVIs decreased in nanopure water body. On contrary, the efficiencies were significantly improved in a river water body. While in case of sea water, groundwater and wastewater, each type of nZVI gave mixed performances. Meanwhile another contaminant, arsenic, was treated with zero-valent iron particles in a simulated groundwater [223] and geothermal waters [226]. Low concentration of sulfate and phosphate caused a drop in arsenic removal, but high concentration of sulfate and nitrate slightly increased the removal, while humic acid marginally retarded it. However, the arsenic removal rates decreased in geothermal water with the coexistence of nitrate ions. Furthermore, contaminants and interferences, Chromium (VI) removal by nZVI-Fe_3O_4 was promoted in presence of cations and organic matter, and hindered for the action of anions. To sum up, the interference impact is a function in several components and parameters: the target contaminant, interfering contaminant (s) and their concentration levels, and the water body that contains other co-existing interfering ions and organic matters.

In this part of investigation of this chapter, nitrate is the target contaminant and is simultaneously removed along with/without phosphorus by nZVI-based reagents. The removal of nitrate and phosphorus by nZVI has been deeply studied well in our works. However, their mutual interference, with each other and with the coexisting common ions in ground water and wastewater, affects their removal by nZVI-based reagents, which is not well-investigated. For each promotion and inhibition effect on the removal of a target contaminant, due to the presence of different coexisting matters, there are different explanations which are explored throughout this research. This work scrutinizes the influence of interference on nitrate and phosphate removal from their aqueous solutions by nZVI and a promising modified nZVI-based material, which is the composite of nZVI supported on treated activated charcoal ($F_1^2AT_2^{950}$), denoted now generally as nFe(0)/AC. The entire

research includes the investigation of contaminants interference of domestic wastewater, humic acid, anions of sulfate and phosphate, cations of cuprous and cupric, and calcium carbonate (hardness) with the removal efficiency of nitrate pollutant from its aqueous solution. Also the study is provided with a kinetic modeling of interferences including the determination of the type and strength of the interference effect using the equation rate parameters, which is unprecedented, according to our best knowledge, in this type of studies.

4.9.2. Batch tests

Batch experiments were divided into three main types: batch experiments A which treated concentrations of nitrate of 45.18 mg $NO_3^- - N/L$; batch experiments B for phosphate remediation of 50 mg $PO_4^{3-} - P/L$; and batch experiments C which examined the removal of both coexisting contaminants at 45.18 mg $NO_3^- - N/L$ and 50 mg $PO_4^{3-} - P/L$. Batch experiments were performed using nZVI (200 mg) or nFe(0)/AC composite (2:1 wt Fe^0/wt AC of 200 mg nZVI) added to 200 mL aqueous solutions of batch experiments A, B and C in 300 mL closed conical flasks under 250 rpm shaking at a maintained room temperature (25 ± 2 ºC).

The nZVI-based reagents (nZVI and nFe(0)/AC) were applied in batch experiments for interference studies (For example, effect of existing $CaCO_3$, humic acid or so forth on pollutants degradation). The comparison in performances was illustrated by plotting profiles of treatment concentrations and formulating kinetic models of these results. Batch experiments related to interference studies were operated in the same manner as previously stated, against 200 mL solutions of batch experiments A and C in 300 mL conical flasks shaken at 200 rpm. The interference studies focused on nitrate reduction, while the impact of interference of minerals and organic matters on phosphorus removal was considered quite insignificant as deduced from results of preliminary experiments.

The interference effect in a typical wastewater was studied. Mikasagawa municipal wastewater was modified to contain the under-investigated concentration of nitrate of 45.18 mg $NO_3^- - N/L$. The data and properties of Mikasagawa wastewater is presented in Table 4-3.

Table 4-3. Properties of the basic Mikasagawa municipal wastewater.

Contaminant	Value or conc. in mg/L
pH	7.3
Total $PO_4^{3-} - P$	4.45
Total $NH_4^+ - N$	28
Total N	37
BOD	229
COD	424
Suspended solids	175

Interference investigations included cuprous chloride (CuCl) and cupric chloride (CuCl$_2$) presence in batch experiments A and C to demonstrate their promoting effect on nitrate reduction and phosphate adsorption kinetics by nZVI and nFe(0)/AC. Cu$^+$ was injected into batch A with amounts of 50 and 125 mg Cu/L, and into batch C with an amount of 250 mg Cu/L by adding certain amounts of CuCl, whereas Cu^{2+} was used with the same amounts of copper and the same procedure as in Cu$^+$ interference experiments.

The influences of humic substances, hardness, and sulfate anions were also inspected for their interfering behavior. The intervening effect of the organic matter was inspected at 50 mg/L of humic acid and of sulfate ion (SO$_4^{2-}$) at 500 mg/L, while hardness of batch experiment A solution was altered by inserting determined amounts of CaCO$_3$. 40 mg/L CaCO$_3$ of soft hardness and 180 mg/L CaCO$_3$ of hard hardness were tested for batch experiments A, and 120 mg/L CaCO$_3$ for batch experiment C. These concentrations were picked out to represent common and high values of groundwater conditions to detect the limits and degrees of interference.

Samples were periodically withdrawn, and their filtrate was separated out using a 0.22 μm membrane filter for measuring concentrations of nitrate-nitrogen and phosphorus. Experiments were performed at least two times to ensure the validity of the produced results.

4.9.3. Performance in simultaneous removal of contaminants

The modified composite (nFe(0)/AC) proved its reliability and efficient performance over nZVI in batch experiments A, B and C in Fig. 4-19. The removal efficiencies of nitrate and phosphate by nZVI were individually 39% and 45%, respectively in separate experiments (batch A and B). However, nFe(0)/AC had higher kinetic rates and treatment efficiencies, around 67.5% and 86%, respectively in the same experiments as seen in Fig. 4-19. In other experiments (batch C), when phosphate coexisted with nitrate at close concentrations of phosphorus (50 mg/L) and nitrogen (~45.18 mg/L), P had a negative and demolishing interference with NO_3^--N removal but NO_3^--N had a positive interference with P removal. The inset of Fig. 4-19 Showed ~96% removal of P using either nZVI or nFe(0)/AC in nitrate-phosphate aqueous solution. Nitrate removal decreased by ~60% and 37% for nZVI and nFe(0)/AC, respectively. However, if both nitrate removal profiles of nZVI and nFe(0)/AC were compared (in Fig. 4-19 inset), the performance of nFe(0)/AC exceeds that of nZVI by ~183% increase in removal efficiency of nitrate. The larger negative charge of phosphate ion (-4) facilitates its path towards the surface of nZVI, which has a positively charged surface especially at pH values lower than the isoelectric point (IEP ≈ pH 8). Afterwards the pH of the solution increases till reaches a value around 11 and the surface charge changes [166]. This could be the possible reason for fast kinetics and improved removal for phosphate over nitrate, especially at the initial period (pH <8). Adding that the effect of thermal modification built up the positive charge of AC surface [214] which attracted more the negatively-charged ions.

4.9.4. Municipal wastewater, organic matters and anions interference

As illustrated in Fig. 4-20, all interfering components had a negative impact on the nitrate removal by supported nZVI in batch experiments A. Mikasagawa municipal wastewater (WW, refer to its properties in Table 4-3) had the highest interference with nitrate reduction by decreasing the rate of removal and minimizing the removal efficiency (RE) by 56.3% compared to the control efficiency of nitrate removal in a pure DDW. The presence of several contaminants in wastewater, such as phosphorus, ammonia, organic carbons, minerals and others, led to this high impact on performance. If the water body is contaminated with various pollutants, precautions should be engaged in the design of treatment equipment and process,

determination of the number of operating units (pre-treatment, primary, advanced, etc.) and especially, the calculation of dosage amounts of the treating reagent. One of the municipal wastewater constituents (phosphorus) was individually examined at a close concentration (5 mg/L) to that found in the WW. Phosphorus interfered with nitrate removal by 32.6% reduction in treatment efficiency, about more than half the interference reduction percentage of the WW (56.3%). A high concentration of sulfate anions (500 mg SO_4^{2-}/L) showed the same interference impact as phosphorus ions (15.33 mg PO_4^{3-}/L) in nitrate removal resulting in two roughly identical profiles observed in Fig. 4-20. The active sites of nZVI have initially a positive charge state then a competition between different negatively-charged anions (NO_3^-, PO_4^{3-} and SO_4^{2-}) takes part in covering these surface active locations, resulting in a decline in nitrate reduction rate and removal deficiency. Despite using high concentration of sulfate ions, their equivalent interference impact to that of phosphate ions (at lower concentration) is another indication on the greater effect of valences and negative charge value of an anion more than the concentration parameter in the interference process. Low phosphorus content (5 mg/L) can cause more than 50% of the interference impact of a higher phosphorus content (50 mg/L, batch c) on nitrate removal. In another interference study, humic acid, due to its organic acid nature and incomplete ionization in water, had the lowest negative interference among other interfering substances by ~10% reduction in nitrate RE.
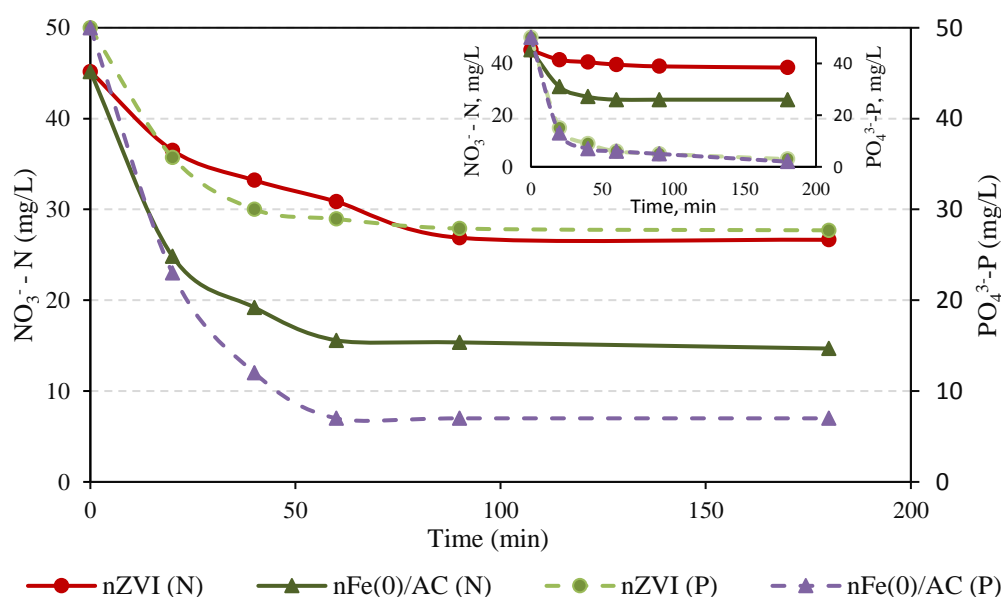
Fig. 4-19. The removal profiles of nitrate and phosphate in batch experiments A and B, and in batch experiments C (inset) by nZVI and nFe(0)/AC.
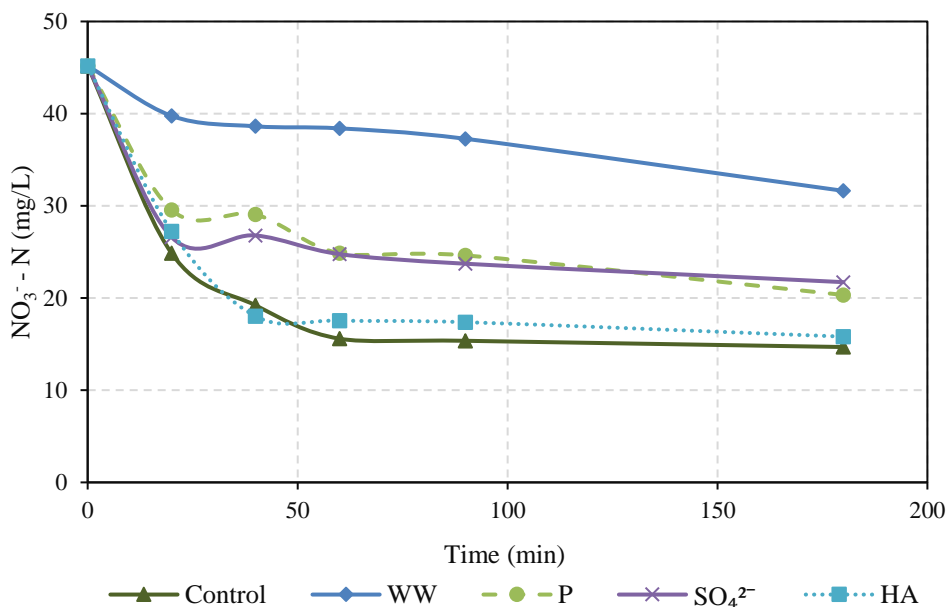
Fig. 4-20. Nitrate removal rates regarding the Interference of municipal wastewater contaminants (WW), phosphorus (P, 5 mg/L), sulfate (SO_4^{2-}, 500 mg/L) and humic acid (HA, 50 mg/L) with nFe(0)/AC in batch experiments A.

4.9.5. Hardness effect

Hardness had a considerable interfering action on nitrate removal in batch experiments A and C as concluded from Fig. 4-21. At 40 mg/L $CaCO_3$ (soft hardness), a reduction by ca. 18% in nitrate removal occurred in batch A. However, the negative impact reached a reduction by ca. 29% in removal efficiency within batch A at the hard hardness (180 mg/L $CaCO_3$). These results indicated that shifting from soft hardness level to a hard one reduced nitrate RE by further 13.5% stated as lower than the interference reduction percentage of the original (18%) exhibited by the soft hardness solution. Hence, the highest interfering effect could meet a low concentration of calcium carbonate then the impact of interference could be lower than expected as the concentration of $CaCO_3$ increases. The performance of nitrate removal in the presence of phosphate, carbonate and calcium ions is described in the inset of Fig. 4-21 (batch C), the moderate hardness (125 mg/L $CaCO_3$) in phosphate presence had a large impact on nitrate removal by around 62% reduction, which is considered the highest negative interference in this study. To explain this drop in nitrate removal process, it was reported that calcium ions greatly retarded the removal of nitrate by microscale ZVI [222]. Ca^{2+} ions precipitate at high pH value with hydroxide ions. That suppresses the release of ferrous ions from nZVI surface, which participate in a major role in nitrate removal as the ferrous ions

are one of the main products of nitrate reduction by nZVI and their rapid release increases the rate of nitrate reduction described by the following equation (Eq. (3.6)) from the whole mechanism [85, 145]:

$$4Fe^0 + NO_3^- + 10H^+ \rightarrow 4Fe^{2+} + NH_4^+ + 3H_2O$$
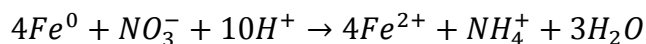
Moreover, the presence of carbonate ions with calcium ions (CaCO₃) forms a coating onto nZVI surface, which strongly inhibits the nitrate removal.

4.9.6. Influence of copper cations

Copper ions proved to promote removal efficiencies and kinetics in aqueous solutions of nitrate and phosphate [145, 146]. They also enhanced nZVI removal efficiency towards heavy metals in the pilot plant treatment of non-ferrous smelting wastewater [132]. CuCl and CuCl₂ were tested at the same copper concentration in order to understand the role of valences and electrons in remediation performance. Figure 4-22 depicts the interference of copper ions (Cu^+ and Cu^{2+}) with nitrate removal of batch experiments A and C by nZVI and nFe(0)/AC. In batch A (connected to Fig. 4-22a) , concerning nZVI and Cu^+, nitrate removal efficiency was promoted and increased ca. 29% and 50% at 50 and 125 mg Cu^+/L (by addition in value), respectively. However, Cu^{2+} increased the efficiency 51% and 47.5% at 50 and 125 mg Cu^{2+}/L, respectively, which means that increasing amount of Cu^{2+} can slightly decrease the removal efficiency, and the optimum amount was at lower mass [145]. In Fig. 4-22b, nitrate removal of nZVI increased from 15% to ca. 73.5% at 250 mg Cu^+/L and to 62.5% at 250 mg Cu^{2+}/L. In batch experiments A conducted using the nZVI composite, cuprous cations (Cu^+) increased the removal efficiency by ca. 21.5% and 23.7% at 50 and 125 mg Cu/L while cupric cations (Cu^{2+}) increased the decontamination of nitrate by ca. 46% resulting in a complete removal at 50 mg Cu/L and by ca. 41% at 125 mg Cu/L. Excessive occupation of active sites by zero valent copper and copper ferrite compounds along with the interference of chloride ions at high concentrations could be related to the lowered performance on increasing cupric dosage [145]. These results elucidated the enhancing effect of copper ions especially using Cu^{2+} at optimum concentrations with the supported nZVI. Cu^+ can enhance nitrate removal efficiency but at high concentrations, and that showed clearly the important role played by valences and transfer of electrons in promoting nitrate removal kinetics and efficiency. Although Batch experiments C, presented Fig. 4-22b, composed of a high concentration of

phosphate (50 mg P/L), but copper ions were able to increase both sequestration of phosphate [146] and removal of nitrate by supported nZVI at the same time. Thus, the trend of results agreed with the results of batch A, and nitrate removal elevated from 45% by ca. 23% at 250 mg Cu^+/L and by ca. 62% at 250 mg Cu^{2+}/L, which is considered the highest positive interference in this study. Moreover, as expected, phosphate removal efficiencies in batch C exceeded 90% within 20 min in the presence of copper ions. Concerning the residual contaminants, copper ions were detected after the treatment process of batch experiments below 0.6 mg/L, which is lower than the safe regulation (2 mg Cu/L) of world health organization for drinking water.
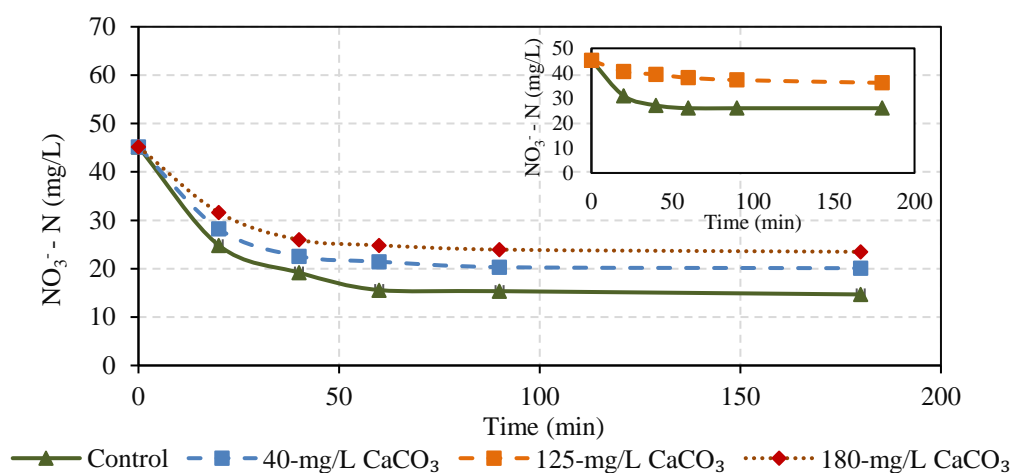
Fig. 4-21. Interference of $CaCO_3$ (Hardness) with nitrate removal rates by nFe(0)/AC at different concentrations of 40 mg/L and 180 mg/L in batch A and 125 mg/L in batch C (inset).
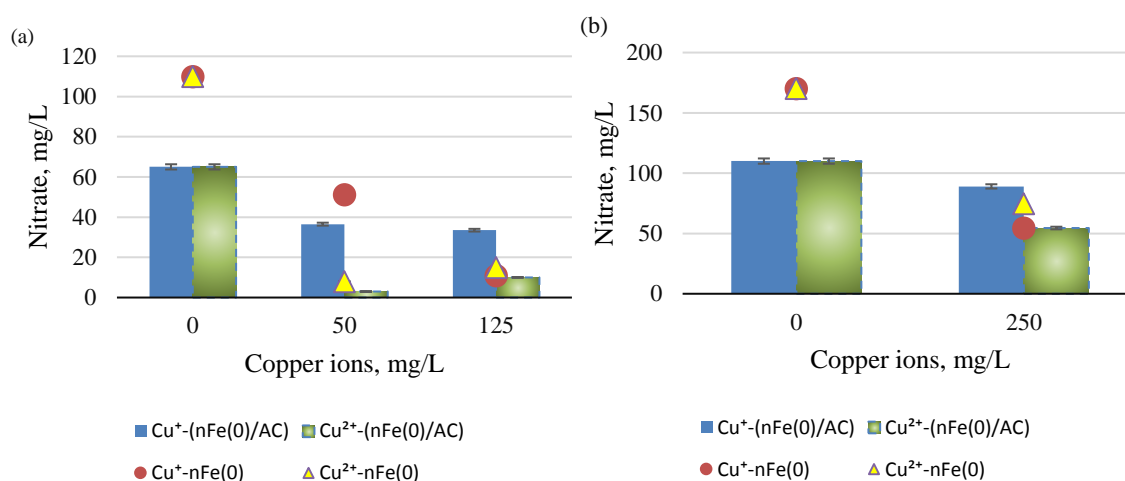
Fig. 4-22. Influence of copper compounds on nitrate removal by nZVI and nFe(0)/AC at constant copper concentration (a) 50 and 125 mg/L for batch I and (b) 250 mg/L for batch III.

4.9.7. Overall comparison and kinetics formulations

The performance of nZVI and nFe(0)/AC in nitrate removal process of batch experiments A is described in Fig. 4-23 against all interfering substances involved in this study at specific concentrations. In general, the supported composite outperformed nZVI in most of interference studies. The interference acted by the municipal wastewater was detrimental for both nZVI-based reagents, however, the nitrate removal efficiency by nFe(0)/AC in DDW or WW increased by around 75% than that by nZVI in the same water bodies. The rest of the improvement/increase percentages in case of other negative interfering contaminants ranges between ca. 27% to ca. 53%. In case of copper ions (especially Cu^{2+}), they enhanced the nitrate reduction in both nZVI-based experiments by ca. 150% (for nZVI) and completely eliminated nitrate contamination in case of nFe(0)/AC.

The formulation of nitrate removal kinetic models was essential to further understand the effect of interfering substance on the kinetic model parameters and overall removal performance. The reaction kinetics formulation was based on the interpretation of experimental data by pseudo first order reaction combined with first order deactivation model [149]. This approach comprises a well-known and widely implemented approach, which is pseudo first order reaction, and a deactivation model that describes the passivation layer formation on the ZVI surface [85, 145]. Hence, the ensuing pseudo first order kinetic equation combined with first order deactivation of nZVI-based reagents was used:

$$\frac{dC}{dt} = -\mathrm{k}C \times e^{-\alpha t} \tag{4.1}$$

where C is the nitrate concentration (mg/L), k is known as the observed pseudo first order rate constant (h^{-1}) while α is considered as the first order deactivation constant for nZVI-based reagents (h^{-1}).

The proposed kinetic model was examined for some investigated interference studies involved in this research, especially which are related to Fig. 4-23 along with batch C experiments. The kinetic parameters were evaluated based on the minimization of the least square error method using Generalized Reduced Gradient (GRG) Nonlinear solving method built in Excel® solver, and the coefficients of determination were determined as well. Figs. 4-24 (a to f) show some examples of the kinetic models of nitrate removal using the combined pseudo first order kinetic equation with first order deactivation and compared to pseudo first

order kinetic equation. Each plot in the graph is related to the following denotation that defines the components and reagent used in performing the nitrate decontamination experiments either in batch experiments A or C:

nZVI or nFe(0)/AC reagent–interfering substance (the concentration of interfering substance in mg/L)

The symbol M beside the aforementioned denotation refers to the proposed (combined) kinetic model, while the word "Expon." in the beginning of the denotation indicates the pseudo first order model only used in that fitting.

Usually the pseudo first order reaction equation succeeds in describing the initial period of nitrate removal with high determination coefficient (R^2), if it is applied only in this duration [145], but it totally fails to describe the whole period. On contrary, the proposed model succeeds in fitting to the experimental data with high accuracy and precision ($R^2>0.95$). The calculated parameters of this suitable kinetic model are presented in Table 4-4.

Comparing the values of both kinetic formulation parameters shown in Table 4-4 could give explanations to the over performance of the composite in nitrate removal, effect of negative interferences and promotional impacts. Concerning case no. 1 to 3, the observed pseudo first order rate constant (k) is less than the first order deactivation constant (α) when nZVI reduced nitrate in DDW (case #1) or WW (case#3), and the ratio k/α is lower than 1. However, when the ratio k/α is higher than 1 for nFe(0)/AC in DDW (case#2), the performance of nitrate reduction is improved by ca. 75% compared to that of nZVI in the same water matrix as stated before. The ratio k/α is higher than 1 in other cases no. 10 to 14 and 19 to 22 in which most of these experiments involved the coexistence of copper ions which had a positive effect on the removal performance and kinetics of nitrate. The higher the ratio k/α, the faster kinetic rate and more positive interference can occur. All negative interference cases include k/α less than 1. This provides an interpretation to the crucial effect of negative interfering substances, which gives rise to the passivation of the active sites on nZVI-reagent surface and suppression of rapid ferrous dissolution resulting in a higher deactivation rate that works against the forward rate of the nitrate reduction reaction.

Table 4-4. The evaluated kinetic parameters of pseudo first order kinetic equation with first order deactivation of nZVI-based reagents for specific interference batch experiments A and C.

Case number	Reagent-interf. sub. (Conc. mg/L)	k (h^{-1})	α (h^{-1})
Batch A			
1	nZVI-0 (0)	0.734	1.331
2	nFe(0)/AC- 0 (0)	2.543	2.243
3	nZVI-WW	0.205	1.529
4	nFe(0)/AC- WW	0.249	0.641
5	nZVI-P (5)	0.782	1.590
6	nFe(0)/AC- P (5)	1.410	1.996
7	nZVI-SO_4^{3-} (500)	0.653	1.089
8	nFe(0)/AC- SO_4^{3-} (500)	2.777	4.312
9	nZVI-HA (50)	1.0003	1.697
10	nFe(0)/AC- HA (50)	2.368	2.258
11	nZVI-Cu^+(125)	3.842	1.267
12	nFe(0)/AC-Cu^+(125)	10.630	5.944
13	nZVI-Cu^{2+}(50)	8.042	1.781
14	nFe(0)/AC-Cu^{2+}(50)	10.817	1.750
15	nZVI-$CaCO_3$(180)	1.618	2.989
16	nFe(0)/AC-$CaCO_3$ (180)	1.984	2.575
Batch C			
17	nZVI-0 (0)	0.319	2.009
18	nFe(0)/AC- 0 (0)	1.936	3.453
19	nZVI-Cu^+(250)	1.435	0.912
20	nFe(0)/AC-Cu^+(250)	1.511	1.504
21	nZVI-Cu^{2+}(250)	1.615	1.407
22	nFe(0)/AC-Cu^{2+}(250)	2.419	1.611
23	nFe(0)/AC-$CaCO_3$(125)	0.346	1.591
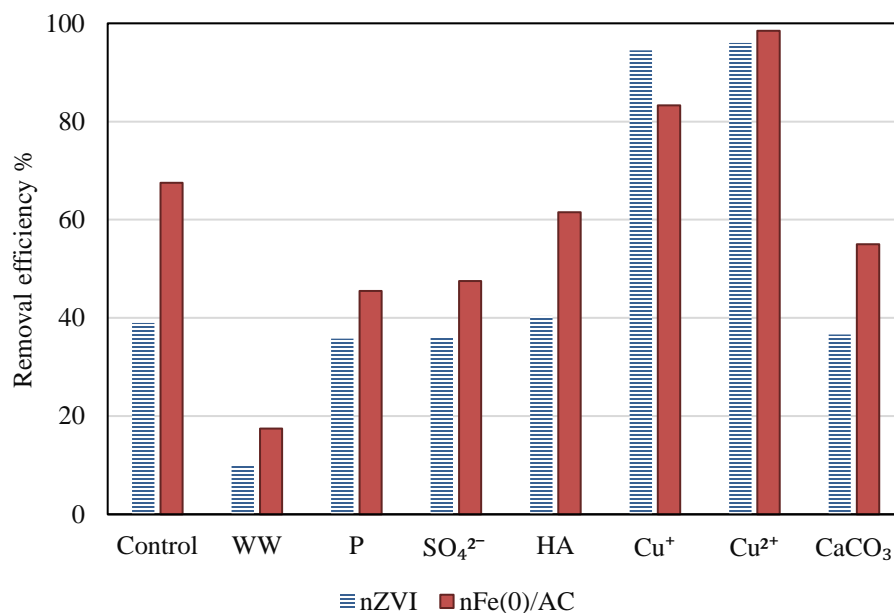
Fig. 4-23. Treatment efficiencies (after 180 min) of nitrate by nZVI and nFe(0)/AC against interference of WW, phosphorus (P, 5 mg/L), sulfate (SO_4^{2-}, 500 mg/L), humic acid (HA, 50 mg/L), cuprous (Cu^+, 125 mg/L), cupric (Cu^{2+}, 50 mg/L) and hardness ($CaCO_3$, 180 mg/L) in batch experiments A.
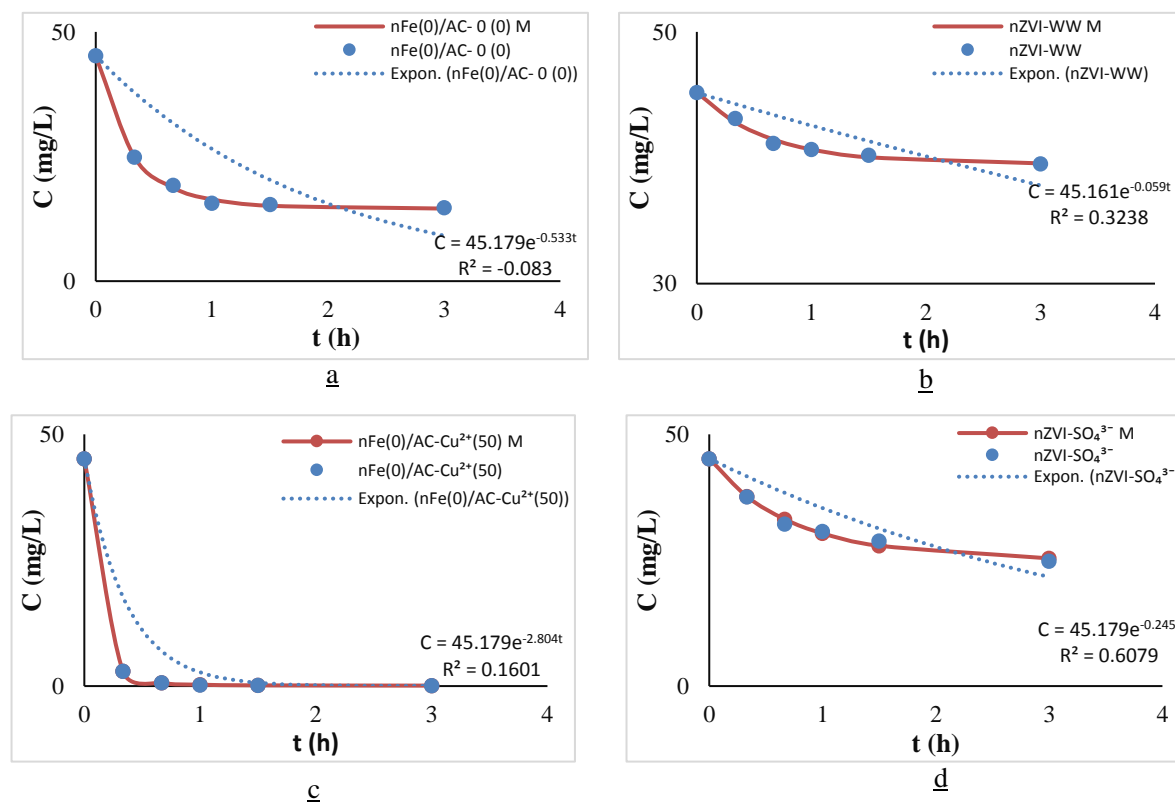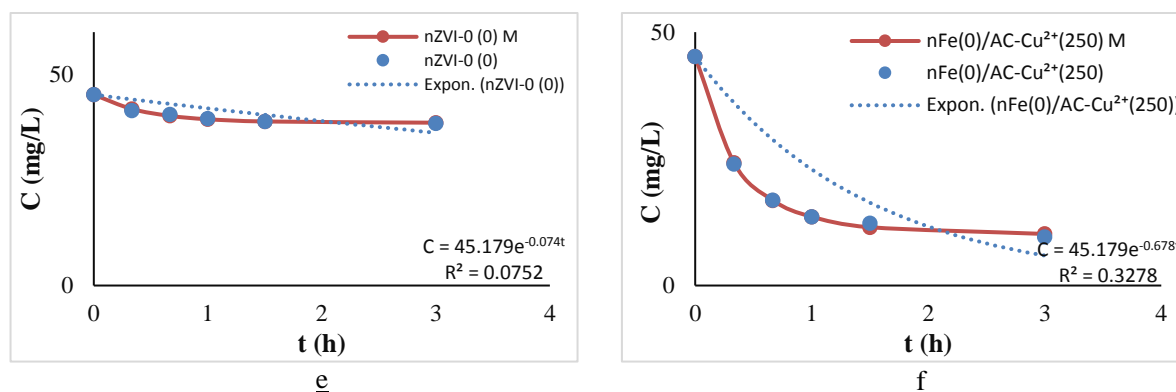
Fig. 4-24. Graphical representations of kinetic formulation of some experiments as examples to the suitable fitting of kinetic model of nitrate reduction in batch experiments A (case a, b, c and d) and batch experiments C (case e and f) by nZVI-based reagents.

4.10. Conclusions

The process to achieve the best conditions of treated AC-supported nZVI needed tuning and optimization. Treatment methods were basically applied to solve problems of nZVI oxidation and poor pore diffusion for AC-supported nZVI. Synthesis in ethanol medium, one of the suggested methods, increased the corrosion of nZVI. Thermal, nitric-acid and nitric-acid thermal treatments were used for modifying textural structure and surface chemistry of AC. Resulting from tuning of the mass ratio, ratio 2:1 of nZVI to AC was the optimum ratio, and, from treatment methods, thermal treatment of AC at 950 $^{\circ}$C for 2 hours was the chosen treatment at optimum conditions to cause the highest removal efficiency of nitrate and phosphate in their aqueous solutions. Thermal treatment modified AC surface chemistry and charge to attract nitrate and phosphate anions which eased direct contact with nZVI. $F_1^2AT_2^{950}$ eliminated nitrate from its solution 1.5 times more than nZVI and adsorbed phosphate from its solution 2 times more than nZVI. In a solution of nitrate and phosphate, the removal of nitrate reached 3 times more than that of nZVI along with almost the same complete elimination of phosphate. In order to fully examine the novel treated composite, it was tested for various interference under different concentrations of interfering substances. It was found that the presence of a low concentration of any tested interfering substance, except for copper ions, had the greatest reduction value in nitrate removal efficiency in aqueous nitrate solution, subsequently by raising the interfering component concentrations, the reduction in removal value decreased according to their type. This drop in removal efficiency (12-38%) should be

considered in the design process of treatment equipment and estimation of dosage amount required for treatment. Regarding copper ions, the nitrate removal was promoted for $F_1^2AT_2^{950}$ by 1.2 to 1.5 times. Finally, it is recommended to produce treated AC-supported bimetallic nZVI for wastewater treatment of highly efficient results.

In this chapter, nZVI and nZVI supported on heat-modified activated charcoal were tested in a nitrate removal study for various interferences under different concentrations of anions (phosphate and sulphate), cations (cuprous and cupric), organic matters (humic acid) and hardness (calcium carbonates), in addition to testing in a municipal wastewater matrix. According to the characterization results of nZVI-based synthesized materials, aggregation of nZVI particles was prevented to a certain extent on using the support. This reflected on the overall performance of nFe(0)/AC that surpassed the original performance of nZVI in nitrate removal efficiency by ca. 27% to 183% in case of negative interferences or no interference. Anions, in general, competed for the possession of active sites on the surface of nano iron particles leading to negative interferences with the contaminant removal. The larger negative charge of an anion gave more contribution to the negative interference effect than increasing its composition by quite significant increments. The same principal could be applied to the positive interference of the cations of copper in a reversed way. The cupric ions (Cu^{2+}) were more effective than cuprous ions (Cu^+), and they full reduced the nitrate contamination. Due to their weak acidic (ionic) nature, the organic matters of humic acid slightly and negatively interfered with nitrate reduction.   The nitrate reduction in municipal wastewater body resulted in a high drop in nitrate removal efficiency. Also calcium carbonate had a significant and negative interference effect due to its tendencies to form coating layers that passivated the surface of nZVI-based materials and inhibited the dissolution of nitrate reduction product (Fe^{2+}) from their surface. To give a clear relation between nitrate reduction and passivation behaviour of interfering substances, kinetic rate equation was implemented to fit the experimental data. It combined between the common pseudo first order model and deactivation model of enzymes which suited all experimental data along the whole experimental period. The ratio between the rate constant and deactivation constant (k/α) could give information about the type of interference, whether negative or positive, and degree of interference, whether high or low.

CHAPTER 5

REGENERATION OF NZVI

Chapter 5 Regeneration of nZVI

Chapter 5 presents the essential steps of handling a material used in a remediation process, the regeneration and recycle. The chapter manages to compare between different types of nZVIs. It shows the lack of stability of nZVI particles upon ordinary storage represented in an aged old-purchased nZVI, the effect of controlled acid treatment on this aged type of nZVI, and the potent influence of the regeneration process on a spent nZVI extracted from nitrate batch experiments with fresh prepared type. This presentation is demonstrated by methods of characterizations and batch experiments to compare performances of removal.

5.1. Introduction

Nano-scale zero-valent iron (n-Fe^0) is not a stable form of iron. It can slowly oxidize with air and/or water to its (hydr)oxides with increasing its oxidation number and valences (Fe^{2+}, Fe^{3+}). By this way, nZVI particles' reactivity collapses by passing of time [188, 229]. So a lot of care and concern should be directed to the method of storage of nZVI. In addition, it is important to emphasize on this deactivation behavior by comparing nitrate removal profiles or kinetics to that of fresh nZVI synthesized at optimum synthesis (of chemical emulsion reduction method) conditions so far. The morphology of nZVI particle states that they have core-shell structure. The core is composed of Fe^0 whereas the shell side contains two layers of iron (II, III) oxides/hydroxides (FeO(OH)) [229]. The shell layer gets enlarged by oxidation slowly with air in case of incautious storage or rapidly in case of nitrate reduction process. Treatment and regeneration processes should be applied in the two cases, respectively. The reason of application is that the primary step of nitrate reduction is its sorption in the shell layer until reaching the core at which the reduction occurs. The thick layer acts as a resisting barrier for nitrate diffusion and electrons transfer to the core resulting in a lower removal performance. By using the treatment method, the thick shell layer is partially dissolved for the purpose of reactivating nZVI particles and regaining reactivity. This method was indirectly mentioned and reported by a few researches as a sort of washing to clean the surface [229]. The acid treatment method had been applied to aged nZVI

purchased since one year from usage in batch experiments. In the other case, the regeneration method targets reviving Fe^0 and reconverting spent iron (oxides/hydroxides) in the enlarged thicker shell layer to fresh nZVI. This regeneration process is employed to regain reactivity of spent synthesized nZVI.

According to the author's acquired knowledge, the literature lacks investigation of this topic related to the study of the reactivity of nZVI towards removal of nitrate from water in different states of nZVI, which are aged (denoted as A-nZVI), treated (T-nZVI), fresh synthesized (S-nZVI) and recovered/regenerated (R-nZVI). This study compares the performances (and difference in reactivity) of these four types in nitrate removal process. The success of treatment and regeneration processes can add benefits and strength points of applying the nZVI technology for contaminated water and wastewater remediation systems.

5.2. Methods

5.2.1. Preparations of different nZVIs

Four nZVIs were prepared in this study. The basic bare nZVI was synthesized following up the method described in chapter 2 of this dissertation. A-nZVI is a commercial nano-scale zero-valent iron (Nano Iron Co., Czech Republic) procured one year before using in batch experiments. In this case, HCl was applied to treat both A-nZVI and spent S-nZVI at different conditions. The rest of nZVIs (derivatives) were produced from the subsequent preparations.

5.2.1.1. T-nZVI preparation

The acid treatment/washing process was applied to the surface of A-nZVI using 0.1 M HCl. An amount of 10 grams of the commercial iron was introduced to 250 mL of HCl solution in 300 mL Erlenmeyer (conical glass) flask, and then the whole produced slurry was placed on a shaker adjusted at 200 rpm (reciprocating motion) for 1 h. After shaking, filtration process took place then the obtained wet solids were washed with 200 mL of deoxygenated DW and 100 mL absolute ethanol numerous times in order to clean the surface of nanoparticles from any acid traces. The filtered solids were anaerobically dried prior to batch experimental processing.

5.2.1.2. R-nZVI acquirement

The R-NZVI was prepared by dissolving the spent S-nZVI, which was collected and filtered after spending in nitrate decontamination experiments, in HCl solution. The method is based on the following chemical reaction equation (5.2) by the dissolution of the spent magnetite (Fe_3O_4) resulting from iron oxidation in a hydrochloric solution [145, 230]:

$$NO_3^- + 3Fe^0 + 3H_2O \rightarrow Fe_3O_4 + NH_4^+ + 2OH^- \tag{5.1}$$

$$Fe_3O_4(s) + 8HCl\,(aq.) \rightarrow FeCl_2(aq.) + FeCl_3(aq.) + 4H_2O \tag{5.2}$$
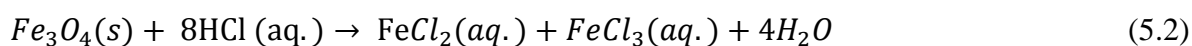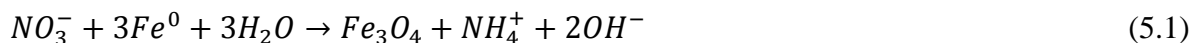
It involves the reconversion of oxidized iron compounds to iron chlorides, which can participate again as a precursor in a regenerating synthesis process with NaBH$_4$ reductant to produce R-nZVI. However, executing the reaction at stoichiometric amounts is slow but beneficial in preventing any excess of acid solution to react with NaBH$_4$ during the regeneration process and waste some of the reductant concentration. Also another problem exists that of converting the whole ferrous chloride to ferric chloride, which is more effective and has faster kinetic rates in reduction with NaBH$_4$ due to the higher number of electron transferred. The process of oxidation of ferrous to ferric ion can be full-filled using oxidizing agent, such as air, hydrogen peroxide, potassium permanganate, etc. In this study, the spent nano iron was treated with stoichiometric amount of 0.5 M HCl in 300 mL Erlenmeyer (conical glass) flask under continuous magnetic stirring and continuous flow of air for 20 h. Hydrogen peroxide solution can greatly reduce the oxidation time, but an effective optimization process is needed to find the optimum conditions under a safe environment. The preliminary experiments showed complete dissolution of spent iron compounds in HCl solution in less than 2 h, but the obtained colorless solution participated in the regeneration process then in batch experiments to recover a low efficiency of nitrate removal. Whereas the oxidized mixture of orange color (after longer time) was the treated spent iron that entered the regeneration process with NaBH$_4$. In this method, the original S-nZVI was prepared with half-original amount (half conc. at 10 g/L and same volume) of NaBH$_4$ reductant and then the other half was used in the regeneration process. Both S-nZVI, synthesized at half reductant amount, and R-nZVI were handled after the reaction in the same way as mention in section "S-nZVI production" then they were utilized in batch experiments.

5.2.2. Experimental

Nitrate removal performance was evaluated through executing a main batch experiment in 500 mL four-neck glass flask by applying dosage of 2 g/L of nZVI in a 100 mg/L of nitrate solution. The nitrate solution was stirred with nZVI reagent (as A-nZVI, T-nZVI, S-nZVI or R-nZVI) at 250 rpm, maintained at 25 ± 0.5 $^{\circ}$C using a water bath for a maximum duration of 480 min and kept under anoxic condition using a continuous flow of nitrogen gas. The whole system of experiment was closed by using different plugs with one or two holes. The batch configuration was set up to monitor pH, ORP, concentrations of samples, volume of gas collected, and concentration of stripped ammonia. Samples of 5 mL were withdrawn at certain given time intervals then filtered through a 0.22 μm membrane, and then analyzed for numerous components (nitrate, ammonia, nitrite, total nitrogen, ferrous, ferric and total iron ions). The vent gas from the flask was directed to absorb in 100 mL (0.1 M) acidic solution in a 200 mL beaker for the analysis of the stripped ammonia gas. An inverted graduated cylinder full of acidic solution (supported by a stand) was used in one batch experiment, in which no nitrogen purging was applied, in order to collect nitrogen gas (by product) produced from nitrate reduction above the liquid level inside it. Most of batch experiments were performed in doubles to check on the reproducibility of results.

5.3. Properties of nZVIs

The characterization results of both A-nZVI and S-nZVI showed high degree of agglomeration as indicated in TEM images of Fig. 5-1. Fig. 5-1i and 5-1iii show the morphology of A-nZVI particles, and Figs. 5-1ii, and 5-1iv represent that of S-nZVI particles. The magnetic nature of these nanoparticles combines them together to form necklace-like structures, which agrees with the observations of different reports [112, 145]. The shell layer of iron nanoparticle can be distinguished from the core area as it appears in a brighter color justifying the presence of lighter atomic masses (Fe + O). Figs. 5-1iii and 5-1iv present a close observation at resolution of 50 nm that clearly shows the core-shell structure, especially the thicker shell layer of A-nZVI particle compared to that of S-nZVI particle. This obviously reflects the effect of storage time and conditions on the structure and morphology of nZVI.
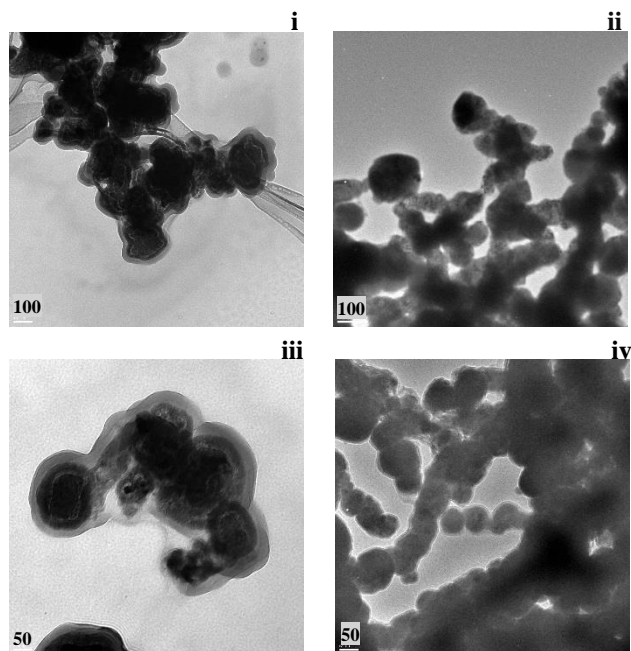
Fig. 5-1. TEM images of A-nZVI (i, iii) and S-nZVI (ii, iv) at different resolutions (100 and 50 nm, respectively).

The particle size distribution was obtained using laser-scattering particle size analysis under an internal sonication condition for both A-nZVI and S-nZVI (appeared in the graph of Fig. 5-2). The average aggregated particle sizes of both A-nZVI and S-nZVI were measured to be 1.993 µm and 42 nm, respectively. These results hypothetically match up with the observed particle sizes of TEM images (in Figs. 5-1iii and 5-1iv) showing the particle sizes of A-nZVI more than 50 nm and that of S-nZVI less than/around 50 nm. However, the results of particle sizes observed in TEM images are more related to a single particle size than an aggregated size, especially at high-resolution power. The particle size distribution of the synthesized nanoparticles seems narrower than the distribution of the aged nanoparticles (shown in Fig. 5-2), adding that the aggregate particle size is smaller. Although the S-nZVI has finer particle size than A-nZVI which increases its tendency towards agglomeration, but the aging period was sufficient to build up these agglomerations. This reflected upon the lower Brunauer–Emmett–Teller (BET) specific surface area value of A-nZVI particles (of 14.5 m^2/g) compared to the value of BET specific surface area of fresh S-nZVI (62 m^2/g) obtained at optimum synthesis conditions.
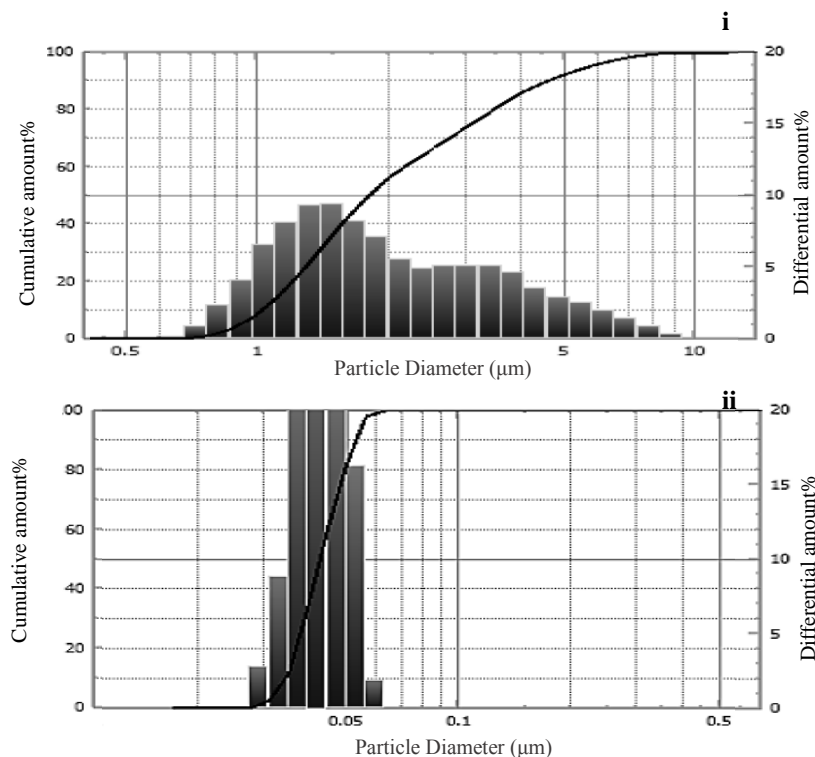
Fig. 5-2. Particle size distribution of i) A-nZVI and ii) S-nZVI.

The XRD patterns of both aged and fresh synthesized nanoparticles are shown in Figure 5-3. These patterns are semi-identical detecting zero valent iron (Fe^0) at its major deflection angle 2θ of 44.8◦ and other angle 82.6◦. The XRD analysis did not detect iron oxides attributed to their relative small amounts and low degree of crystallinity. The higher intensity peak of A-nZVI in XRD pattern indicates a more crystalline structure than that of S-nZVI. The incomplete drying process of S-nZVI particles was the reason of its lower crystallinity to prevent probabilities of iron oxidation.

5.4. Performance of nZVIs in nitrate removal

The mechanism of nitrate reduction was carefully scrutinized in order to describe the removal process for T-nZVI and S-nZVI only (as A-nZVI had a very low reactivity and R-nZVI had a close performance to the S-nZVI, which are shown in the forthcoming section). Spectrophotometric analysis results (revealed in Figure 5-4) showed that ammonia (NH_4^+) was detected in high concentrations indicating being the main product. Nitrite (NO_2^-) was also found at a relatively higher concentration (around 5 mg/L produced from utilizing S-

nZVI) at the initial period of the batch experiment, which was reduced and eliminated throughout the course of the treatment reaction. It was proven beforehand in chapter 3 that nitrate reduction mechanism involves reducing nitrate into nitrite and ammonia, the former product was then consumed to produce ammonia and nitrogen. According to the discussion and results obtained previously, the following reactions occurred with every type of nZVI with only different rates [85, 145]:

$$4Fe^0 + NO_3^- + 10H^+ \rightarrow 4Fe^{2+} + NH_4^+ + 3H_2O$$
$$Fe^0 + NO_3^- + 2H^+ \rightarrow Fe^{2+} + H_2O + NO_2^-$$
$$3Fe^0 + NO_2^- + 8H^+ \rightarrow 3Fe^{2+} + 2H_2O + NH_4^+$$
$$3Fe^0 + 2NO_2^- + 8H^+ \rightarrow 3Fe^{2+} + 4H_2O + N_2$$
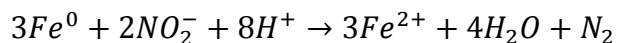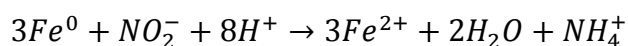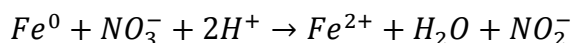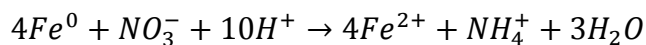
As indicated by the precedent reaction mechanism, ammonia should have the largest concentration value followed up with nitrite then nitrogen concentrations. This mechanism agrees with the results of analysis in Figure 5-4 that depicts the concentration profiles of nitrate reduction products.
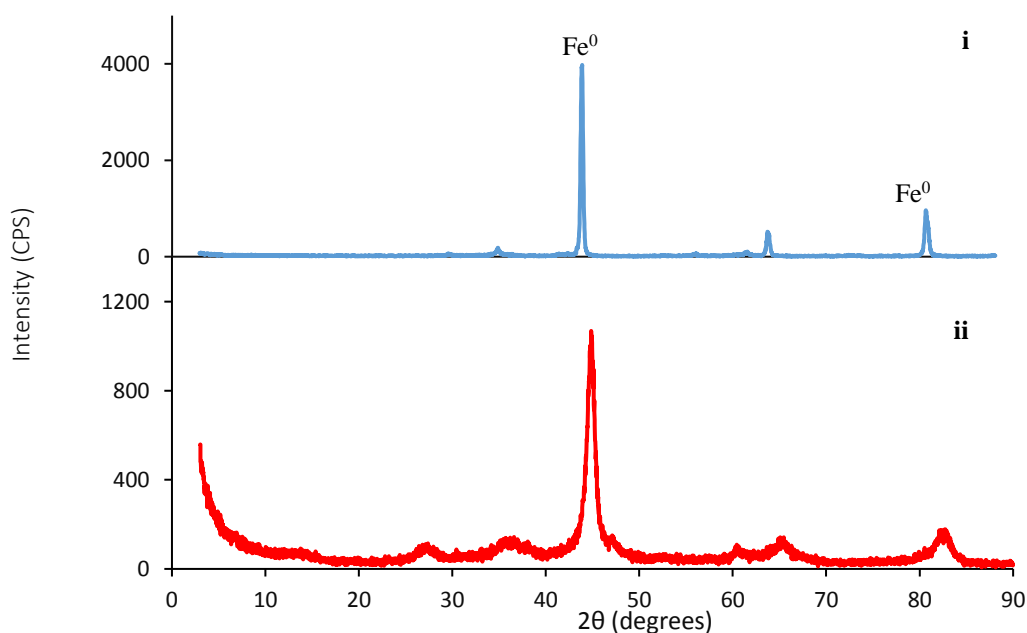
Fig. 5-3. XRD patterns of i) A-nZVI and ii) S-nZVI.
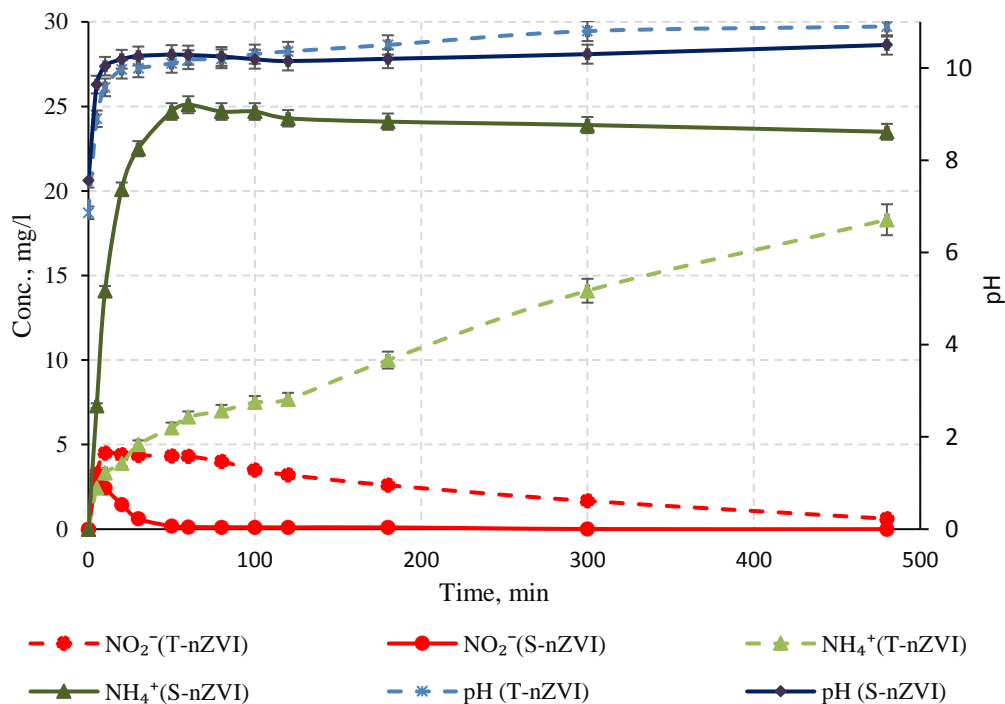
Fig. 5-4. Tracking concentrations of produced nitrogen compounds and pH from nitrate reduction using T-nZVI and S-nZVI.

The produced ammonia concentration value is an indication of the reactivity of the utilized nanoparticles in the batch process. The highest ammonia production was for the S-nZVI (and R-nZVI) evidencing high reactivity and performance compared to other nZVIs. The nitrite in both cases (S-nZVI and T-nZVI) exhibited the same trend of concentration profiles, which proves that nitrite was consumed in other reactions to produce ammonia and nitrogen. Ammonia is an unpleasant product, which needs further treatment. However, the high monitored pH of the solution mixture can strip out ammonia that was collected in a graduated cylinder at 7 mL volume at NTP, which corresponds, to a total concentration of $NH_4^+ - N$ equal to 9.74 mg N/L (50% of total) and the rest was absorbed in water under the inverted graduated cylinder. Also the gas chromatograph (GC 3200, GL Sciences Co., Japan) analysis detected nitrogen gas in that collected gas volume at low concentration (2%). In addition, the total nitrogen amount of all produced nitrogen compounds was lower than the initial total amount of nitrogen (22.58 mg N/L corresponding to 100 mg nitrate/L) confirming the production of the nitrogen gas. The spent nZVI in nitrate reduction reactions is mainly composed of magnetite (Fe_3O_4) and FeO(OH) from depositions and reactions of ferrous and

ferric ions and unreacted Fe^0. In addition, Figure 5-5 presented XRD pattern of the spent nZVI providing a support to the previously mentioned statement regarding the presence of magnetite and iron oxide products.
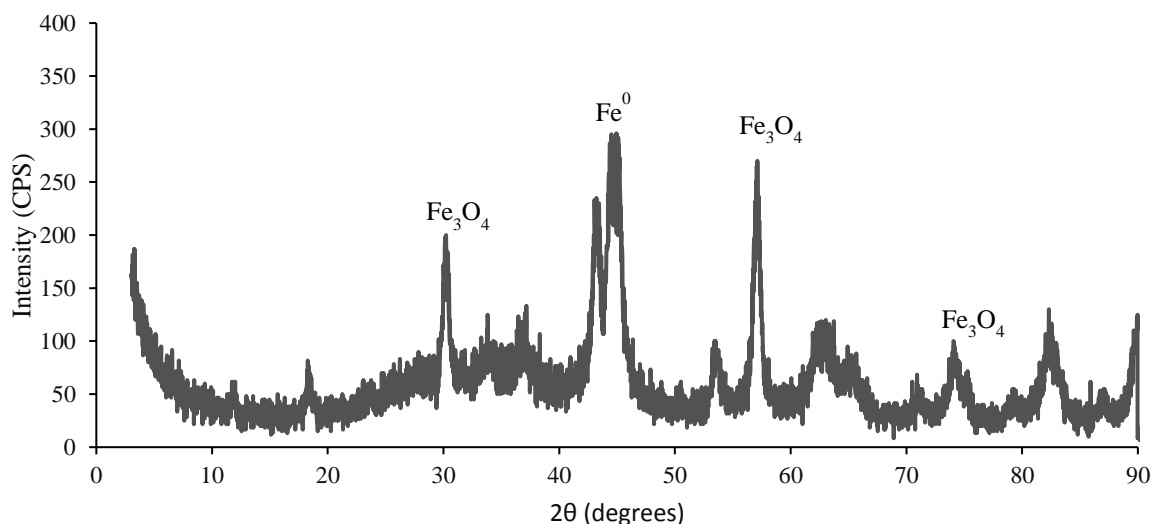
Fig. 5-5. XRD pattern of the spent S-nZVI featuring iron (II, III) oxides.

The spent nZVI from S-nZVI batch experiments was dissolved in dil. HCl solution and sampled then analyzed for the existence of nitrate remaining, which might be still adsorbed within shell layers. The results indicated that the whole amount of the nitrate was reduced and no adsorbed nitrate was still detected. In general, nitrate reduction mechanism starts with adsorption of nitrate on the shell layer of the iron nanoparticle then followed by the complete chemical reduction to almost all adsorbed amount at the core of zero-valent iron with being this step the controlling step (slowest step) in the whole process. This nitrate reduction step is described by first-order kinetic rate equation [145].

The reactivity of A-nZVI, T-nZVI, S-nZVI and R-nZVI were examined using 1-gram dosage of nZVI and starting with initial concentration 100 mg NO_3^--N/L under the same conditions. The profiles of removal efficiency representing their results versus the experimental time are observed in Fig. 5-6. The removal efficiencies were calculated based on the percentages of the difference in concentrations, between initial concentration and specific concentration at the selected sampling time, referred to (or divided by) the initial concentration of the investigated solution.
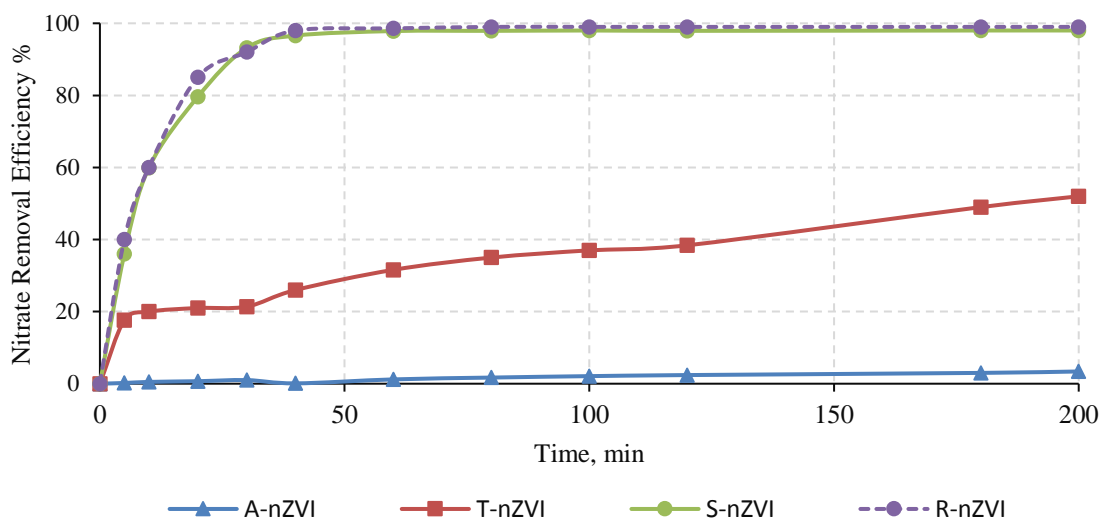
Fig. 5-6. The performance of the four nZVIs in nitrate removal batch experiments.

It is clear that A-nZVI has the lowest performance and reactivity, which cannot even reach 10% after 8 h. The effect of aging is crucial on the reactivity of these nanoparticles. Originally, the new commercial nano-iron with its specific BET surface area (25 m^2/g) can give 50 % as a nitrate removal after two hours when equilibrium is achieved. The investigations on its new BET specific surface area after aging was found to be around 15 m^2/g with about 40 % decrease in surface area available for reaction. Adding that the formation of larger shell layer as referred to TEM images (in Figure 5-1) of iron (hydr)oxides severely contributed in that drop in reactivity. However, the acid treatment of A-nZVI restored a great portion of the fallen removal efficiency. The T-nZVI succeeded in removing half of the whole nitrate load within 3 h. The dilute acid can dissolve all the iron components, so the molarity of acid and time of treatment are important factor to consider so as to only dissolve a part of a shell layer without consuming the ZVI core. That is why the acid was used at a low molarity and limited time for that purpose.

Regarding the fresh synthesized and regenerated iron nanoparticles, S-nZVI obtained a high efficiency and completely removed the nitrate load after 1 h of reaction. Surprisingly, R-nZVI performed in almost the same way as that of S-nZVI and achieved a removal efficiency of 100% within the same period. Also nZVI was regenerated from S-nZVI prepared with half original concentration of sodium borohydride reductant, and the other half was used to regenerate acidified spent S-nZVI. The results of this process are shown in Fig.

5-7. The results are close to that of Fig. 5-6 except for that the removal of S-nZVI at half original [NaBH$_4$] is being slightly lower than that of S-nZVI at full original [NaBH$_4$]. The correlation between the nitrate removal efficiency (expressing S-nZVI reactivity) and the effect of reductant concentration can be reviewed elsewhere [149], and these results here agree with that relation.

Comparing between results of Fig. 5-7 with Fig. 5-6, there is an indication that the S-nZVI and R-nZVI in Fig. 5-7 can treat approximately double load of nitrate at a summation of NaBH$_4$ amount equal to that used to produce S-nZVI (appeared in Fig. 5-6) at full NaBH$_4$ amount. The only change is the addition of diluted HCl as a part of regeneration process. The low molarity of HCl is used for stoichiometric conversion of iron oxides to iron (II, III) chlorides, which is economic but takes a long time for reaction. However, the rate of reaction is clearly increased when applying high molarities of HCl. The problem with this procedure is that the excess HCl can consume a part of reductant during regeneration process, even neutralizing the excess acid generates salts unfavourable to be found in the synthesis and regeneration processes of nZVI. The bubbling of acidified spent S-nZVI with air was not too effective in increasing ferric ions, as indicated by the initial masses of ferrous and ferric ions before bubbling: 0.7 g Fe^{2+} and 0.3 g Fe^{3+}, and after bubbling: 0.53 g Fe^{2+} and 0.47 g Fe^{3+}. However, this did not affect the results to obtain a reactive R-nZVI. The search on a good oxidant is going on to completely convert Fe^{2+} to Fe^{3+} in a shorter time without affecting the efficiency of the regeneration process. It is important to mention that the amount of total iron in the acidified S-nZVI was measured to be almost 1 gram (without losses in mass).

In general, the performance of regenerated nanoparticles seems slightly higher than the original synthesized nanoparticles as it appears in Fig. 5-7. This can be attributed to the lower pH of the entering regenerated solution of ferric chloride (pH 0.9) compared to the pH of the original ferric chloride solution (pH 2.4). The slightly lower pH solution is capable of dissolving iron (hydr)oxides and decreasing surface passivation of iron as previously mentioned in the treatment process.
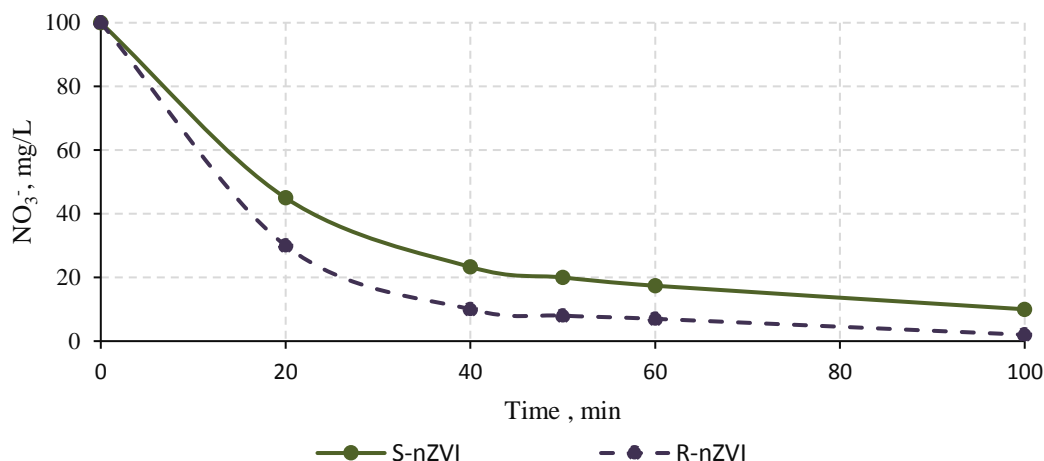
Fig. 5-7. Nitrate concentration profiles resulted from utilizing of S-nZVI and its regenerated nanoparticles R-nZVI (synthesized and regenerated at half reductant concentration) in batch experiments.

5.5. Conclusions

This chapter investigated the nitrate reduction reactivity and performance of four different types of nZVIs under the same batch experimental conditions. The effect of aging on nZVI was highlighted and found to have a collapsing effect on the reactivity. The nitrate removal efficiency for A-nZVI did not exceed 10% after a long period of time. Nevertheless, the aged nZVI was treated in an acid treatment process using a dilute HCl at a controlled and limited treatment time. This kind of washing surface removed portion of shell layer of nZVI particle leaving its surface exposed to the reduction reaction obtaining 50% removal of nitrate within three hours. While a one hour was sufficient to remove the whole nitrate load on applying the S-nZVI, which was used immediately after synthesis and characterized by its high value of BET-SSA. The spent S-nZVI was not wasted, it was regenerated using a diluted acid and reductant at specific conditions. A regeneration process was applied on the spent to produce R-nZVI which successfully reduced the whole amount of nitrate within the same short period (1h). The regeneration process of nZVI seems to be a promising process, especially for nZVI used in systems resembling pump-and-treat technologies and conventional activated sludge systems, but further optimization of this process should be executed to shorten its time, as this regeneration step of nZVI is a very important topic to be addressed. Summing up, the treatment and regeneration process suggested by this study can be employed to reactivate aged and spent reagent of nZVI particles used in water remediation.

THE DEVELOPMENT OF NANO-SCALE ZERO-VALENT IRON TECHNOLOGY FOR APPLICATION IN WATER TREATMENT

Chapter 6 The Development of Nano-scale Zero-Valent Iron Technology for Application in Water Treatment

Chapter 6 displays the method of developing the application of nZVI reagent in a laboratory-scale continuous-flow system. It describes the importance of this procedure before application on a large scale as it depicts the contemporary issues related to the remediation of a certain contaminant (nitrate) by a specific nZVI reagent in a type of design at certain operational conditions. Process and equipment designs are illustrated and performances are reported.

6.1. Introduction

It is still this new progressive technology of nano-scale zero-valent iron cannot spread for application in water treatment [133]. The process of application and the development of nZVI technology is by far continuously optimized to be more effective with a lower cost. Successful few applications were found recently. A nZVI pilot plant was founded to treat arsenic and heavy metals in a smelting non-ferrous wastewater as an additional unit to an established treatment process [132]. Alkaline process is known to be a common alternative to get rid of heavy metal through precipitation, and this is the only mechanism for removal via overdosing. This method results in major consequences and problems such as large amounts of hazardous sludge and generating additional costs, and other problems can arise as solids removal, poor settling and cementation of filters [231]. Upon the success of nZVI pilot plant, the nZVI treatment facility was built in April 2012, and operated by the Jiangxi Copper Company, Jiangxi, China, which is one of the largest copper producers in the world that manufactures 340,000 tons of copper annually from its mines [87]. The facility served as a pretreatment unit to remove arsenic and metals from the wastewater. The project proved the capability of nZVI in water treatment applications in which it was involved.

On another side, zero-valent iron-based materials can fit in different applications and confronted with various problems. For instance, the longevity of ZVI packed column seems to be a major concern [124, 232, 233]. Details on the hydraulic and reactive performance of PRBs as long-term data are available in few studies [121, 234]. Although nZVI has been tested and qualified to remediate wastewaters and groundwater, limited applications and scarce works were executed, which are not equivalent to the degree of efficacy that it shows.

According to the purpose of application, different types of technologies are implemented to achieve high performance and successful treatment. The permeable reactive barriers can treat shallow ground water, and otherwise it could be costly in dealing with the deep ground waters. Injection of nZVI in these deep wells could be beneficial in that case. For surface water and shallow groundwater, pump and treat technology could offer a more efficient solution than other methods. Economic study and basic knowledge on the pros and cons of these technologies are the key factors for the final verdict on the best decision. According to the life-cycle comparisons of PRBs versus pump and treat systems conducted by Higgins et al. (2009) [234], material production requirements in addition to energy usage during construction are main influential factors that affect the PRB erection whereas energy demands of processing and operation restrict pump and treat application. Moreover, the researchers stated that in order for granular ZVI-PRB to out-compete pump and treat systems, a minimum longevity of 10 years is required. Otherwise, the PRBs would perform lower than pump and treat systems.

6.1.1. Aim of work

This chapter introduces the concept of continuous treatment of nitrate contamination, which is different from the batch tests conducted throughout the all previous chapters. This is the first step towards full-scale application, as in order to construct pilot plant then a treatment facility unit, a laboratory-scale continuous-flow system (LSCFS) was designed and erected to decontaminate nitrate from water using nZVI-based materials.

One of the targets of this work is to check that nZVI process is scalable and efficient for application in water treatment using a cost-effective design. Moreover, LSCFS process is more reliable to give a clear depiction of nZVI performance in full-scale pump-and-treat technologies and conventional activated sludge systems. It is easy to detect, in this stage, the

problems of (by) products (ferrous, ferric, ZVI, nitrate, nitrite and ammonia, and their impact on the environment). Finding the solution at this point will save many efforts in advanced stages and designs.

Although the work contained in the preceded chapters has well-documented and illustrated nitrate removal in different situations, conditions and water bodies, nonetheless, treating a nitrate-contaminated river water in a real world conditions is challenging and beyond the limit of batch tests due to the complexity of actual water's composition. Therefore, a modified river water contaminated with nitrate was tested in LSCFS by using nZVI-based reagents.

Finally, this study is unique and based on our research; the lab-scale remediation of this process on nitrate removal by nZVI has not been executed until the documentation of this thesis.

6.2. Methods

6.2.1. Process of LSCFS and equipment design

The LSCFS process consists of three sequential units: a basic nZVI continuous stirring flask reactor, a settler or clarifier followed by a recirculating nZVI peristaltic pump, and a polishing unit to further treat the effluent water. The flow diagram of the process was best described in Fig. 6-1.
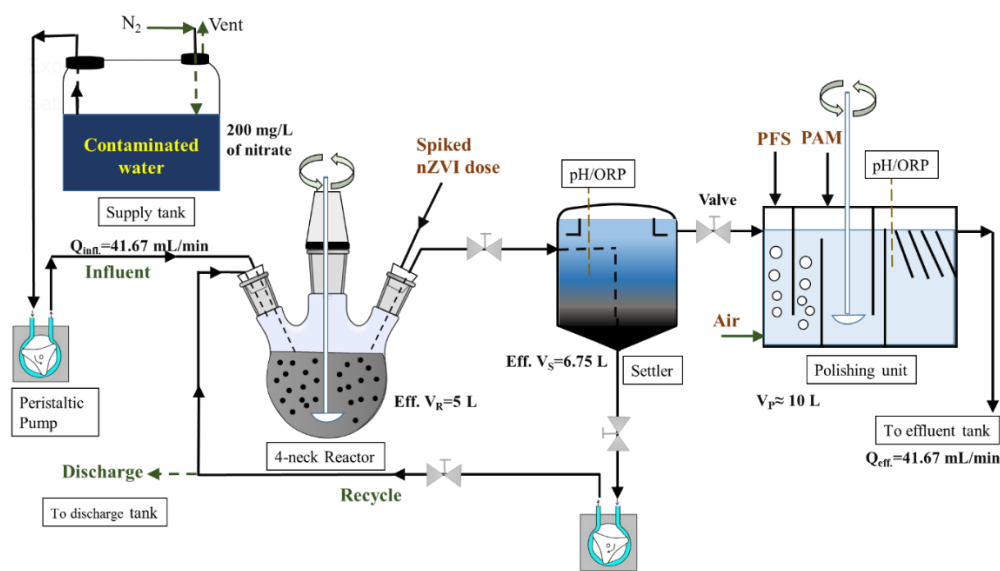
Fig. 6-1. The flow diagram of laboratory-scale continuous-flow system.

The LSCF system was operated at 2.5 L/h and 40-60 L of nitrate-contaminated water was treated with specific focus on remediating the first 20 L of the contaminated water, because the concentration in the treatment of this stage might be considered 1g/L as the amount of nZVI always used in LSCFS was 20 grams.

The design equation of a continuous stirring reactor can be derived from the law of mass conservation combined with first order rate equation of nitrate reduction by nZVI to obtain the following equation [235]:

$$C_{NO_3^-|out} = \frac{C_{NO_3^-|in}}{1+k\tau}$$ (6.1)

where $C_{NO_3^-|out}$ is the effluent desired nitrate concentration, $C_{NO_3^-|in}$ is the inlet concentration of nitrate to the reactor, k is the first order rate constant and τ is the residence time related to volume of the reactor (V_R) and its influent flowrate (Q_R) according to this relation: $\tau = V_R / Q_R$.

Based on the results of batch experiments of chapter 4, specifically in shaken flasks, k equals 0.37 h^{-1}, ($C_{NO_3^-|in} = 200$ mg/L, pH = 7, anaerobic, and dosage of nZVI = 1 g/L). If the desired outlet concentration was 114 mg/L (the same as that of batch test), the reaction/residence time is estimated to be 2 h and the reactor volume is designed to be 5 L (at Q_R=2.5 L/h). In another case, k equals 0.9 h^{-1} when using a continuous stirring reactor at the same mentioned conditions. By substituting in the design equation with residence time of 2 h, the obtained outlet nitrate concentration was lower than 114 mg/L. It was anticipated that the performance of LSCS would outstrip batch experiments due to various reasons, which will be discussed later. The effective volume of reactor was decided to be 5 L, and that of the settling unit to be close in volume (V_s =6.75 L). The selection of separator/settler size was also based on design calculations. Starting from Stokes law which states that denser and large particles maintain a higher settling velocity, Stokes equation to estimate aggregates settling velocities (v_T) was derived [236] :

$$v_T = \frac{gd^2(\rho_p - \rho_m)}{18\mu}$$ (6.2)

where g is the acceleration of gravity, d is the particle diameter of aggregates, ρ_p is the density of particle, ρ_m is the density of medium or slurry and μ is the viscosity of medium.

The design should use the minimum possible diameter of particles as they have the slowest settling velocity. At least d_{10} should be chosen for design. Estimating terminal

velocity at 1.563 µm (d_{10} of aggregate acquired from the particle size distribution data found in Fig. 5-2ii), v_T was about 25.2 mm/h which can offer a design (height of settler H_s and its diameter D_s) calculated from the following equality: $\tau = H_s/v_T = V_s/Q_{in}$. The estimated values of $D_s (d = 1.563 \text{ µm}) \approx 25.3$ cm and minimum required $H_s (\tau = 4h) = 10.08$ cm. Due to the high value of residence time and relative short height, the design of settler was modified and managed to be 18 cm Ds, 20 cm H_s (cylindrical part) and 5 cm H_s (conical bottom) that was able to settle ca. 3 µm with ~9 cm/h and residence time ~2.7 h. The conical part was essential to facilitate aggregation and settling of particle on the inclined surfaces. The longer height contributed to the setting improved efficiency because it allowed further settling of larger and aggregated particles that increased in size successively along the depth of settler.

The final unit is the polisher. It is composed of three compartments: the aeration chamber (to oxidize unreacted nZVI), coagulation chamber (to agglomerate and coagulate the particles of nZVI), and settling chamber (responsible for separation of oxidized iron and residual particles). The aeration time was adjusted at ca. 80 min to guarantee sufficient time for iron oxidation. Also for the same reason, in order to achieve adequate time for coagulation and settling process to occur in adequate time, the volumes of the three compartments were equal, and the whole volume of the polishing unit equaled approximately 10 L. PFS (Poly ferric sulfate hydrate, 97%, Sigma-Aldrich Co., USA) dose of 100 mg/L was added in chamber of aeration and coagulation, whereas PAM (poly acrylamide, number average molecular weight M_n 40,000, Sigma-Aldrich Co., USA) dose of 2 mg/L was added in the middle compartment. Both polymers were injected periodically to observe their effect on polishing process. All tube internal diameters used in this LSCFS setup were 5 mm, which was found to handle nZVI and its derivatives except for the supported nZVI on GAC that was subjected to severe clogging during operation.

6.2.2. Production of iron-based reagents

The iron-based reagents were simply produced by scaling-up the synthesis process mentioned in section "Synthesis of bare nZVI" located in Chapter 2. Bare nZVI was prepared in this case in a 5-L four-neck flask. Consequently, the volumes of reductant and precursors were equal to 2.5 L. Same conditions were maintained to produced 20 grams of fresh nZVI, which

was used after ethanol washing, drying and storage for 1 day at -18 °C. The bimetallic nZVI-Cu was prepared following the same methodology of pristine nZVI along with the addition of 1gram of anhydrous cupric chloride onto the precursor of ferric salt solution to adjust the concentration of copper in the final product 2.363% (wt Cu^0/wt Fe^0). This weight percent is the same attainable value caused by the modification of nZVI during the process of nitrate remediation via addition of 1 gram of anhydrous $CuCl_2$. The aspects of the improved performance due to the addition were discussed elsewhere (Chapter 3 of this thesis).

6.2.3. Experimental processes of LSCFS

There was a considerable number of experimental works and studies of different nZVI-based reagents and nitrate in different water bodies. However, due to few technical failures in some experiments (mainly clogging), 5 types of experiments were reported, which were replicated twice without any issue. CFNZVI 1 (Continuous-flow nZVI) is the first experiment that involved the treatment of nitrate contamination in initially deoxygenated distilled water at constant flowrate (41.67 mL/min). CFNZVI 2 considered the variation in residence times in the reactor and settler in the start-up stage (4.7 h) to be close to that of batch tests (2 h) by raising the flowrate at the beginning to~98 mL/min before entering the polishing step then the flowrate was adjusted again to 41.67 mL/min. CFNZVI 3 was conducted using a bimetallic nZVI-Cu material instead of pristine nZVI, while this bare nZVI was utilized in CFNZVI 4 against nitrate-contaminated river water brought from Ushikubi River, Kasuga, Fukuoka, Japan. The river water physical and chemical properties are reported below in Table 6-1. This water body was nitrate-free, but in order to simulate an actual case, this water was modified to accommodate nitrate pollution. Finally, CFNZVI 5 was identical to the process running in CFNZVI 4 except in the addition of copper salt ($CuCl_2$) as a surface modifier, electron stimulator and catalytic improver. In general, for all processed experiments, the amount of nZVI was initially spiked to the reactor and left to recycle from the settler to the reactor. The LSCFS treated nitrate contamination of initial concentration ca. 46.7 mg NO_3^-/L (ca. 207 mg NO_3^-/L) in all experiments. ORP and pH were monitored during fixed intervals of time in settler and polisher. 14 mL samples were obtained every hour available for nitrogen and iron compounds analyses. Iron compounds (ferrous and ferric ions or total iron ions) were detected twice, one time as dissolved Fe^{2+} and Fe ions in treated water; and

another determination in case of total iron presence whether it was ferrous or iron (dissolved and suspended Fe^{2+} and Fe^{3+}). This involved the dissolution of well-agitated homogenous sample in conc. HCl plus dilution to the suitable pH of spectrophotometric analyses.

Table 6-1. River water properties.

Property	Value or Conc. (mg/L)
pH	7.4
NO_3^-	2
Total NH_4^+	0.02
Total PO_4^{3-}-P	2
Total Alkalinity (mg $CaCO_3$/L)	673
COD	30
BOD	10
TDS	81
TSS	4

6.3. Outputs of implementations

Experimental studies of CFNZVI 1 are expressed in Figs. 6-2, 6-3 and 6-4. The nitrate concentration (Fig. 6-2) from the beginning until 8 h of producing effluent (20 L) was below 11 mg N/L (WHO threshold concentration), which reflects the significance of treatment process to maintain environmental regulations. The first outlet nitrate concentration was 1.44 mg N/L corresponding to ca. 97%, then a gradual increase of nitrate concentration (Fig. 6-2) and decrease of RE (Fig. 6-4) took place because of iron corrosion and consumption. Nevertheless, the reported removal efficiencies were higher than batch experiments of nZVI against the same nitrate concentration and water matrix whether they occurred in shaken

conical flasks (RE 45%) or continuous N_2-purging and stirred four-neck flasks (85%) mentioned in previous chapters. Adding that the LSCFS was not a completely closed system, and it was more prone to the intervention of dissolved oxygen, which might decrease the RE by 40%. The major role exhibited by recirculation of unreacted nZVI from the settler to the reactor was effective and influential factor in improving RE. In addition, the vigorous stirring (250 rpm) in reactor ensured the homogenous mixing and constant concentration flow to the gravitational separator, and the flow process itself increased the chances of molecules to face each other.

The nZVI converted nitrate into ammonium (average conc. ~35.5 mg/L) with a trend of generation opposite to that of nitrate reduction. Although there are no established US EPA action levels or WHO guidelines for ammonium in drinking water [237, 238], but it still acts as an unfavoured (non-desired) product. Nitrate reduction also produced nitrite in quantities lower than the guideline for nitrite (3 mg/L, 0.913 mg N/L) assigned by WHO [7]. The total nitrogen line represents the summation of all expected nitrogen compounds in the reduction reaction according to our deep study of mechanisms (revealed in chapter 3). Strangely, the line showed several drop values, confirming the evolution of nitrogen gas and ammonia gas that stripped out from the high alkaline solution of pH >10 (refer to Fig. 6-4). It is important to note that ammonium ions (NH_4^+) and ammonia molecules (NH_3^+) both coexist with each other in the solution then depending on the high degree of alkalinity of the medium, ammonia phase dominates and becomes easier to unleash.

Concerning rest of products, dissolved iron compounds shown in Fig. 6-3 increased gradually throughout the process of LSCFS for about 40 L effluent. The dissolved ferrous Fe^{2+}(D) and iron (Fe) ions did not exceed 2.5 mg/L and 10 mg/L, respectively, which are acceptable in drinking water [239]. Again, there is no proposed health-based guideline value for iron by WHO. Nevertheless, the quality standards of drinking water may differ from country to another. Japan, for example, has set its drinking water quality standard to 0.3 mg Fe/L [240], therefore, further improvements should occur to the polishing unit to comply with this quality standard. Another case, when studying the concentrations of total iron Fe^{2+} (T) and Fe (T), including dissolved and non-dissolved amounts, the values of Fe^{2+} (T) and Fe (T) were maximum at the beginning (6.65 and 68 mg/L, respectively) then gradually or sharply decreased, as a result of polymer addition, to less than 5 mg Fe^{2+} (T) /L and around

20 mg Fe (T) /L, respectively. The high values of Fe (T) are consistent with the production and release of iron oxide compounds from nitrate reduction (Eq. 3.12) which was then proceeded by acute oxidation in the polishing unit. However, these results pointed out to the low efficiency of the two other compartments of the prototype design of the polishing unit, which was progressively modified to suppress the maximum Fe (T) down to around or lower than 30 mg Fe (T) /L.
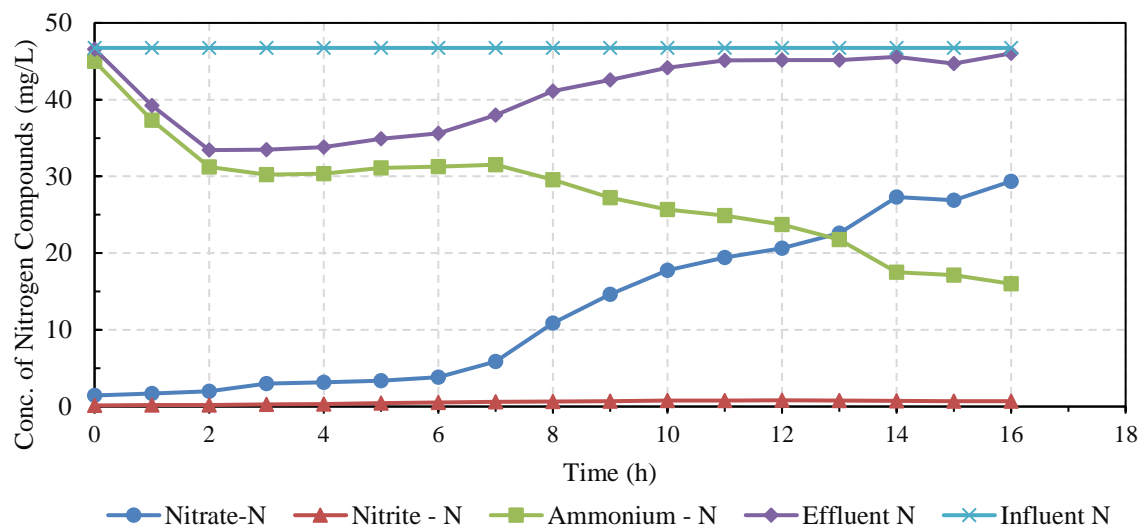
Fig. 6-2. Concentrations of nitrogen compounds in the effluent of CFNZVI experiment 1 (Reagent: nZVI, water body: DW, and type: constant flow rate).
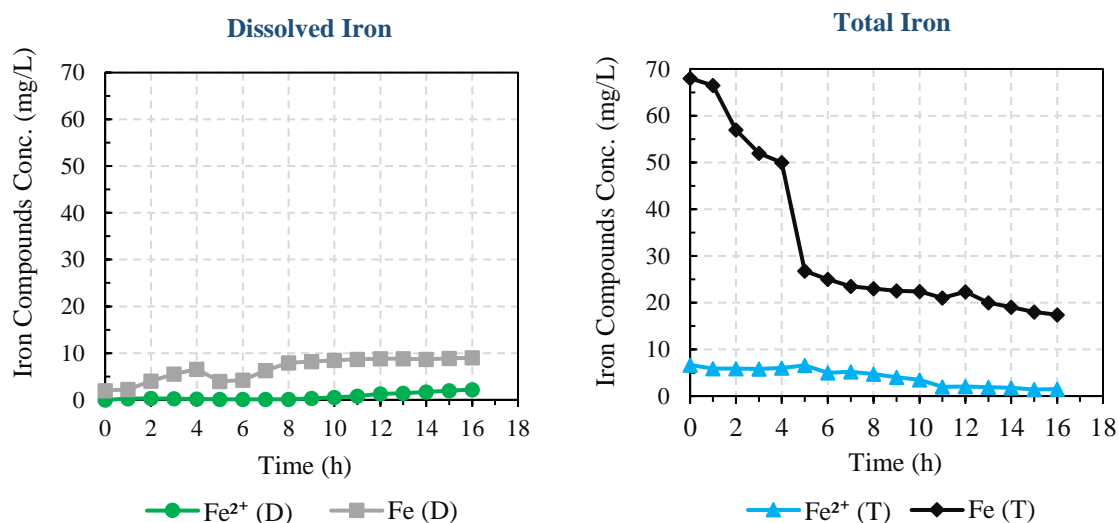
Fig. 6-3. Concentrations of Iron compounds in the effluent of CFNZVI experiment 1 (Reagent: nZVI, water body: DW, and type: constant flow rate).

There is a clear relation between RE% of nitrate and pH and ORP values in both settler and polisher units. The removal efficiency was found to be above 90% in the first 6 h (collecting 15 L) represented by a line of small inclination (Fig. 6-4), after that the RE% noticeably decreased. During the first period, the pH of settler and polisher increased followed by a slight decrease that seems to be approximately constant afterwards. The behavior of ORP apparently was the same, but occasionally it started at low negative value, continued decreasing to a lower value (-700 mV in the settler and -189 mV in the polisher) witnessed in the first 8-h period, ending with the gradual increase of ORP in the last stage when the reactivity of nZVI vanished with time. These results manifested that ORP could be a strong indicator of nZVI lifespan and reactivity inside reactors, and additional amounts of nZVI might be added based on the data monitoring of pH and ORP [87].
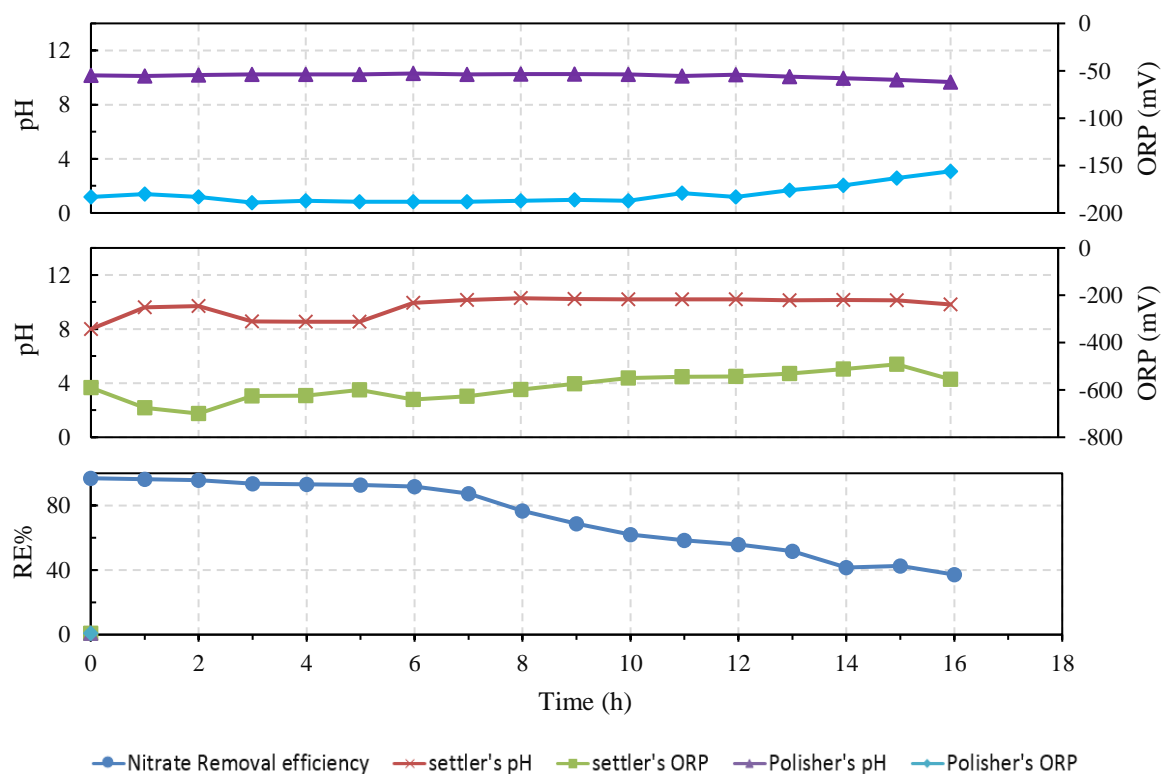
Fig. 6-4. Monitoring pH and ORP in both settler and Polishing unit of CFNZVI experiment 1 (Reagent: nZVI, water body: DW, and type: constant flow rate).

By comparing the performance of pristine nZVI in two types of operation of LSCFS in two experiments (CFNZVI 1 and CFNZVI 2), constant flowrate against constant (lower) residence time, the results of Fig. 6-5 showed the higher reactivity of nZVI in CFNZVI 1 than the same material under different condition of shorter and constant residence time. The most affected region was the initial interval of 8 h after that the two profiles of nitrate reduction seemingly coincide. The indication of the influential part contributed by residence time was shown clearly in the differential performance between both nitrate reduction profiles. Revisiting concentration of iron compounds, in that case of CFNZVI 2, the amendments in the polisher unit kept the value of the total iron under 25 mg Fe/L in Fig. 6-6. Both dissolved and total iron content in treated water showed peaks and troughs, which could be explained as an effect of polymer addition that suppressed the rising iron content, specially the doses of PFS and PAM were inserted according a discrete schedule and not as a continuous flow. As mentioned before, monitoring pH and ORP along the remediation process was an important factor to emphasize on the relation between these measurements and the concerned reactivity of nZVI. Fig. 6-7 yet shows the monitor process for extended periods (20 h). It appears plainly the decrease of both pH values of that of settler and polisher accompanying the decrease of nZVI reactivity. A more reliable indication was portrayed by ORP when its value inside the settler increased significantly from -688 to -101 mV and inside the polisher from a negative value (-203) to a positive one (165).
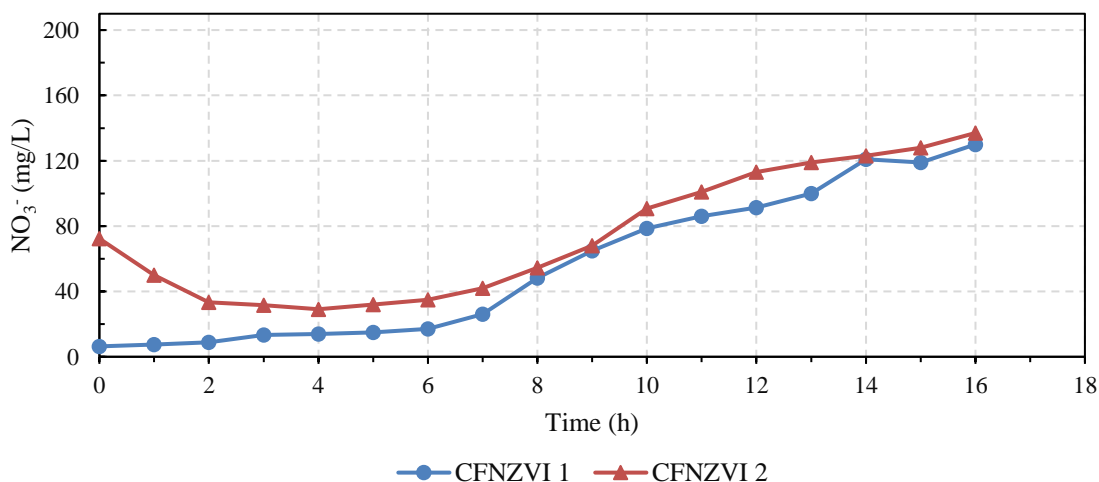
Fig. 6-5. Nitrate removal profile in CFNZVI 1 and CFNZVI 2 (Reagent: nZVI, water body: DW, and type: constant flow rate versus constant residence time).

Fig. 6-6. Concentrations of iron compounds in the effluent of CFNZVI experiment 2 (Reagent: nZVI, water body: DW, and type: constant residence time).
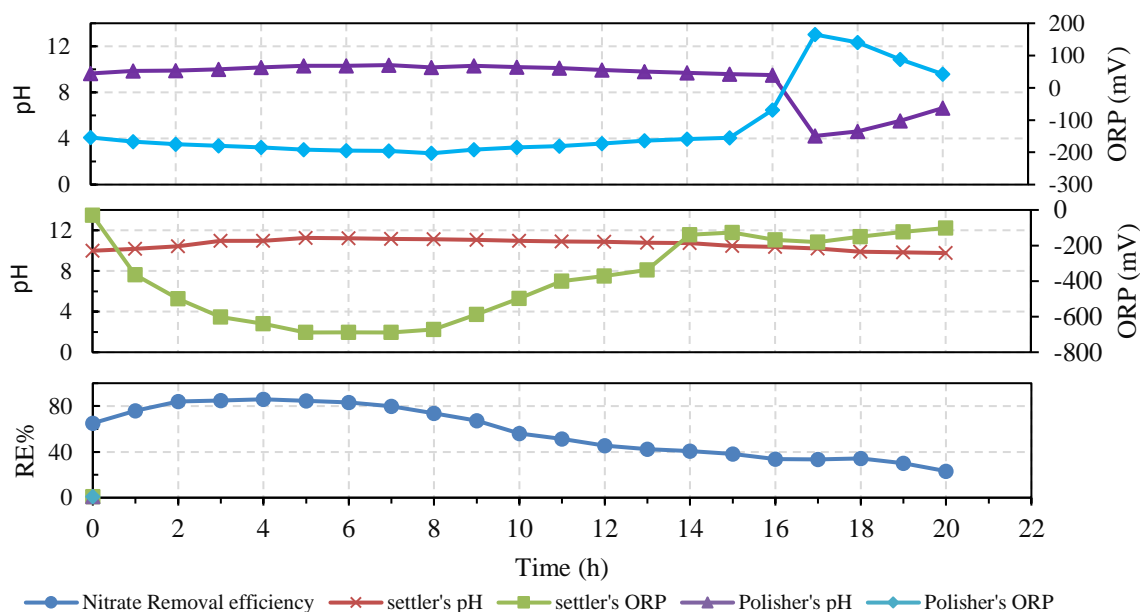
Fig. 6-7. Monitoring pH and ORP in both settler and Polishing unit of CFNZVI experiment 2 (Reagent: nZVI, water body: DW, and type: constant residence time).

Unlikely, the bimetallic nFe(0)-Cu(0) demonstrated unexpected slightly little effectiveness and capability in CFNZVI 3 lower than bare nZVI, clearly illustrated in Fig.

6-8. The reasons of that little deficiency might be linked to the higher reactivity of this composite, which could lead to accidental oxidation in air during filtration, drying or storage, taking into account the large amounts produced in this work compared to other literature mentioned studies. Another possible reason is that the used coating/ loading ratio of Cu(0) to nFe(0) might not be the optimum value for coating and enhancing the surface [167]. Considering the products of nitrate reduction, ammonia production did slightly decrease compared to that of CFNZVI 1, while nitrite concentration exceeded 2 mg N/L. The latter result is a recognized observation found in different studies of bimetallics and modifying by copper salt addition amidst treatment. Other results (not shown) of iron concentrations, pH and ORP values gave close similar observations to that performed by CFNZVI 1.

In this thesis, chapter 4 unfolded the effect of interference on nZVI performance in several scrutinized studies. The part of detrimental effect on nZVI reactivity could change design and operation calculation because of the unexpected results as shown in Fig. 6-9. Despite being a river water body not a wastewater, the best removal efficiency (recorded at the beginning) by nZVI only was less than 50 % in CFNZVI 4. The addition of copper ions as surface modifiers was deeply discussed in details throughout this thesis. At this time, the effect of this modification improved nZVI reactivity to the extent of achieving a maximum RE% (CFNZVI 5) more than double the corresponding one of CFNZVI 4. The improved nZVI (in the essence of reactivity perspective) had the ability to stabilize operational conditions and return the effectiveness of design to a certain approximate value.

An important check was executed concerning copper ions in the effluent of CFNZVI 5. The detected levels of these ions were always smaller than 1 mg/L depicted in Fig. 6-10, which matches with regulations, guidelines and water quality standard worldwide [240].

To get a better comparison, the overall RE% was calculated after determining the removed mass of nitrate ($R.m_{NO_3^-}$):

$$R.m_{NO_3^-} = C_0 V(t) - \int_{C_0}^{C_t} C_t dV(t) \tag{6.3}$$

where $R.m_{NO_3^-}$ was evaluated by subtracting nitrate effluent mass (the integral part) from the total mass $C_0 V(t)$ as C_0 is the concentration at t=0 and V is the volume treated at a certain time t. The most important period is the target region of collecting 20 L of treated water as described before. The integral part was estimated using the Trapezoidal rule starting from

initial concentration C_0 to final desired C_t that contained the target region. After that the overall nitrate RE% was calculated from comparing $R.m_{NO_3^-}$ with respect to nitrate total mass $C_0 V(t)$ carried in the flow, or determining total nitrate removal capacity of nZVI from comparing $R.m_{NO_3^-}$ with respect to total mass of nZVI used in experiments (20 g). The results revealed the order of reactivity of nZVI in CFNZVI from 1 to 5 as 92.22%, 80.9%, 87.21%, 30.04% and 65.5% with removal capacities 190.9, 167.5, 180.5, 62.2 and 135.6 mg nitrate/g nZVI. These output values strengthen the discussed points aforementioned in this section and emphasize on the retarding factor of short reaction time and matter intervention affecting negatively the reactivity. This stands against the positive contribution of modifiers that can fix what these retarders spoiled of reactivity.
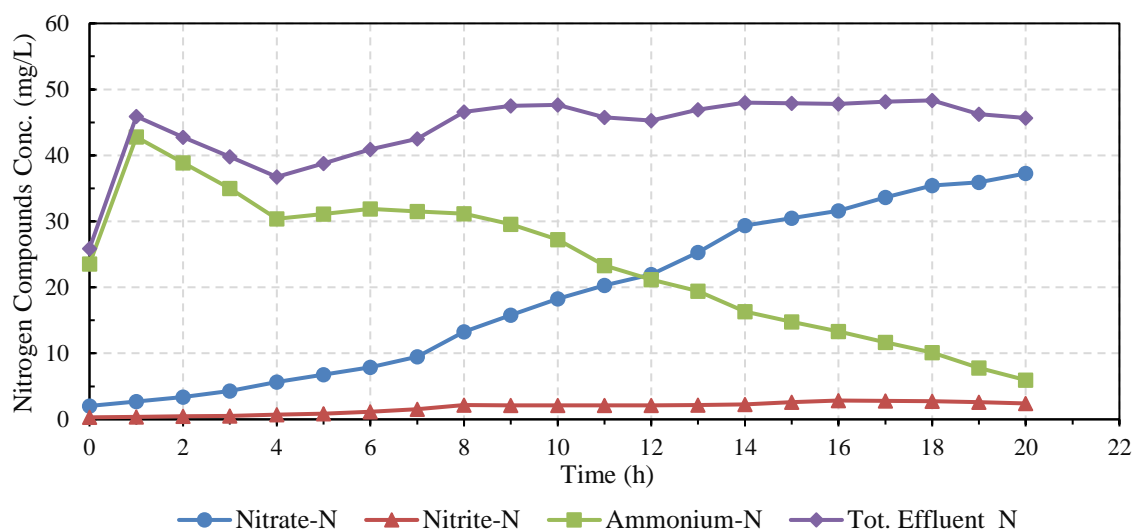
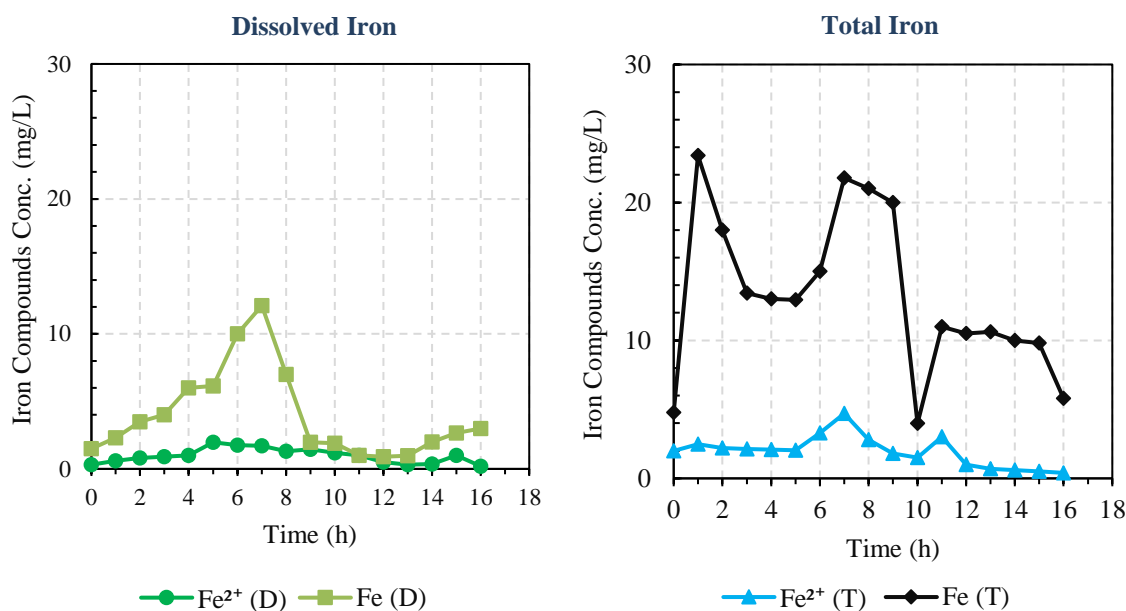**Fig. 6-8.** Concentrations of nitrogen compounds in the effluent of CFNZVI experiment 3 (Reagent: nFe(0)-Cu(0), water body: DW, and type: constant flow rate).
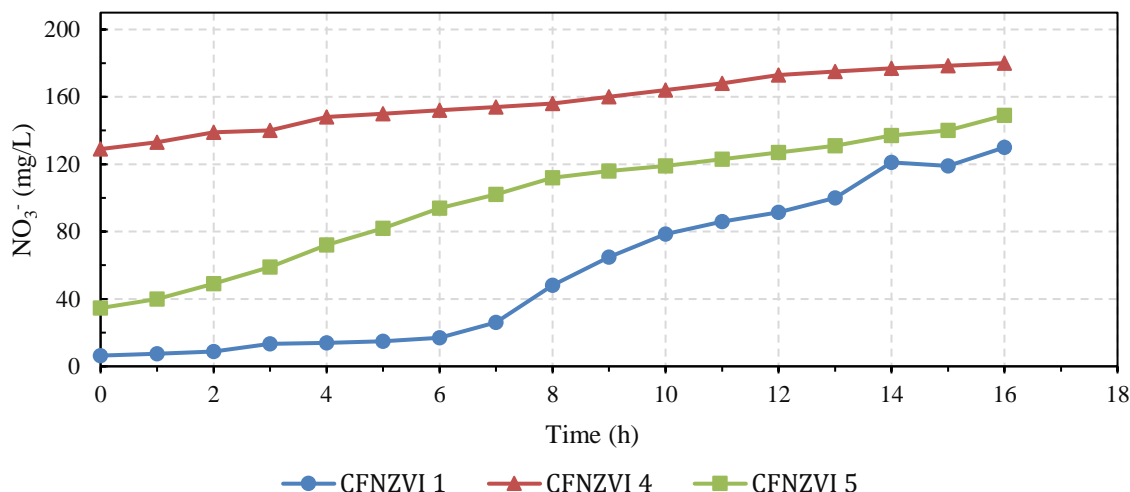
Fig. 6-9. Nitrate removal profile in CFNZVI 1, CFNZVI 4 and CFNZVI 5.
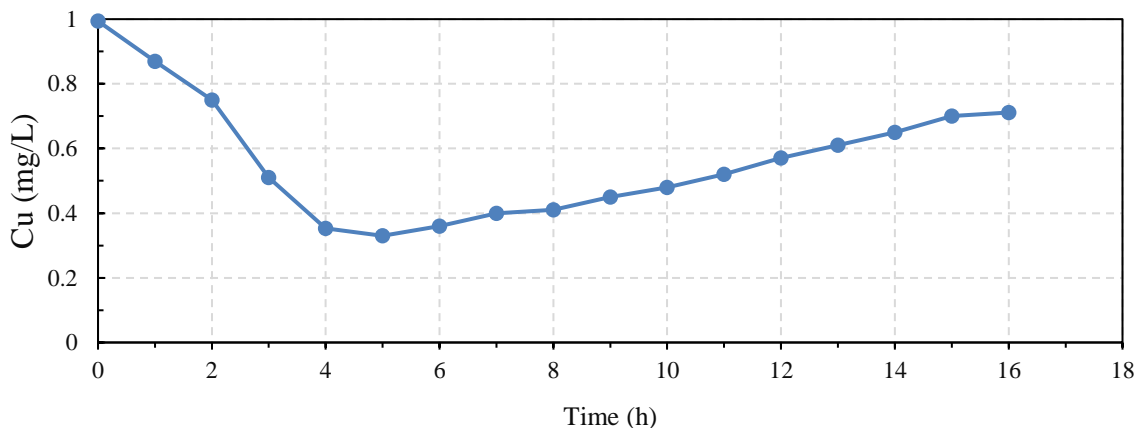
Fig. 6-10. Remaining copper ions in effluent stream of CFNZVI 5.

6.4. Issues facing nZVIs-LSCFS technology for nitrate treatment

The products of nZVI reactions with nitrate are iron oxides and hydroxides, ammonia, nitrite and nitrogen. Iron oxides and hydroxides are environmentally benign, and they could present minimal environmental and health risks at certain reasonable low levels. Nitrogen gas is a desired byproduct and nitrite concentration can be maintained at lower concentration via slightly increasing the dosage of nZVI or reaction (residence) time. However, ammonia generation is still a great problem in the treatment using nZVI. The main purpose of whole work was to promote the reactivity of nZVI in the treatment while the full treatment requires further more steps. Hence, nitrate could be treated in a combined system of nZVI and

heterotrophic-autotrophic denitrification biological treatment [212] or use zeolite derivatives to remove ammonium within the basic treatment stage or polishing unit [241]. Besides, zeolites mixtures with nZVI have the ability to increase the reaction kinetics of nitrate reduction by nZVI through continuous consumption of the main product (ammonia) after its release [168]. The previous solutions could also be used to cure problems of relatively high nitrite concentration in case of copper ions modified nZVI, which can sometimes surpass 4 mg N/L in case of CFNZVI 5. With respect to elimination of iron products in the effluents, the separator and polisher are the most important role players in this LSCFS to control the concentrations of these kinds of products. Developing new efficient designs and making use of iron magnetic properties in their separation could offer effective solutions for a better water quality.

6.5. Conclusions

The modest number of nZVI applications was the motivation of developing this technology and conducting this work. The laboratory-scale continuous-flow system was a successful trial to imitate real treatment facilities on the available lab scale. It is considered as a new system, which is difficult to find in the literature. This system presented great convenience in management, process control and operation offered by properties of nZVI especially its diminished size. It completely utilized the reactivity of nZVI particles in comparison with their performance in batch experiments. The design, arrangement, layout and operation should be tested on that lab scale as it reflects on the improvement or degradation of treatment. The recycle stream provided an access for remaining nZVI surfaces to further reactions and for iron hydr(oxides) shell layer to adsorb more nitrate with high contact time. The relatively long residence time, even higher than the time required reaching equilibrium in batch experiments, was yet effective in the treatment process. As a result of their high reactivities, nZVI particles were vulnerable against interference of low concentrations of common ions. The interference interrupted removal performance and defied validity of design and reliability of operation. Alternatives were few to regain removal performance in a close proximity to the original. The best method was applying modification of nZVI reactive surface with a more noble metal (as copper) during a treatment process. The high efficacy of nZVI/CuCl$_2$ was attributed to the in-situ deposition of copper and the recirculation

design of LSCFS. Overall, the nZVI-LSCFS showed a close resemblance to the performance of nZVI in actual applications including necessary unit operations, such as pumping, continuous flow reaction, separation, recirculation and polishing. The benefits extracted from such implementation exposed performance issues that needs to work on for a reliable design, operation and treatment quality.

CHAPTER 7

CONCLUSIONS AND

RECOMMENDATIONS

Chapter 7 Conclusions and Recommendations

Nano-scale zero-valent is a type of nanoparticles formed by a cutting-edge technology that carries future prospects for a promising emerging water treatment technology. Although nZVI has been studied for more than two decades to remove undesired constituents from water, its potential in water treatment is yet largely unexploited. In order to put nZVI in efficient use for water treatment, this research was developed. In this chapter, the major findings and anticipated future work included in this thesis are given. One of recommendations is suggested based on these findings that the combination of both modifications of copper salt addition and supporting nZVI on heat-modified activated carbon at optimum loading ratios and treatment condition (obtained from numerous investigations) forms a promising material that suits groundwater and wastewater treatment systems.

7.1. Major Findings and Recommendations

This thesis was developed relying upon a straightforward strategy organized as follows:

- Studying the nature of nZVI and its major drawbacks in water treatment applications
- Suggesting hypotheses about possible methods of modifications, especially innovating new methods such as addition of a promoting contaminant and the use of thermal treatment action on the support.
- Synthesizing nano iron-based reagent and characterizing the produced materials
- Careful selection of contaminants (nitrate and phosphorus) to deal with nZVI as presenters of their removal techniques
- Optimizing parameters of modifications by performing numerous batch tests under various conditions of reaction
- Deducing the steps or mechanisms of contaminants removal techniques by nZVI and modified nZVI (nZVI-based reagents)
- Characterizing the spent of iron-based reagent from treatment provided necessary evidences to support hypotheses

- Testing the validity of nZVI-based reagents in a lab-scale application

    The success of this strategy produced the subsequent major findings:

✓ The electrochemical stimulating corrosion and hydrogen catalytic effects of copper ions addition, during the remediation process of eutrophication causing contaminants, promoted removal kinetics (reactivity) of nZVI by two up to ten times more than that by ordinary pristine nZVI solely. The degree of enhancement depends on the reaction condition and presence of interfering substances. This effect is attributed to the formation of copper ferrite spinels on nZVI surface that also increases the adsorption capacities of contaminants.

✓ Promotion of nZVI reactivity reduced the negative effects generated from coexisting of interfering substances, dissolved oxygen and high pH of medium required treatment.

✓ The optimum addition ratio of $CuCl_2/Fe^0$ was found to be a mass ratio of 0.05 for best nitrate removal and 0.1 for best phosphorus removal. As the ratio 0.1 (wt $CuCl_2$/wt Fe^0) was not tested in nitrate removal experiments and the difference in performance prior to ratio of 0.05 is minor. Therefore, the optimum addition ratio of $CuCl_2/Fe^0$ is 0.1 (corresponding to 4.73% Cu^0/Fe^0).

✓ Recovery of phosphorus was well executed at high pH, proving the ability and reliability of nano iron materials to recycle an important nutrient as phosphorus in water treatment.

✓ The thermal treatment of AC support modified its textural and surface chemistry properties to attract contaminant anions with a higher affinity towards nZVI supported on that carrier.

✓ AC-supported nZVI ($F_1^2 AT_2^{950}$) was selected at optimum nZVI/AC mass ratio of 2:1 and treatment conditions of 950 ºC for 2 h for maximum performance.

✓ Interference studies showed that the negative impact on a certain contaminant (nitrate) resulted in over 40% drop in removal efficiency by nZVI

✓ Regeneration of spent nZVI particles regained full and complete removal efficiency of nitrate, the same as the synthesized nZVI.

✓ The performance exhibited by nZVI in nitrate treatment in the laboratory-scale continuous-flow system was the highest compared to all experiments performed by bare nZVI, due to the recirculation design and efficient mixing.

✓ Critical issues of treating nitrate by nZVI were revealed when applying in the laboratory-scale continuous-flow system.

Based on these finding, here are some suggestions and recommendations:

➢ The supported nZVI on treated activated carbon and modified by copper salt addition (CuCl$_2$/ $F_1^2AT_2^{950}$) is capable to enhance reactivity up to 15 times the original. The novel composite can be implemented as a promising reagent in environmental wastewater and groundwater technologies.

➢ Regeneration process of nZVI requires further optimization of conditions.

➢ Interferences studies and lab-scale practical application are important to undergo before scaling up to a pilot plant or a treatment unit facility. The drop in removal efficiency, because of interference, should be considered in the design process of treatment equipment and estimation of dosage amount required for treatment.

7.2. Future work

This work represents the forthcoming stage of my research in a further continuation of the accomplishments of this thesis.

7.2.1. Purpose of proposed future research

The main purpose of the research is to conduct full treatment of wastewater bodies by nZVI and its modified derivatives using LSCFS, refer to the schematic flow diagram of this process in Fig.7-1. The description of the process in this figure is similar to that mentioned in Chapter 6. One of the wastewater bodies that attracted our attention is the petroleum or oil refinery effluents (ORE). These discharges are wastewaters originating from the treatment and refining process of crude oil. This ORE is considered as a worldwide issue. According to Coelho et al. [242], the volume of ORE generated during processing can reach from 0.4 up to 1.6 times that of the crude oil processed, globally yielding a total of 38.8-155.2 million barrels per day (mbpd) of ORE accompanied with 97 mbpd of crude oil in 2017 [243]. In addition, treatment of such industrial wastewaters is challenging due to the presence of a variety of contaminants the natural oil contains. Usually the treatment is conducted in a number of stages. However, in case of applying a versatile material such as nZVI, the number of stages that could be used is anticipated to be lower.
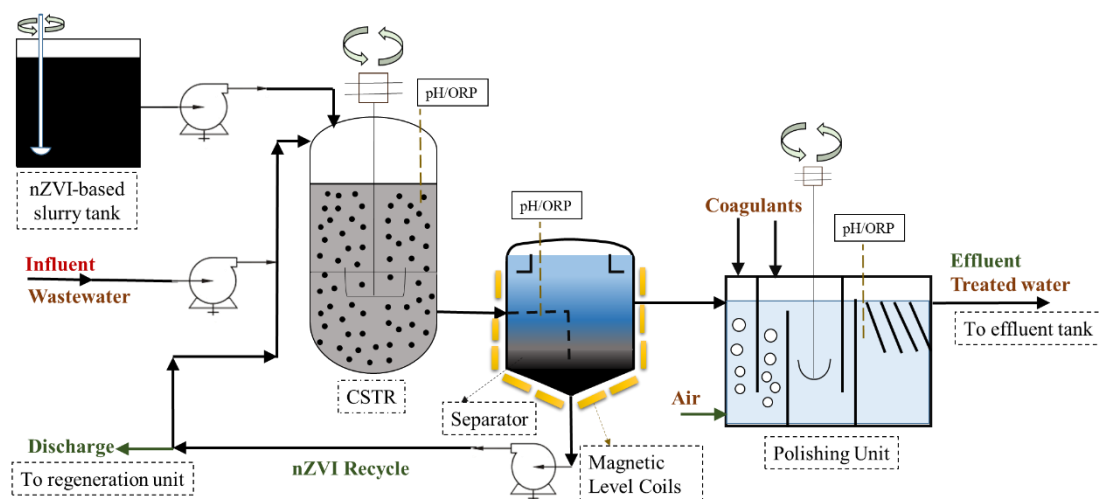
Fig. 7-1. The LSCFS for ORE wastewater treatment using nZVI-based reagents (associated with magnetic level coils and a polishing unit for improving separation of iron particles).

The amount of petroleum consumption is rapidly increasing, and subsequently, ORE volumes could present a considerable load on treatment units. Here are some general typical pollutants of ORE and their values as follows [244]: oil and grease within a range of 500 to 3000 mg/L, heavy metals (Cr, Cu, V, Zn, Ni, Pb) from 0.1–100 mg/L, BTEX (Benzene, Toluene, Ethylbenzene, Xylene) levels of 1–100 mg/L, COD level of 300-800 mg/L, phenol concentrations at 6–500 mg/L, polyaromatic hydrocarbons, and other inorganic compounds such as sulfates, sulfides, chlorides, ammonia, nitrate and phosphorus. Numerous technologies treated ORE with different efficiencies regarding each contaminant, including electrocoagulation [244], membranes processes, UV/O_3, $UV/H_2O_2/O_3$, photocatalytic degradation, biological processes and so forth [245]. The usage of subsequent number of different technologies increases both capital and operating treatment cost. On contrary, the major advantage of nZVI, as in this thesis, is that it can sustain the remediation of a wide range of contaminants via diverse mechanisms. For example, nZVI can remove phenol via Fenton oxidation, some heavy metals (HMs) by adsorption, other HMs and nitrate through reduction and so on. However, some points should be investigated that include (a) the influence of contaminants interference on each other and its relation with the required nZVI dosage, (b) effect of different parameters on the removal mechanism, involving temperature, dissolved oxygen, nZVI aging, pH, etc., (c) investigating the enhancement actions of modifying nZVI on the treatment of every pollutant of ORE, and (d) ensuring that the

residual contaminants after the treatment abide by regulations of WHO (World Health Organization) and environmental quality standards for human health in Japan. To the best of my present knowledge, the application of this research future work is *novel and unique* in this petroleum field.

7.2.2. Proposed future plan

The title of the project is "The Development of Treatment Technology of Oil Refinery Effluent by Nano-scale Zero-Valent Iron". Examining the performance of nZVI and its modified counterparts to full decontaminate OREs is stated as the main objective statement of this research. The LSCFS units can cover the physicochemical step and advanced treatment step of the ORE processing treatment [14]. Thus, the proposed future research plan should comply with the purpose, and it is composed of the following Work Breakdown Structures (WBS) depicted in the research plan timeline in Fig. 7-2:

WBS 1. REVIEW & PREPARE: (i) Review recent developments via literature survey on the relevant subject and recent advances in nZVI treatment technologies and (ii) prepare and purchase essential materials for the experimental work.

WBS 2. MODIFY & CONDUCT: (i) Modify nZVI surface either by metallic coating or supporting it on a matrix, and (ii) conduct batch (basic) experiments on each individual contaminant of ORE under different parametric conditions of pH, temperature, dissolved oxygen, alkalinity, hardness, etc.

WBS 3. SET UP & APPLY: (i) Set up LSCFS to the most suitable configuration and (ii) apply the optimized nZVI-based reagent for basic tests and ORE treatment (real case studies).

WBS 4. ANALYZE: perform analyses to acquire (i) water samples' physical properties (pH, temp., electric conductivity) and concentrations of chemical components using UV-visible spectrophotometer, gas chromatograph and inductively coupled plasma spectroscopy, and (ii) characteristics of nanoparticles such as morphology using a transmission electron microscope, crystallinity and mineral compositions using X-ray diffraction, particle dimensions by a particle size analyzer, specific surface area by surface characterization analyzer and others.

WBS 5. MODEL & SIMULATE: (i) Develop a simulating model of the ORE treatment by nZVI-based reagents in all experiments and (ii) compare results to the real values.

WBS 6. WRITE, REPORT & PROPOSE: (i) Write and submit research manuscripts to journals and conferences, (ii) report to the project managers who adopted my proposal, and (iii) propose a pilot plant design for a petroleum refinery companies.
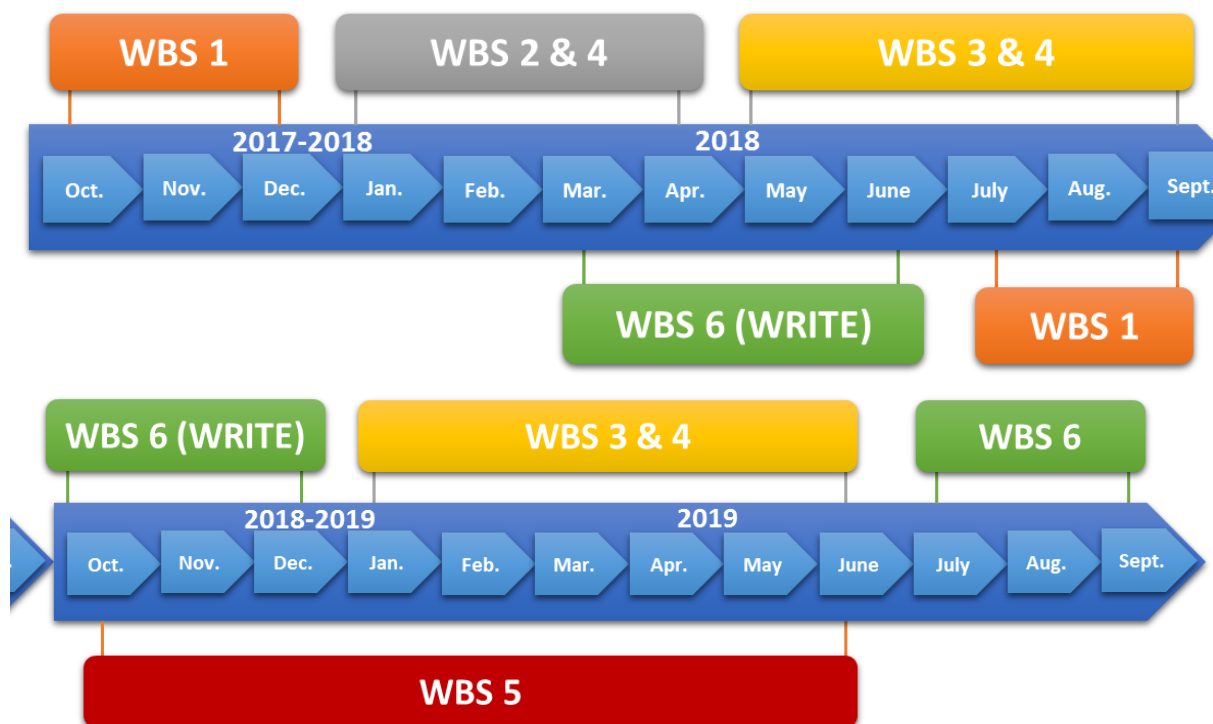
Fig. 7-2. Proposed future research plan timeline.

7.2.3. Expected results and impacts

Based on nZVI's multi-versatile contaminant remediation, there are great expectations, and it is anticipated the following:

(a) Full treatment of oil refinery effluent; (b) The determination of adequate dosage of nZVI-based reagent; (c) Dealing with the influence of contaminant and substance interferences; (d) Deciding on the best modification employed to nZVI particles; (e) Preventing some arising problems and issues related to the LSCFS process to achieve optimum treatment conditions; (f) Producing a scale-up simulating model of nZVI-LSCFS treatment process. Consequently,

the impact of aforementioned results on domestic and industrial wastewater treatment and purification centers could be highly beneficial. They could capitalize on the efficient and reliable performance of nZVI-based reagents and their remediation capability to treat a wide range of contaminants in addition to the simplicity of LSCFS design. According to the outputs of this research work, some petroleum refinery companies in Japan (and the world) along with some other purification centers could shift towards installing this technology to save money required for ORE and wastewater treatment.

References

1. Fu, F., D.D. Dionysiou, and H. Liu, *The use of zero-valent iron for groundwater remediation and wastewater treatment: a review*. Journal of Hazardous Materials, 2014. **267**: p. 194-205.
2. Organization, W.H. and UNICEF, *Progress on sanitation and drinking water–2015 update and MDG assessment*. 2015: World Health Organization.
3. Eckenfelder, W.W., et al., *Industrial water quality*. 2008: McGraw-Hill Professional.
4. National Bureau of Statistics of China. *Environmental statistical data(2013)*. 2017 [cited 2017 14/4]; (in Chinese)]. Available from: http://www.stats.gov.cn/ztjc/ztsj/hjtjzl/2013/201412/t20141216654129.html.
5. UNICEF. *Arsenic Contamination in Groundwater*. Current issues no. 2 (2013). Available from: https://www.unicef.org/media/files/Current_Issues_Paper_-_Arsenic_Contamination_in_Groundwater.pdf.
6. Mueller, N.C., et al., *Application of nanoscale zero valent iron (NZVI) for groundwater remediation in Europe*. Environmental Science and Pollution Research, 2012. **19**(2): p. 550-558.
7. Organization, W.H., *Nitrate and nitrite in drinking-water: Background document for development of WHO Guidelines for Drinking-water Quality*. 2003.
8. Lewis Jr, W.M., W.A. Wurtsbaugh, and H.W. Paerl, *Rationale for control of anthropogenic nitrogen and phosphorus to reduce eutrophication of inland waters*. Environmental science & technology, 2011. **45**(24): p. 10300-10305.
9. Follett, R.F. and J.L. Hatfield, *Nitrogen in the environment: sources, problems, and management*. The Scientific World Journal, 2001. **1**: p. 920-926.
10. Kapoor, A. and T. Viraraghavan, *Nitrate removal from drinking water-review*. Journal of Environmental Engineering, 1997. **123**(4): p. 371-380.
11. EPA. *Basic Information about Nitrate in Drinking Water*. [cited 2015 1/5]; Available from: http://water.epa.gov/drink/contaminants/basicinformation/nitrate.cfm.
12. Minister of the Environment (MOE), J. *Environmental quality standards for water pollution*. [cited 2017 1/4]; Available from: https://www.env.go.jp/en/water/wq/wp.pdf.
13. Huang, C.-P., H.-W. Wang, and P.-C. Chiu, *Nitrate reduction by metallic iron*. Water Research, 1998. **32**(8): p. 2257-2264.
14. Bae, B.-U., et al., *Improved brine recycling during nitrate removal using ion exchange*. Water Research, 2002. **36**(13): p. 3330-3340.
15. Schoeman, J. and A. Steyn, *Nitrate removal with reverse osmosis in a rural area in South Africa*. Desalination, 2003. **155**(1): p. 15-26.
16. Fernández-Nava, Y., et al., *Denitrification of wastewater containing high nitrate and calcium concentrations*. Bioresource Technology, 2008. **99**(17): p. 7976-7981.
17. Zhang, T.C. and Y.H. Huang, *Effects of selected Good's pH buffers on nitrate reduction by iron powder*. Journal of environmental engineering, 2005. **131**(3): p. 461-470.
18. Li, M., et al., *Treatment of nitrate contaminated water using an electrochemical method*. Bioresource technology, 2010. **101**(16): p. 6553-6557.

19.   Anderson, J.A., *Photocatalytic nitrate reduction over Au/TiO₂.* Catalysis Today, 2011. **175**(1): p. 316-321.

20.   Bhatnagar, A. and M. Sillanpää, *A review of emerging adsorbents for nitrate removal from water.* Chemical Engineering Journal, 2011. **168**(2): p. 493-504.

21.   Öztürk, N. and T.E.l. Bektaş, *Nitrate removal from aqueous solution by adsorption onto various materials.* Journal of hazardous materials, 2004. **112**(1): p. 155-162.

22.   Stahl, R.G., *The genetic toxicology of organic compounds in natural waters and wastewaters.* Ecotoxicology and environmental Safety, 1991. **22**(1): p. 94-125.

23.   Vega, M., et al., *Biological and chemical tools in the toxicological risk assessment of Jarama River, Madrid, Spain.* Environmental pollution, 1996. **93**(2): p. 135-139.

24.   Mandel, K., et al., *Layered double hydroxide ion exchangers on superparamagnetic microparticles for recovery of phosphate from waste water.* Journal of Materials Chemistry A, 2013. **1**(5): p. 1840-1848.

25.   Sims, J., R. Simard, and B. Joern, *Phosphorus loss in agricultural drainage: Historical perspective and current research.* Journal of Environmental Quality, 1998. **27**(2): p. 277-293.

26.   Devey, D. and N. Harkness, *The significance of man-made sources of phosphorus: detergents and sewage.* Water Research, 1973. **7**(1-2): p. 35-54.

27.   Smil, V., *Phosphorus in the environment: natural flows and human interferences.* Annual review of energy and the environment, 2000. **25**(1): p. 53-88.

28.   Mezenner, N.Y. and A. Bensmaili, *Kinetics and thermodynamic study of phosphate adsorption on iron hydroxide-eggshell waste.* Chemical Engineering Journal, 2009. **147**(2): p. 87-96.

29.   Eljamal, O., J. Okawauchi, and K. Hiramatsu. *Product Rich in Phosphorus Produced from Phosphorus-Contaminated Water*. in *Advanced Materials Research*. 2014. Trans Tech Publ.

30.   Woumfo, E.D., J.M. Siéwé, and D. Njopwouo, *A fixed-bed column for phosphate removal from aqueous solutions using an andosol-bagasse mixture.* Journal of environmental management, 2015. **151**: p. 450-460.

31.   Penn, C.J. and J.G. Warren, *Investigating phosphorus sorption onto kaolinite using isothermal titration calorimetry.* Soil Science Society of America Journal, 2009. **73**(2): p. 560-568.

32.   Cordell, D., J.-O. Drangert, and S. White, *The story of phosphorus: global food security and food for thought.* Global environmental change, 2009. **19**(2): p. 292-305.

33.   Eljamal, O., et al., *Phosphorus sorption from aqueous solution using natural materials.* Environmental earth sciences, 2013. **68**(3): p. 859-863.

34.   Song, Y., et al., *Nutrients removal and recovery by crystallization of magnesium ammonium phosphate from synthetic swine wastewater.* Chemosphere, 2007. **69**(2): p. 319-324.

35.   De-Bashan, L.E. and Y. Bashan, *Recent advances in removing phosphorus from wastewater and its future use as fertilizer (1997–2003).* Water research, 2004. **38**(19): p. 4222-4246.

36.   Youcef, L. and S. Achour, *Elimination des phosphates par des procédés physico-chimiques.* Larhyss Journal, 2005(04): p. 129-140.

37.   Karaca, S., et al., *Kinetic modeling of liquid-phase adsorption of phosphate on dolomite.* Journal of Colloid and Interface Science, 2004. **277**(2): p. 257-263.

38. Feynman, R.P., *There's plenty of room at the bottom.* Engineering and science, 1960. **23**(5): p. 22-36.

39. *Photo of Physicist Richard Feynman.* [cited 2017 9/3]; Available from: https://www.nano.gov/nanotech-101/what/definition.

40. *Photo of Professor Norio Taniguchi.* [cited 2017 9/3]; Available from: http://friendlyscienceguy.blogspot.jp/2013/05/nanotechnology-industry-of-very-small.html.

41. Drexler, K.E. and M. Minsky, *Engines of creation.* 1990: Fourth Estate London.

42. *Photo of Damascus Blade.* [cited 2017 9/3]; Available from: http://sustainable-nano.com/2013/06/17/nanotechnology-through-history-carbon-based-nanoparticles-from-prehistory-to-today/.

43. Yong, E. *Carbon nanotechnology in an 17ᵗʰ century Damascus sword.* 2008 [cited 2017 9/3]; Available from: http://scienceblogs.com/notrocketscience/2008/09/27/carbon-nanotechnology-in-an-17th-century-damascus-sword/.

44. Kahn, J., *Nanotechnology.* National Geographic, 2006: p. 98–119.

45. Di Sia, P., *Nanotechnology Among Innovation, Health and Risks.* Procedia - Social and Behavioral Sciences, 2017. **237**: p. 1076-1080.

46. Contreras, J., E. Rodriguez, and J. Taha-Tijerina, *Nanotechnology applications for electrical transformers—A review.* Electric Power Systems Research, 2017. **143**: p. 573-584.

47. He, L., J. Xu, and D. Bin, *Application of nanotechnology in petroleum exploration and development.* Petroleum Exploration and Development, 2016. **43**(6): p. 1107-1115.

48. Ferrari, M., *Cancer nanotechnology: opportunities and challenges.* Nature Reviews Cancer, 2005. **5**(3): p. 161-171.

49. Qu, X., P.J. Alvarez, and Q. Li, *Applications of nanotechnology in water and wastewater treatment.* Water research, 2013. **47**(12): p. 3931-3946.

50. Crini, G. and P.-M. Badot, *Sorption processes and pollution: conventional and non-conventional sorbents for pollutant removal from wastewaters.* 2010: Presses Univ. Franche-Comté.

51. Lu, C., H. Chiu, and C. Liu, *Removal of zinc (II) from aqueous solution by purified carbon nanotubes: kinetics and equilibrium studies.* Industrial & Engineering Chemistry Research, 2006. **45**(8): p. 2850-2855.

52. Ji, L., et al., *Mechanisms for strong adsorption of tetracycline to carbon nanotubes: a comparative study using activated carbon and graphite as adsorbents.* Environmental science & technology, 2009. **43**(7): p. 2322-2327.

53. Sharma, Y., et al., *Nano‐adsorbents for the removal of metallic pollutants from water and wastewater.* Environmental Technology, 2009. **30**(6): p. 583-609.

54. Yean, S., et al., *Effect of magnetite particle size on adsorption and desorption of arsenite and arsenate.* Journal of Materials Research, 2005. **20**(12): p. 3255-3264.

55. Diallo, M.S., et al., *Dendrimer enhanced ultrafiltration. 1. Recovery of Cu (II) from aqueous solutions using PAMAM dendrimers with ethylene diamine core and terminal NH₂ groups.* Environmental science & technology, 2005. **39**(5): p. 1366-1377.

56. Ramakrishna, S., et al., *Electrospun nanofibers: solving global issues.* Materials today, 2006. **9**(3): p. 40-50.

57. Maximous, N., et al., *Optimization of Al_2O_3/PES membranes for wastewater filtration.* Separation and Purification Technology, 2010. **73**(2): p. 294-301.

58. Bae, T.-H. and T.-M. Tak, *Effect of TiO_2 nanoparticles on fouling mitigation of ultrafiltration membranes for activated sludge filtration.* Journal of Membrane Science, 2005. **249**(1): p. 1-8.

59. Pendergast, M.T.M., et al., *Using nanocomposite materials technology to understand and control reverse osmosis membrane compaction.* Desalination, 2010. **261**(3): p. 255-263.

60. Lind, M.L., et al., *Influence of zeolite crystal size on zeolite-polyamide thin film nanocomposite membranes.* Langmuir, 2009. **25**(17): p. 10139-10145.

61. Liu, Z., et al., *A low-energy forward osmosis process to produce drinking water.* Energy & Environmental Science, 2011. **4**(7): p. 2582-2585.

62. Haynes, W.M., *CRC handbook of chemistry and physics.* Haynes, WM, ed. 2014, CRC Handbook of Chemistry and Physics, 95th edn.(Boca Raton, FL: CRC Press), ISBN 9781482208689., 2014.

63. Zhang, X., et al., *Kaolinite-supported nanoscale zero-valent iron for removal of Pb^{2+} from aqueous solution: reactivity, characterization and mechanism.* Water Research, 2011. **45**(11): p. 3481-3488.

64. Qiu, X., et al., *Emergency remediation of simulated chromium (VI)-polluted river by nanoscale zero-valent iron: Laboratory study and numerical simulation.* Chemical engineering journal, 2012. **193**: p. 358-365.

65. Lv, X., et al., *Highly active nanoscale zero-valent iron (nZVI)–Fe_3O_4 nanocomposites for the removal of chromium (VI) from aqueous solutions.* Journal of colloid and interface science, 2012. **369**(1): p. 460-469.

66. Neumann, A., et al., *Arsenic removal with composite iron matrix filters in Bangladesh: a field and laboratory study.* Environmental science & technology, 2013. **47**(9): p. 4544-4554.

67. Klas, S. and D.W. Kirk, *Advantages of low pH and limited oxygenation in arsenite removal from water by zero-valent iron.* Journal of hazardous materials, 2013. **252**: p. 77-82.

68. Yin, W., et al., *Experimental study of zero-valent iron induced nitrobenzene reduction in groundwater: the effects of pH, iron dosage, oxygen and common dissolved anions.* Chemical Engineering Journal, 2012. **184**: p. 198-204.

69. Gu, C., et al., *Synthesis of highly reactive subnano-sized zero-valent iron using smectite clay templates.* Environmental science & technology, 2010. **44**(11): p. 4258.

70. Shimizu, A., et al., *Phenol removal using zero-valent iron powder in the presence of dissolved oxygen: roles of decomposition by the Fenton reaction and adsorption/precipitation.* Journal of hazardous materials, 2012. **201**: p. 60-67.

71. Segura, Y., et al., *Enhancement of the advanced Fenton process (Fe^0/H_2O_2) by ultrasound for the mineralization of phenol.* Applied Catalysis B: Environmental, 2012. **113**: p. 100-106.

72. Dorathi, P.J. and P. Kandasamy, *Dechlorination of chlorophenols by zero valent iron impregnated silica.* Journal of Environmental Sciences, 2012. **24**(4): p. 765-773.

73. Shirin, S. and V.K. Balakrishnan, *Using chemical reactivity to provide insights into environmental transformations of priority organic substances: The Fe^0-mediated reduction of Acid Blue 129.* Environmental science & technology, 2011. **45**(24): p. 10369-10377.

74. Greenlee, L.F., et al., *Kinetics of zero valent iron nanoparticle oxidation in oxygenated water.* Environmental science & technology, 2012. **46**(23): p. 12913-12920.

75. Almeelbi, T. and A. Bezbaruah, *Aqueous phosphate removal using nanoscale zero-valent iron.* Journal of Nanoparticle Research, 2012. **14**(7): p. 1-14.

76. Cao, J., et al., *Synthesis of monodispersed CMC-stabilized Fe–Cu bimetal nanoparticles for in situ reductive dechlorination of 1, 2, 4-trichlorobenzene.* Science of The Total Environment, 2011. **409**(11): p. 2336-2341.

77. Su, C., et al., *A two and half-year-performance evaluation of a field test on treatment of source zone tetrachloroethene and its chlorinated daughter products using emulsified zero valent iron nanoparticles.* Water research, 2012. **46**(16): p. 5071-5084.

78. Kustov, L.M., et al., *Pd–Fe nanoparticles stabilized by chitosan derivatives for perchloroethene dechlorination.* Environment international, 2011. **37**(6): p. 1044-1052.

79. Choi, K. and W. Lee, *Enhanced degradation of trichloroethylene in nano-scale zero-valent iron Fenton system with Cu (II).* Journal of Hazardous materials, 2012. **211**: p. 146-153.

80. Stefaniuk, M., P. Oleszczuk, and Y.S. Ok, *Review on nano zerovalent iron (nZVI): From synthesis to environmental applications.* Chemical Engineering Journal, 2016. **287**: p. 618-632.

81. Jou, C.-J.G., et al., *Combining zero-valent iron nanoparticles with microwave energy to treat chlorobenzene.* Journal of the Taiwan Institute of Chemical Engineers, 2010. **41**(2): p. 216-220.

82. Tong, M., et al., *Reduction of nitrobenzene in groundwater by iron nanoparticles immobilized in PEG/nylon membrane.* Journal of Contaminant Hydrology, 2011. **122**(1–4): p. 16-25.

83. Zhang, X., et al., *Degradation of 2,4,6-trinitrotoluene (TNT) from explosive wastewater using nanoscale zero-valent iron.* Chemical Engineering Journal, 2010. **158**(3): p. 566-570.

84. Jiang, Z., et al., *Nitrate reduction using nanosized zero-valent iron supported by polystyrene resins: role of surface functional groups.* Water research, 2011. **45**(6): p. 2191-2198.

85. Hwang, Y.-H., D.-G. Kim, and H.-S. Shin, *Mechanism study of nitrate reduction by nano zero valent iron.* Journal of Hazardous Materials, 2011. **185**(2): p. 1513-1521.

86. Ryu, A., et al., *Reduction of highly concentrated nitrate using nanoscale zero-valent iron: effects of aggregation and catalyst on reactivity.* Applied Catalysis B: Environmental, 2011. **105**(1): p. 128-135.

87. Li, S., et al., *Heavy metal removal using nanoscale zero-valent iron (nZVI): theory and application.* Journal of hazardous materials, 2017. **322**: p. 163-171.

88.   Lv, X., et al., *Removal of chromium (VI) from wastewater by nanoscale zero-valent iron particles supported on multiwalled carbon nanotubes.* Chemosphere, 2011. **85**(7): p. 1204-1209.

89.   Tanboonchuy, V., N. Grisdanurak, and C.-H. Liao, *Background species effect on aqueous arsenic removal by nano zero-valent iron using fractional factorial design.* Journal of hazardous materials, 2012. **205**: p. 40-46.

90.   Jing, C., Y. Li, and S. Landsberger, *Review of soluble uranium removal by nanoscale zero valent iron.* Journal of Environmental Radioactivity, 2016. **164**: p. 65-72.

91.   Shan, G., et al., *Applications of nanomaterials in environmental science and engineering: review.* Practice Periodical of Hazardous, Toxic, and Radioactive Waste Management, 2009. **13**(2): p. 110-119.

92.   Li, S., W. Yan, and W.-x. Zhang, *Solvent-free production of nanoscale zero-valent iron (nZVI) with precision milling.* Green Chemistry, 2009. **11**(10): p. 1618-1626.

93.   Nurmi, J.T., et al., *Characterization and properties of metallic iron nanoparticles: spectroscopy, electrochemistry, and kinetics.* Environmental Science & Technology, 2005. **39**(5): p. 1221-1230.

94.   Hoch, L.B., et al., *Carbothermal synthesis of carbon-supported nanoscale zero-valent iron particles for the remediation of hexavalent chromium.* Environmental science & technology, 2008. **42**(7): p. 2600-2605.

95.   Jamei, M.R., M.R. Khosravi, and B. Anvaripour, *Investigation of ultrasonic effect on synthesis of nano zero valent iron particles and comparison with conventional method.* Asia‐Pacific Journal of Chemical Engineering, 2013. **8**(5): p. 767-774.

96.   Hoag, G.E., et al., *Degradation of bromothymol blue by 'greener'nano-scale zero-valent iron synthesized using tea polyphenols.* Journal of Materials Chemistry, 2009. **19**(45): p. 8671-8677.

97.   Kuang, Y., et al., *Heterogeneous Fenton-like oxidation of monochlorobenzene using green synthesis of iron nanoparticles.* Journal of Colloid and Interface Science, 2013. **410**: p. 67-73.

98.   Yoo, B.-Y., et al., *Electrochemically fabricated zero-valent iron, iron-nickel, and iron-palladium nanowires for environmental remediation applications.* Water science and technology, 2007. **55**(1-2): p. 149-156.

99.   Chen, S.-S., H.-D. Hsu, and C.-W. Li, *A new method to produce nanoscale iron for nitrate removal.* Journal of Nanoparticle Research, 2004. **6**(6): p. 639-647.

100.   Xu, J., et al., *Dechlorination of 2,4-dichlorophenol by nanoscale magnetic Pd/Fe particles: Effects of pH, temperature, common dissolved ions and humic acid.* Chemical Engineering Journal, 2013. **231**: p. 26-35.

101.   Yang, L., et al., *Catalytic dechlorination of monochlorobenzene by Pd/Fe nanoparticles immobilized within a polymeric anion exchanger.* Chemical Engineering Journal, 2011. **178**: p. 161-167.

102.   Shih, Y.-h., M.-Y. Chen, and Y.-F. Su, *Pentachlorophenol reduction by Pd/Fe bimetallic nanoparticles: Effects of copper, nickel, and ferric cations.* Applied Catalysis B: Environmental, 2011. **105**(1–2): p. 24-29.

103.   Wu, L., M. Shamsuzzoha, and S. Ritchie, *Preparation of cellulose acetate supported zero-valent iron nanoparticles for the dechlorination of trichloroethylene in water.* Journal of Nanoparticle Research, 2005. **7**(4-5): p. 469-476.

104.   Wu, L. and S. Ritchie, *Enhanced dechlorination of trichloroethylene by membrane‐supported Pd‐coated iron nanoparticles.* Environmental Progress, 2008. **27**(2): p. 218-224.

105.   Zhu, H., et al., *Removal of arsenic from water by supported nano zero-valent iron on activated carbon.* Journal of Hazardous Materials, 2009. **172**(2): p. 1591-1596.

106.   Ling, X., et al., *Synthesis of nanoscale zero-valent iron/ordered mesoporous carbon for adsorption and synergistic reduction of nitrobenzene.* Chemosphere, 2012. **87**(6): p. 655-660.

107.   Zhang, R., et al., *Reduction of nitrobenzene using nanoscale zero-valent iron confined in channels of ordered mesoporous silica.* Colloids and Surfaces A: Physicochemical and Engineering Aspects, 2013. **425**: p. 108-114.

108.   Du, Q., et al., *Bifunctional resin-ZVI composites for effective removal of arsenite through simultaneous adsorption and oxidation.* Water research, 2013. **47**(16): p. 6064-6074.

109.   Shu, H.-Y., et al., *Using resin supported nano zero-valent iron particles for decoloration of Acid Blue 113 azo dye solution.* Journal of Hazardous Materials, 2010. **184**(1): p. 499-505.

110.   Liu, T., et al., *Enhanced chitosan/Fe^0-nanoparticles beads for hexavalent chromium removal from wastewater.* Chemical Engineering Journal, 2012. **189–190**: p. 196-202.

111.   Liu, T., et al., *Enhanced chitosan beads-supported Fe^0-nanoparticles for removal of heavy metals from electroplating wastewater in permeable reactive barriers.* Water research, 2013. **47**(17): p. 6691-6700.

112.   Zhang, Y., et al., *Enhanced removal of nitrate by a novel composite: nanoscale zero valent iron supported on pillared clay.* Chemical Engineering Journal, 2011. **171**(2): p. 526-531.

113.   Shi, L.-n., X. Zhang, and Z.-l. Chen, *Removal of chromium (VI) from wastewater using bentonite-supported nanoscale zero-valent iron.* Water research, 2011. **45**(2): p. 886-892.

114.   Chen, Z.-x., et al., *Removal of methyl orange from aqueous solution using bentonite-supported nanoscale zero-valent iron.* Journal of colloid and Interface Science, 2011. **363**(2): p. 601-607.

115.   Zhang, X., et al., *Kaolinite-supported nanoscale zero-valent iron for removal of Pb2$^+$ from aqueous solution: Reactivity, characterization and mechanism.* Water Research, 2011. **45**(11): p. 3481-3488.

116.   Kim, S.A., et al., *Removal of Pb (II) from aqueous solution by a zeolite–nanoscale zero-valent iron composite.* Chemical Engineering Journal, 2013. **217**: p. 54-60.

117.   Frost, R.L., Y. Xi, and H. He, *Synthesis, characterization of palygorskite supported zero-valent iron and its application for methylene blue adsorption.* Journal of colloid and interface science, 2010. **341**(1): p. 153-161.

118.   Quinn, J., et al., *Field demonstration of DNAPL dehalogenation using emulsified zero-valent iron.* Environmental Science & Technology, 2005. **39**(5): p. 1309-1318.

119.   Gillham, R.W. and S.F. O'Hannesin, *Enhanced degradation of halogenated aliphatics by zero‐valent iron.* Ground water, 1994. **32**(6): p. 958-967.

120. Gu, B., et al., *Biogeochemical dynamics in zero-valent iron columns: implications for permeable reactive barriers.* Environmental Science & Technology, 1999. **33**(13): p. 2170-2177.

121. Warner, S.D., et al., *The first commercial permeable reactive barrier composed of granular iron: hydraulic and chemical performance at 10 years of operation.* IAHS PUBLICATION, 2005. **298**: p. 32.

122. Obiri-Nyarko, F., S.J. Grajales-Mesa, and G. Malina, *An overview of permeable reactive barriers for in situ sustainable groundwater remediation.* Chemosphere, 2014. **111**: p. 243-259.

123. U.S.EPA. *Field Applications of in-situ remediation technologies: permeable reactive barriers*. EPA 68-W-00-084 (2002). Available from: https://clu-in.org/download/rtdf/fieldapp_prb.pdf.

124. Wilkin, R.T., et al., *Fifteen-year assessment of a permeable reactive barrier for treatment of chromate and trichloroethylene in groundwater.* Science of the total environment, 2014. **468**: p. 186-194.

125. Baric, M., et al., *Coupling of polyhydroxybutyrate (PHB) and zero valent iron (ZVI) for enhanced treatment of chlorinated ethanes in permeable reactive barriers (PRBs).* Chemical Engineering Journal, 2012. **195–196**: p. 22-30.

126. Gibert, O., et al., *In-situ remediation of acid mine drainage using a permeable reactive barrier in Aznalcóllar (Sw Spain).* Journal of Hazardous Materials, 2011. **191**(1–3): p. 287-295.

127. Lu, X., et al., *Electrochemical depassivation for recovering Fe^0 reactivity by Cr(VI) removal with a permeable reactive barrier system.* Journal of Hazardous Materials, 2012. **213–214**: p. 355-360.

128. Liu, S.-J., et al., *An anaerobic two-layer permeable reactive biobarrier for the remediation of nitrate-contaminated groundwater.* Water Research, 2013. **47**(16): p. 5977-5985.

129. Karn, B., T. Kuiken, and M. Otto, *Nanotechnology and in situ remediation: a review of the benefits and potential risks.* Environmental health perspectives, 2009: p. 1823-1831.

130. EPA, U.S. *Cost Analyses for Selected Groundwater Cleanup Projects: Pump and Treat Systems and Permeable Reactive Barriers*. EPA 542-R-00-013 (2001). Available from: https://www.epa.gov/sites/production/files/2015-04/documents/cost_analysis_groundwater.pdf.

131. Cundy, A.B., L. Hopkinson, and R.L. Whitby, *Use of iron-based technologies in contaminated land and groundwater remediation: a review.* Science of the total environment, 2008. **400**(1): p. 42-51.

132. Li, S., et al., *Zero-valent iron nanoparticles (nZVI) for the treatment of smelting wastewater: a pilot-scale demonstration.* Chemical Engineering Journal, 2014. **254**: p. 115-123.

133. Crane, R. and T. Scott, *Nanoscale zero-valent iron: future prospects for an emerging water treatment technology.* Journal of hazardous materials, 2012. **211**: p. 112-125.

134. Elliott, D.W. and W.-X. Zhang, *Field assessment of nanoscale bimetallic particles for groundwater treatment.* Environmental science & technology, 2001. **35**(24): p. 4922-4926.

135. Busch, J., et al., *A field investigation on transport of carbon-supported nanoscale zero-valent iron (nZVI) in groundwater.* Journal of contaminant hydrology, 2015. **181**: p. 59-68.

136. Lee, C., et al., *Bactericidal effect of zero-valent iron nanoparticles on Escherichia coli.* Environmental science & technology, 2008. **42**(13): p. 4927.

137. Auffan, M., et al., *Relation between the redox state of iron-based nanoparticles and their cytotoxicity toward Escherichia coli.* Environmental science & technology, 2008. **42**(17): p. 6730-6735.

138. Chen, P.-J., et al., *Toxicity assessments of nanoscale zerovalent iron and its oxidation products in medaka (Oryzias latipes) fish.* Marine Pollution Bulletin, 2011. **63**(5–12): p. 339-346.

139. El‑Temsah, Y.S. and E.J. Joner, *Impact of Fe and Ag nanoparticles on seed germination and differences in bioavailability during exposure in aqueous suspension and soil.* Environmental toxicology, 2012. **27**(1): p. 42-49.

140. Keenan, C.R., et al., *Oxidative stress induced by zero-valent iron nanoparticles and Fe (II) in human bronchial epithelial cells.* Environ Sci Technol, 2009. **43**(12): p. 4555-4560.

141. Tang, S.C.N. and I.M.C. Lo, *Magnetic nanoparticles: Essential factors for sustainable environmental applications.* Water Research, 2013. **47**(8): p. 2613-2632.

142. Li, Z., et al., *Adsorbed polymer and NOM limits adhesion and toxicity of nano scale zerovalent iron to E. coli.* Environmental science & technology, 2010. **44**(9): p. 3462-3467.

143. Shin, K.-H. and D.K. Cha, *Microbial reduction of nitrate in the presence of nanoscale zero-valent iron.* Chemosphere, 2008. **72**(2): p. 257-262.

144. Phenrat, T., et al., *Partial oxidation ("aging") and surface modification decrease the toxicity of nanosized zerovalent iron.* Environmental science & technology, 2008. **43**(1): p. 195-200.

145. Khalil, A.M., et al., *Promoting nitrate reduction kinetics by nanoscale zero valent iron in water via copper salt addition.* Chemical Engineering Journal, 2016. **287**: p. 367-380.

146. Eljamal, O., et al., *Phosphorus removal from aqueous solution by nanoscale zero valent iron in the presence of copper chloride.* Chemical Engineering Journal, 2016. **293**: p. 225-231.

147. Khalil, A.M., et al., *Optimized nano-scale zero-valent iron supported on treated activated carbon for enhanced nitrate and phosphate removal from water.* Chemical Engineering Journal, 2017. **309**: p. 349-365.

148. Khalil, A.M., et al., *Treatment and Regeneration of Nano-scale Zero-valent Iron Spent in Water Remediation.* EVERGREEN Joint Journal of Novel Carbon Resource Sciences & Green Asia Strategy, 2017. **4**(1): p. 21-28.

149. Hwang, Y.-H., D.-G. Kim, and H.-S. Shin, *Effects of synthesis conditions on the characteristics and reactivity of nano scale zero valent iron.* Applied Catalysis B: Environmental, 2011. **105**(1): p. 144-150.

150. Hach. *HACH METHODS Quick Reference Guide*. DOC052.53.25020.Augl16 (2016). Available from: https://www.hach.com/asset-get.download.jsa?id=7639983567.

151. Eaton, A.D., et al., *WE Federation.* Standard Methods for the Examination of Water and Wastewater, American Public Health Association, 2005.

152. Fresenius, W., K.E. Quentin, and W. Schneider, *Water analysis; a practical guide to physico-chemical, chemical and microbiological water examination and quality assurance.* 1988: Springer-Verlag.

153. Cheng, I.F., et al., *Reduction of nitrate to ammonia by zero-valent iron.* Chemosphere, 1997. **35**(11): p. 2689-2695.

154. Liou, Y.H., et al., *Chemical reduction of an unbuffered nitrate solution using catalyzed and uncatalyzed nanoscale iron particles.* Journal of Hazardous Materials, 2005. **127**(1): p. 102-110.

155. Yang, G.C. and H.-L. Lee, *Chemical reduction of nitrate by nanosized iron: kinetics and pathways.* Water research, 2005. **39**(5): p. 884-894.

156. Su, Y., et al., *Simultaneous removal of cadmium and nitrate in aqueous media by nanoscale zerovalent iron (nZVI) and Au doped nZVI particles.* Water research, 2014. **63**: p. 102-111.

157. Young, G., et al., *Chemical reduction of nitrate in water.* Journal (Water Pollution Control Federation), 1964: p. 395-398.

158. O'Carroll, D., et al., *Nanoscale zero valent iron and bimetallic particles for contaminated site remediation.* Advances in Water Resources, 2013. **51**: p. 104-122.

159. Flis, J., *Corrosion of metals and hydrogen-related phenomena: selected topics.* 2013: Elsevier.

160. Siantar, D.P., et al., *Treatment of 1,2-dibromo-3-chloropropane and nitrate-contaminated water with zero-valent iron or hydrogen/palladium catalysts.* Water Research, 1996. **30**(10): p. 2315-2322.

161. Zawaideh, L.L. and T.C. Zhang, *The effects of pH and addition of an organic buffer (HEPES) on nitrate transformation in Fe 0-water systems.* Water science and technology, 1998. **38**(7): p. 107-115.

162. Song, H. and E.R. Carraway, *Catalytic hydrodechlorination of chlorinated ethenes by nanoscale zero-valent iron.* Applied Catalysis B: Environmental, 2008. **78**(1): p. 53-60.

163. Suzuki, T., et al., *Mechanism of nitrate reduction by zero-valent iron: equilibrium and kinetics studies.* Chemical Engineering Journal, 2012. **183**: p. 271-277.

164. Xu, J., et al., *Promotion effect of Fe $^{2+}$ and Fe$_3$O$_4$ on nitrate reduction using zero-valent iron.* Desalination, 2012. **284**: p. 9-13.

165. Zhang, J., et al., *Kinetics of nitrate reductive denitrification by nanoscale zero-valent iron.* Process Safety and Environmental Protection, 2010. **88**(6): p. 439-445.

166. Sun, Y.-P., et al., *A method for the preparation of stable dispersion of zero-valent iron nanoparticles.* Colloids and Surfaces A: Physicochemical and Engineering Aspects, 2007. **308**(1): p. 60-66.

167. Sparis, D., et al., *Reduction of nitrate by copper-coated ZVI nanoparticles.* Desalination and Water Treatment, 2013. **51**(13-15): p. 2926-2933.

168. Fateminia, F.S. and C. Falamaki, *Zero valent nano-sized iron/clinoptilolite modified with zero valent copper for reductive nitrate removal.* Process Safety and Environmental Protection, 2013. **91**(4): p. 304-310.

169. Petala, E., et al., *Nanoscale zero-valent iron supported on mesoporous silica: Characterization and reactivity for Cr (VI) removal from aqueous solution.* Journal of hazardous materials, 2013. **261**: p. 295-306.

170. Zhang, H., et al., *Synthesis of nanoscale zero-valent iron supported on exfoliated graphite for removal of nitrate.* Transactions of Nonferrous Metals Society of China, 2006. **16**: p. s345-s349.

171. Zhang, W.-x., C.-B. Wang, and H.-L. Lien, *Treatment of chlorinated organic contaminants with nanoscale bimetallic particles.* Catalysis today, 1998. **40**(4): p. 387-395.

172. Schrick, B., et al., *Hydrodechlorination of trichloroethylene to hydrocarbons using bimetallic nickel-iron nanoparticles.* Chemistry of Materials, 2002. **14**(12): p. 5140-5147.

173. Hosseini, S.M., B. Ataie-Ashtiani, and M. Kholghi, *Nitrate reduction by nano-Fe/Cu particles in packed column.* Desalination, 2011. **276**(1): p. 214-221.

174. Li, T. and J. Farrell, *Reductive dechlorination of trichloroethene and carbon tetrachloride using iron and palladized-iron cathodes.* Environmental science & technology, 2000. **34**(1): p. 173-179.

175. Tu, Y.-J. and C.-F. You, *Phosphorus adsorption onto green synthesized nano-bimetal ferrites: equilibrium, kinetic and thermodynamic investigation.* Chemical Engineering Journal, 2014. **251**: p. 285-292.

176. Wen, Z., Y. Zhang, and C. Dai, *Removal of phosphate from aqueous solution using nanoscale zerovalent iron (nZVI).* Colloids and Surfaces A: Physicochemical and Engineering Aspects, 2014. **457**: p. 433-440.

177. Yuvakkumar, R., et al., *Preparation and characterization of zero valent iron nanoparticles.* Dig. J. Nanomater. Biostruct, 2011. **6**: p. 1771-1776.

178. Liu, Y., et al., *TCE dechlorination rates, pathways, and efficiency of nanoscale iron particles with different properties.* Environmental Science & Technology, 2005. **39**(5): p. 1338-1345.

179. Woo, H., et al., *Effects of washing solution and drying condition on reactivity of nano-scale zero valent irons (nZVIs) synthesized by borohydride reduction.* Chemosphere, 2014. **97**: p. 146-152.

180. Song, H.-C., E.R. Carraway, and Y.-H. Kim, *Synthesis of Nano-Sized Iron for Reductive Dechlorination. 1. Comparison of Aerobic vs. Anaeriobic Synthesis and Characterization of Nanoparticles.* Environmental Engineering Research, 2005. **10**(4): p. 165-173.

181. Song, H.-C., E.R. Carraway, and Y.-H. Kim, *Synthesis of nano-sized iron for reductive dechlorination. 2. Effects of synthesis conditions on iron reactivities.* Environmental Engineering Research, 2005. **10**(4): p. 174-180.

182. Kuznetsov, M., Y.G. Morozov, and O. Belousova, *Synthesis of copper ferrite nanoparticles.* Inorganic Materials, 2013. **49**(6): p. 606-615.

183. Sleiman, N., et al., *Phosphate removal from aqueous solution using ZVI/sand bed reactor: Behavior and mechanism.* Water research, 2016. **99**: p. 56-65.

184. Chitrakar, R., et al., *Phosphate adsorption on synthetic goethite and akaganeite.* Journal of Colloid and Interface Science, 2006. **298**(2): p. 602-608.

185. Zeng, L., X. Li, and J. Liu, *Adsorptive removal of phosphate from aqueous solutions using iron oxide tailings.* Water Research, 2004. **38**(5): p. 1318-1326.

186.   Yan, L.-g., et al., *Adsorption of phosphate from aqueous solution by hydroxy-aluminum, hydroxy-iron and hydroxy-iron–aluminum pillared bentonites.* Journal of hazardous materials, 2010. **179**(1): p. 244-250.

187.   Xiong, J., et al., *Phosphate removal from solution using steel slag through magnetic separation.* Journal of Hazardous Materials, 2008. **152**(1): p. 211-215.

188.   Yan, W., et al., *Nanoscale zero-valent iron (nZVI): Aspects of the core-shell structure and reactions with inorganic species in water.* Journal of contaminant hydrology, 2010. **118**(3): p. 96-104.

189.   Bard, A.J. and L.R. Faulkner, *Electrochemical methods: fundamentals and applications.* 2 ed. Vol. 2. 2001: Wiley New York. p. 808.

190.   Bard, A.J. and L.R. Faulkner, *Electrochemical methods: fundamentals and applications.* 2 ed. 2001: Wiley New York. p. 18-22.

191.   Choe, S., H.M. Liljestrand, and J. Khim, *Nitrate reduction by zero-valent iron under different pH regimes.* Applied Geochemistry, 2004. **19**(3): p. 335-342.

192.   Wang, J. and J. Farrell, *Investigating the role of atomic hydrogen on chloroethene reactions with iron using Tafel analysis and electrochemical impedance spectroscopy.* Environmental science & technology, 2003. **37**(17): p. 3891-3896.

193.   Rieger, P., *Electrochemistry, Chapman & Hall.* 2 ed. New York. 1994. p. 109-125.

194.   Rastogi, A., S.R. Al-Abed, and D.D. Dionysiou, *Sulfate radical-based ferrous–peroxymonosulfate oxidative system for PCBs degradation in aqueous and sediment systems.* Applied Catalysis B: Environmental, 2009. **85**(3): p. 171-179.

195.   Janda, V., et al., *Kinetic models for volatile chlorinated hydrocarbons removal by zero-valent iron.* Chemosphere, 2004. **54**(7): p. 917-925.

196.   Khalil, A.M., S.-E.K. Fateen, and A. Bonilla-Petriciolet, *MAKHA—A New Hybrid Swarm Intelligence Global Optimization Algorithm.* Algorithms, 2015. **8**(2): p. 336-365.

197.   Fogler, H.S., *Elements of chemical reaction engineering.* 3 rd ed. 2004: Prentice-Hall p. 73-77.

198.   Lagergren, S., *About the theory of so-called adsorption of soluble substances.* 1898.

199.   Ho, Y.-S. and G. McKay, *The kinetics of sorption of divalent metal ions onto sphagnum moss peat.* Water Research, 2000. **34**(3): p. 735-742.

200.   Wang, W., et al., *Enhanced separation of nanoscale zero-valent iron (nZVI) using polyacrylamide: Performance, characterization and implication.* Chemical Engineering Journal, 2015. **260**: p. 616-622.

201.   Bhowmick, S., et al., *Montmorillonite-supported nanoscale zero-valent iron for removal of arsenic from aqueous solution: kinetics and mechanism.* Chemical Engineering Journal, 2014. **243**: p. 14-23.

202.   Li, J.-J., et al., *Nanoporous silica-supported nanometric palladium: synthesis, characterization, and catalytic deep oxidation of benzene.* Environmental science & technology, 2005. **39**(5): p. 1319-1323.

203.   Busch, J., et al., *A field investigation on transport of carbon-supported nanoscale zero-valent iron (nZVI) in groundwater.* Journal of contaminant hydrology, 2015. **181**: p. 59-68.

204.   Zhan, J., et al., *Multifunctional iron− carbon nanocomposites through an aerosol-based process for the in situ remediation of chlorinated hydrocarbons.* Environmental science & technology, 2011. **45**(5): p. 1949-1954.

205. Busch, J., et al., *Investigations on mobility of carbon colloid supported nanoscale zero-valent iron (nZVI) in a column experiment and a laboratory 2D-aquifer test system.* Environmental Science and Pollution Research, 2014. **21**(18): p. 10908-10916.

206. Liu, P., J. Keller, and W. Gernjak, *Enhancing zero valent iron based natural organic matter removal by mixing with dispersed carbon cathodes.* Science of the Total Environment, 2016. **550**: p. 95-102.

207. Guan, X., et al., *The limitations of applying zero-valent iron technology in contaminants sequestration and the corresponding countermeasures: the development in zero-valent iron technology in the last two decades (1994–2014).* water research, 2015. **75**: p. 224-248.

208. Cho, M. and S. Ahn, *The influence of activated carbon support on nitrate reduction by Fe(0) nanoparticles.* Korean Journal of Chemical Engineering, 2012. **29**(8): p. 1057-1062.

209. Katsigiannis, A., et al., *Removal of emerging pollutants through Granular Activated Carbon.* Chemical Engineering Journal, 2015. **280**: p. 49-57.

210. Liu, F., et al., *Graphene-supported nanoscale zero-valent iron: removal of phosphorus from aqueous solution and mechanistic study.* Journal of Environmental Sciences, 2014. **26**(8): p. 1751-1762.

211. Sun, H., et al., *Nano-Fe0 encapsulated in microcarbon spheres: synthesis, characterization, and environmental applications.* ACS applied materials & interfaces, 2012. **4**(11): p. 6235-6241.

212. Huang, G., et al., *Remediation of nitrate–nitrogen contaminated groundwater using a pilot-scale two-layer heterotrophic–autotrophic denitrification permeable reactive barrier with spongy iron/pine bark.* Chemosphere, 2015. **130**: p. 8-16.

213. Xiao, J., et al., *Performance of activated carbon/nanoscale zero-valent iron for removal of trihalomethanes (THMs) at infinitesimal concentration in drinking water.* Chemical Engineering Journal, 2014. **253**: p. 63-72.

214. Ota, K., et al., *Removal of nitrate ions from water by activated carbons (ACs)—Influence of surface chemistry of ACs and coexisting chloride and sulfate ions.* Applied Surface Science, 2013. **276**: p. 838-842.

215. Delgado, J., et al., *Separation of ethanol–water liquid mixtures by adsorption on BPL activated carbon with air regeneration.* Separation and Purification Technology, 2015. **149**: p. 370-380.

216. Zhu, Y., et al., *Impacts of nitrate and electron donor on perchlorate reduction and microbial community composition in a biologically activated carbon reactor.* Chemosphere, 2016. **165**: p. 134-143.

217. Cho, D.-W., et al., *Adsorption of nitrate and Cr (VI) by cationic polymer-modified granular activated carbon.* Chemical Engineering Journal, 2011. **175**: p. 298-305.

218. Abdul, A. and F. Aberuagba, *Comparative study of the adsorption of phosphate by activated charcoal from corncobs, groundnut shells and rice-husks.* AU J Technol, 2005. **9**: p. 59.

219. Vassileva, P., P. Tzvetkova, and R. Nickolov, *Removal of ammonium ions from aqueous solutions with coal-based activated carbons modified by oxidation.* Fuel, 2009. **88**(2): p. 387-390.

220. Drever, J.I., *The Geochemistry of Natural Waters: Surface and Groundwater Environments, 436 pp.* 1997, Prentice Hall, Upper Saddle River, NJ.

221. Su, Y., et al., *Magnetic sulfide-modified nanoscale zerovalent iron (S-nZVI) for dissolved metal ion removal.* Water research, 2015. **74**: p. 47-57.

222. Ruangchainikom, C., et al., *Effects of water characteristics on nitrate reduction by the Fe^0/CO_2 process.* Chemosphere, 2006. **63**(2): p. 335-343.

223. Sun, H., et al., *Treatment of groundwater polluted by arsenic compounds by zero valent iron.* Journal of Hazardous Materials, 2006. **129**(1): p. 297-303.

224. Lv, X., et al., *Effects of co-existing ions and natural organic matter on removal of chromium (VI) from aqueous solution by nanoscale zero valent iron (nZVI)-Fe_3O_4 nanocomposites.* Chemical engineering journal, 2013. **218**: p. 55-64.

225. Su, Y., et al., *Effects of nitrate on the treatment of lead contaminated groundwater by nanoscale zerovalent iron.* Journal of hazardous materials, 2014. **280**: p. 504-513.

226. Tyrovola, K., et al., *Arsenic removal from geothermal waters with zero-valent iron—effect of temperature, phosphate and nitrate.* Water Research, 2006. **40**(12): p. 2375-2386.

227. Mehta, V.S. and S.K. Chaudhari, *Arsenic removal from simulated groundwater using household filter columns containing iron filings and sand.* Journal of Water Process Engineering, 2015. **6**: p. 151-157.

228. Almeelbi, T. and A. Bezbaruah, *Aqueous phosphate removal using nanoscale zero-valent iron.* Journal of Nanoparticle Research, 2012. **14**(7): p. 900.

229. Luo, J., et al., *Mechanism of enhanced nitrate reduction via micro-electrolysis at the powdered zero-valent iron/activated carbon interface.* Journal of colloid and interface science, 2014. **435**: p. 21-25.

230. Rennie, R., J. Law, and J. Daintith, *A Dictionary of Chemistry.* 2016: Oxford University Press.

231. Wang, W., et al., *Removal of Pb (II) and Zn (II) using lime and nanoscale zero-valent iron (nZVI): A comparative study.* Chemical Engineering Journal, 2016. **304**: p. 79-88.

232. Rangsivek, R. and M. Jekel, *Removal of dissolved metals by zero-valent iron (ZVI): Kinetics, equilibria, processes and implications for stormwater runoff treatment.* Water Research, 2005. **39**(17): p. 4153-4163.

233. Phillips, D.H., et al., *Ten year performance evaluation of a field-scale zero-valent iron permeable reactive barrier installed to remediate trichloroethene contaminated groundwater.* Environmental Science & Technology, 2010. **44**(10): p. 3861-3869.

234. Higgins, M.R. and T.M. Olson, *Life-cycle case study comparison of permeable reactive barrier versus pump-and-treat remediation.* Environmental science & technology, 2009. **43**(24): p. 9432-9438.

235. Nauman, E.B., *Chemical reactor design, optimization, and scaleup.* 2008: John Wiley & Sons.

236. Crowder, T.M., et al., *Fundamental effects of particle morphology on lung delivery: predictions of Stokes' law and the particular relevance to dry powder inhaler formulation and development.* Pharmaceutical research, 2002. **19**(3): p. 239-245.

237. Organization, W.H., *Ammonia in drinking-water. Background document for preparation of WHO Guidelines for drinking-water quality. Geneva, World Health Organization (WHO/SDE/WSH/03.04/1).* 2003.

238. Association, W.Q. *Ammonia Fact Sheet* 2013 [cited 2017 10/4]; Available from: https://www.wqa.org/Portals/0/Technical/Technical%20Fact%20Sheets/2014_Ammonia.pdf.

239. Organization, W.H., *Iron in Drinking-water Background document for development of WHO Guidelines for Drinking-water Quality.* 2003.

240. Wakayama, H. *Revision of Drinking Water Quality Standards and QA/QC for Drinking Water Quality Analysis in Japan*. MHLW, japan [cited 2017 10/4]; Available from: http://www.nilim.go.jp/lab/bcg/siryou/tnn/tnn0264pdf/ks0264011.pdf.

241. Widiastuti, N., et al., *Removal of ammonium from greywater using natural zeolite.* Desalination, 2011. **277**(1): p. 15-23.

242. Corrêa, A.X., et al., *Use of ozone-photocatalytic oxidation (O₃/UV/TiO₂) and biological remediation for treatment of produced water from petroleum refineries.* Journal of Environmental Engineering, 2009. **136**(1): p. 40-45.

243. Agency, I.E. [cited 2017 17/3]; Available from: https://www.iea.org/about/faqs/oil/.

244. Estrada-Arriaga, E.B., J.A. Zepeda-Aviles, and L. García-Sánchez, *Post-treatment of real oil refinery effluent with high concentrations of phenols using photo-ferrioxalate and Fenton's reactions with membrane process step.* Chemical Engineering Journal, 2016. **285**: p. 508-516.

245. Diya'uddeen, B.H., W.M.A.W. Daud, and A.R.A. Aziz, *Treatment technologies for petroleum refinery effluents: a review.* Process Safety and Environmental Protection, 2011. **89**(2): p. 95-105.